UNIVERSITÀ DEGLI STUDI DI MILANO BICOCCA
DIPARTIMENTO DI FISICA G.OCCHIALINI

CORSO DI DOTTORATO IN FISICA E ASTRONOMIA
CICLO XXVI

DEVELOPMENT OF LOW LEVEL COUNTING SYSTEMS FOR HIGH SENSITIVITY MEASUREMENTS

Settore Scientifico Disciplinare FIS/04

Tesi di dottorato di
Elena Sala

Tutore: Prof. Ezio Previtali

Anno Accademico 2013-2014

Contents

Introduction

Low level counting techniques are a powerful tools in many different fields including biological and chemical tracer studies, archaeological and geological dating, investigation of natural and induced radioactivities and the study of fundamental particles physics. Since they play a crucial role in many applications, developments are continuously pursue to improve the extreme sensitivity typical of these techniques.

The fundamental request of low level counting techniques is the capability to detect feeble signals, characterized by low counting rates, above the background composed of spurious counts; they thus have the capability to measure very low activities of natural and artificial radionuclides.

During my PhD work I have focused on two main applications using low level counting systems: the search of rare physics events and the environmental monitoring.

Both the studied systems use γ spectroscopy with High Purity Germanium detectors (HPGe). This technique is one of the most sensitive, it exploits the excellent energy resolution typical of such detectors and their low intrinsic background.

The first system is composed of two *n-type* HPGe GMX 100-95 in Low Background configuration, they have been designed with radiopure selected materials to reach an intrinsic background as low as possible. This work has brought to a unique configuration associated to an electrical cooling system, different from the one that was available on market. Since the two GMX detectors have been conceived to work in coincidence I have optimized the measuring system studying different radionuclide decay schemes to consider the most probable coincidences between the γ-rays emitted during the decay of the isotope under study.

A dedicated data acquisition has been developed with particular attention to the coincidence detection efficiency. Furthermore I have developed the analysis software to

analyze these peculiar measurements exploiting all the important features of the system with the help of Monte Carlo simulations.

For some rare physics events experiments the only way to enhance the sensitivity is the background reduction; for this purpose all the materials of the experimental facility should be selected as radiopure as possible.

The development and optimization of the low background system composed of the two GMX detectors, working in coincidence, can select suitable materials through the measurement of very low radionuclide concentrations.

The other system I have worked on is a Broad Energy Germanium (BEGe5030) in low background configuration. This detector can register with excellent energy resolution and high efficiency a wide energy spectrum, from 3 keV up to 3 MeV, thanks to some of its peculiar features. The thin dead layers surrounding the active volume and the thin entrance window on its top are responsible for its capability to detect very low energy radiations.

I have optimized this system using Monte Carlo simulations to detect low contaminations of radionuclides in several samples.

In particular in the last century, the environmental monitoring has became an important aspect of radio-protection; nuclear tests, nuclear accidents, wastes and fall-out in general can release a large quantity of radionuclides. Since toxicity and radioactivity of these contaminations are dangerous it is mandatory an environmental monitoring at the area of interest.

Plutonium isotopes significantly contribute to the contamination due to nuclear fall-out events in environment; since they are very toxic it is important to quickly monitor a large number of samples in the area of interest.

Using the BEGe I have developed a quick and sensitive method to detect Plutonium isotopes concentration in environmental samples through the detection of the X-rays emitted during their decays.

This result is a very important improvement in Plutonium detection for monitoring measurements since the counting methods commonly used are characterized by long measuring and sample treatments time.

Chapter 1

Sources of Radioactive Background

In low level counting measurements the experimental sensitivity is limited by some parameters, the one that affects the most the measurement of the signal rates under study is the background radioactivity. Background sources can be, in general, divided in five components:

- Environmental Radioactivity
- Contaminations in detector and shielding materials
- Radon and its progenies
- Cosmic rays
- Neutrons

The understanding of all the experimental background sources is mandatory before data taking.

1.1 Environmental Radioactivity

Energetic radiation in environment comes from primordial, anthropogenic (man-made) and cosmogenic radionuclides. This radiation has to be understood because it could be an important interference for the signal to detect or an important subject we want to study. Sources of radioactive background could be both external or internal to the counting system. The former is due to contaminations in Th, K and U predominantly present in laboratory, in particular in building materials. Internal radiations come from primordial and artificial radioactivity in shielding and detectors materials. The primordial

radioactivity origins from the synthesis of matter of our solar system and consists in radioisotopes with a half-life of the same order of magnitude as the age of our Earth.

1.1.1 Primordial radionuclides

^{232}Th, ^{235}U and ^{238}U (tab. 1.1)are the first isotopes of three chains of radioactive nuclides that all end in a stable Lead isotope, ^{208}Pb, ^{207}Pb and ^{206}Pb, respectively. Since isotopic abundance is only of about 0.7% for ^{235}U its contribution to the total activity of Uranium is of about 4%.

Another primordial radionuclide is ^{40}K which presence is about 10^4 times that of Thorium and Uranium in soil therefore although ^{40}K isotopic abundance is 0.0118% and the emission of the intense gamma ray, 1460 keV, following the disintegration has a probability of 11%, its contribution to gamma radiation is comparable to the other primordial nuclides [2].

Parent radioisotope	Isotopic Abundance %	$T_{1/2}$ *years*	Emitted radiation
^{232}Th	100	1.4×10^{10}	α, β, γ
^{238}U	99.27	4.47×10^{9}	α, β, γ
^{235}U	0.72	7.04×10^{8}	α, β, γ
^{40}K	0.0118	1.29×10^{9}	β, γ

Table 1.1: Primordial radionuclides

The complete decay chain of ^{232}Th and ^{238}U are shown in figure 1.1 and 1.2 respectively.

The original source of Potassium, Thorium and Uranium is the crust of the Earth and the underlying magma; their contaminations can vary widely in nature depending on geomorphological properties of bedrock and water possible transport. When the activity of all daughters nuclides in a decay chain is equal to the activity of their respective parents a condition called *secular equilibrium* is established A. Some chemical and physical

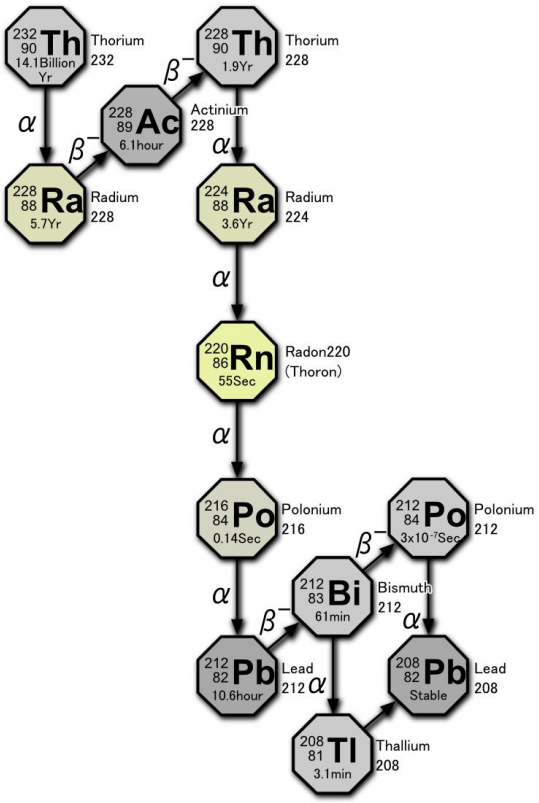

Figure 1.1: ^{232}Th decay chain

processes can cause the transfer of some nuclides producing the break of this condition in environment.

In gamma spectroscopy with HPGe the γ induced background is obviously the most significant and primordial radionuclides contribute with emitted γ with a broad energy range. Some of the ^{238}U and ^{232}Th progenies emit gamma rays accompanying their decays; their energies start from tens of keV to the maximum energy of 2614.5 keV of ^{208}Tl, an isotopes belonging to the ^{232}Th decay series. Some of the most intense γ emissions for ^{232}Th and ^{238}U chain isotopes are listed in table 1.3.

Radon, an element belonging to the noble gas family, has some radioactive isotopes in the Uranium an Thorium series and deserves a particular attention.

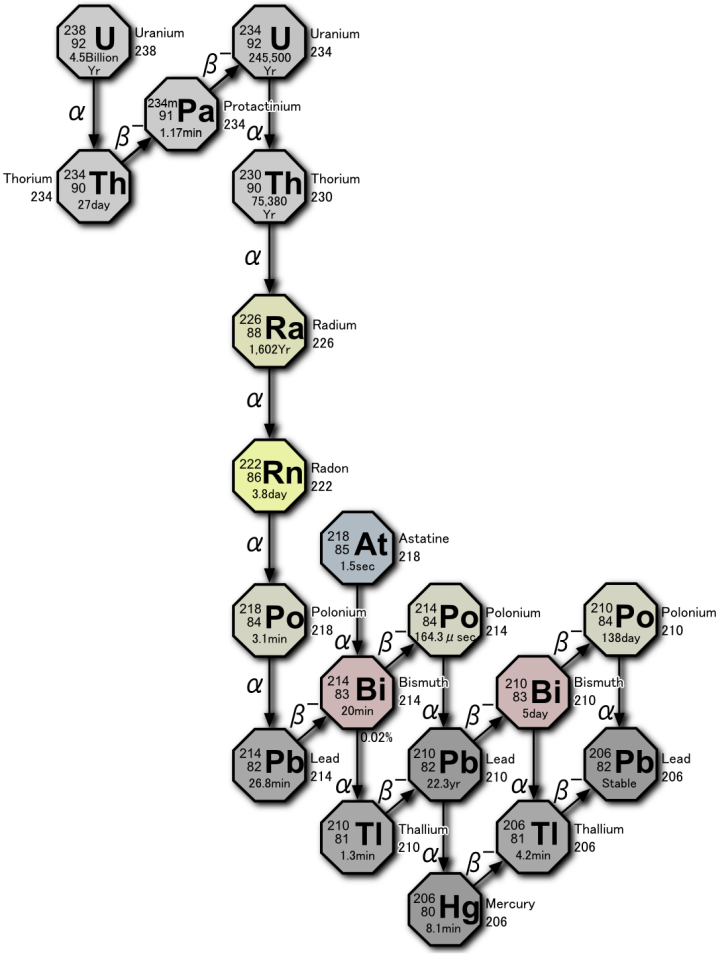

Figure 1.2: ^{238}U decay chain

Radon

Radon isotopes from radioactive primordial chains are:

^{232}Th chain:	^{220}Rn	half-life	54.5 *s*
^{235}U chain:	^{219}Rn	half-life	3.92 *s*
^{238}U chain:	^{222}Rn	half-life	9.82 *days*

Because of its gas nature, Radon can be carried away from its place of formation by air, water or by diffusion process; in minor part it also can escape from solid matrix, such as building materials, by recoil due to α particle ejection or by diffusion.

Energy *keV*	B.R. %
338.3	11.27
794.9	4.25
911.2	25.8
964.8	4.99
968.9	15.8

(a) **^{228}Ac (^{232}Th chain)**

Energy *keV*	B.R. %
277	6.31
510.8	22.6
583.2	84.5
860.6	12.4
2614.5	99

(b) **^{208}Tl (^{232}Th chain)**

Energy *keV*	B.R. %
53.2	1.2
241.9	7.43
295.2	19.3
351.9	37.6
785.9	1.07

(c) **^{214}Pb (^{238}U chain)**

Energy *keV*	B.R. %
609.3	46.1
1120.3	15.1
1238.1	5.8
1764.5	15.4
2204.2	5.1

(d) **^{214}Bi (^{238}U chain)**

Figure 1.3: Most intense γ lines of decay series.

^{219}Rn has a low concentration because of its short half-life, it cannot diffuse very far from its source and is therefore negligible in most low radioactivity background considerations.

^{220}Rn is present in soil, rock and building materials, its concentration decreases with the distance from the emanating source therefore its concentration in air is low due to its short half-life. Its progenies have half-lives up to 11 *hours* of ^{212}Pb (fig. 1.1). If the ^{220}Rn diffuses from the matrix source, its series can be divided in two parts. Since ^{212}Pb has an half-life longer than that of its parent, 0.15 s of ^{216}Po, it can break the secular equilibrium

and gives the depletion of the series. The ^{212}Pb progenies are isotopes with half-lives shorter than that of their parent therefore the secular equilibrium will be established in this last part of the chain.

^{222}Rn is the Radon isotope that contributes most to environmental radioactivity because of its half-life and of its daughter products emitting many gamma radiations. Its progenies are α and β emitters, in particular ^{214}Pb and ^{214}Bi are responsible for the high B.R. γ emissions following their β^- decays. Of its daughters, ^{210}Pb has the longest half-life: about 22 *years*.

Radon indoor concentration depends on different aspects:

- building materials
- underlying soil and rocks
- Rn concentration in tap water
- ventilation in the building

1.1.2 Cosmogenic radioactivity

Cosmic Rays

The primary particles of cosmic rays are nuclei with very high energy: about 86% of protons, 12.7% of α particles and 1.3% of heavier nuclei. These particles interact with the nuclei in atmosphere producing secondary particles: neutrons, electrons, neutrinos, protons, muons and pions. The production rate reaches its maximum at about 15 km of height where the production of new particles is balanced by the loss of particles that have lost all their energy through nuclear collisions or ionization. The intensity of the secondary particles decreases rapidly below this altitude where the loss of particles is higher than the production. Usually for cosmic rays it is used the depth measured by the mass per unit area of overlying gas in g/cm^2 or meters water equivalent: 1 *mwe* = 100 g/cm^2[2].

The two components of cosmic rays at sea level are called hard and soft. The hard component consists in the muon flux produced in the high atmosphere from the primary cosmic rays. Muons have a great energy (1-100 GeV) and therefore they are very penetrating. Since the muon life-time is of 2.2μs the flux is partially reduced due to the muon

decay, but in materials muons can lose all their energy through different electromagnetic processes: ionization and excitation are the most probable, but bremsstrahlung and pair production are also possible[2].

The interactions of muons with electrons and nuclei in matter produce the cosmic ray soft component mainly composed of electrons and photons with a wide energy spectrum.

Muons are also accountable for the production of neutrons due to the interaction with the shielding materials. Because neutrons can possibly interact with the detector, despite the low production intensity this background component should be contemplated [6].

In low background techniques muons and neutrons are the most relevant particles while electrons and photons are generally absorbed by shielding materials. Cosmic rays produce also some cosmogenic radioactive nuclides, with either short and long half-life, in their interaction with atmospheric nuclei; the most significant are: ^{14}C, ^{3}H, ^{7}Be, ^{10}Be and ^{36}Cl [1].

1.1.3 Neutrons

Neutrons have no electric charge therefore they lose their energy through elastic and inelastic collisions or nuclear reactions with nuclei. Since cross sections for these processes are rather low, neutrons are highly penetrating particles. In elastic collisions the energy loss for neutrons is significant only if the nucleus mass is comparable to the neutron mass therefore they experience an effective slowing down process during interactions with low Z materials.

The typical energy spectrum, for neutrons originated from nuclear reactions, ranges from few keV up to several MeV, considering natural occurring process such as the nuclear fission. Such neutrons are called fast neutrons[6].

In penetration processes the neutron energy decreases and, if not absorbed, it can become thermal; as the velocity decreases the probability of capture or absorption by nuclei increases. This process produces nuclei that are generally unstable and consequently they emit some radiations; a nucleus, left in an excited state, emits neutrons depending on its mass number [2].

1.1.4 Anthropogenic radioactivity

From the half of the twentieth century nuclear weapons production and testing programs as well as the use of nuclear power for electricity generation, have produced many radionuclides in different waste forms and have spread them, causing environmental contamination across the whole earth.

Moreover the present use of radioactive elements for medical and industrial applications has increased the general diffusion of radioactive wastes that can be sometime dispersed in the environment.

Nuclear weapon tests during the period 1952-1962 and the Chernobyl and Fukushima catastrophes in 1986 and 2011 respectively, have spread radioactive fission products in environment. ^{137}Cs is one of these products, it has an half-life of about 30 *years* and decays through the β process followed by a 661 *keV* γ with 85% of B.R. Weapon tests and nuclear accidents have released also large quantity of Plutonium isotopes and ^{90}Sr, particularly important for their abundance.

1.2 Contaminations in detector and shielding materials

The radioactive background of a detector is evaluated through its count rate in absence of a sample to be measured. A measuring system is composed of detector, electronic components, a cryostat and shielding materials so that to fully understand the background it is mandatory to consider the count rate from all these parts of the system. The significant sources of background generally vary for different kind of detectors and systems, in this work I will focus on Germanium detectors.

Primordial radionuclides are always present in ores and in some raw materials that, for this reason, are often contaminated in K, Th and U. Firstly I will consider some materials commonly used in detector fabrication.

Aluminum (Z = 13, ρ = 2.7 g/cm^3)

Measurements on Aluminum samples have confirmed contaminations mainly from the Uranium series, that generally is not at the secular equilibrium but has lost the main part of its Radium.

Uranium concentration in Aluminum samples are usually of about 1-10 *Bq/kg*, but during the past years rather expensive methods to produce a pure Aluminum, High Purity Aluminum, with 2 *mBq/kg* of Th and U have been developed. Thanks to its properties this material is often used for various components of Germanium detectors[2].

Plastic Materials

The most commonly used plastic materials are polyethylene, mylar and Teflon. Since most of the plastic materials are mainly composed of C, H and O the possible contaminants are ^{14}C and Tritium, but industrial organic synthesis starts from low contaminated gases. Additives or catalysts can add some contaminations. But these type of materials are generally extremely pure [1].

Glass

Glass is generally used for photomultiplier tubes of scintillator detectors and it is always contaminated in K, Th and U. Glass used for this purpose should have particular features, and a development work has been carried out to produce materials with low contaminations since phototubes are widely used in rare event physics experiments [2].

Electronic components

Although the growing development in electronic circuit that allows low radioimpurities levels in Th and U, some components as boards, soldering and capacitors can have traces of radioactive contaminants. Generally the electronic part, i.e. the preamplifier, of a detector should be placed far from the active volume even better if outside the shielding materials.

Copper (Z = 29, ρ = 8.92 g/cm^3)

Copper is an important material used for detector components and as inner shielding layer. It can be fabricated with a very high purity thanks to its high redox potential compared to that of K, Th, U and most of their daughters [1]. Electrolytically refined Copper, OFHC (Oxygen Free High Conductivity) Copper, is purified after smelting by electrolytic dissolution and redeposition in solution separating Copper from all the radionuclides in

the environment. This process therefore produces Copper completely free of primordial and man-made radioimpurities.

Shielding materials

Materials used as shield from external radiations should have a low intrinsic activity in addiction to high atomic number Z and high density to reduce the environmental γ rays. Some suitable materials are:

Mercury (Z = 80, ρ = 13.6 g/cm^3)

Thanks to its properties Mercury is an excellent, though rather expensive, material capable to absorb environmental γ radiation. Mercury is easily purified by distillation and for this reason it was commonly used as shielding material. A layer of 2-4 cm placed in a steel enclosure was the typical inner shield. Nowadays, due to its high toxicity, this material has been replaced with Copper since it could reach a very high level of purity.

Iron (Z = 26, ρ = 7.874 g/cm^3)

Iron was commonly used as external shielding material in low level counting system. Iron and steel produced after 1952 could contain amount of artificial radioactivity, especially ^{60}Co since it was widely used in furnaces. Old ship Iron early produced can be cleaned reaching the mBq/kg level [1], since it is often recycled some contaminations could always be present [2]. Iron is however used as material for some system components, but it was replaced by Lead as shielding material.

Lead (Z = 82, ρ = 11.34 g/cm^3)

It is the most important shielding material not only for its high atomic number and high density but also for the good mechanical properties and the fair cost. Unfortunately Lead has the disadvantage of a not negligible ^{210}Pb contamination.

Thorium and Uranium have small concentrations in lead ores and can be separated from Lead in the refining processes thanks to the differences in chemical properties. Since the ^{210}Pb isotope cannot be separated from the Lead with the refining process the same ^{210}Pb/Pb concentration ratio is maintained; this value can vary from one mine to other.

Concentration of ^{210}Pb in Lead material varies starting from its production; ^{210}Pb decays with an half-life of 22 *years* thus after 100 *years* it will have decayed to 4.3% of its initial concentration value and after 200 *years* to about 0.2% [2].

The intrinsic radioactivity of Lead derives also from ^{210}Pb daughters nuclides: ^{210}Bi and ^{210}Po. ^{210}Pb decays beta with a transition energy of 63 keV that produces, with a B.R. of 85%, an exited state of 46 keV, the gamma associated with the de-excitation of the nucleus shows a 4.2% probability. The 1.16 *MeV* energetic β of ^{210}Bi produces bremsstrahlung and characteristic X-rays in Lead ranging from about 70 *keV* up to 90 *keV* (72.8, 75.0, 84.9 and 87.4 *keV*). ^{210}Po, the α emitters of this chain with an energy of 5.30 *MeV*, can diffuse increasing the surface contamination [1].

For low level counting system an old Lead is preferably used, this material should have been produced several ^{210}Pb half-life ago. Some Lead from 150-200 *years* ago are available even if in limited quantities.

1.3 Radon background

Building materials, water, soil and rocks can have significant contamination in Radium since this element is chemically active can interact with other elements. The Radium isotopes of the decay chains decay producing Radon radionuclides. These isotopes are therefore present in different concentrations in all buildings and in free air.

The Radon contamination in low level counting systems is due to its diffusion in free space volume surrounding the detector producing a background contribution proportional to its concentration.

1.4 Cosmic rays background

Cosmic rays contributes to the measurement background in different ways according to the considered component. Energetic charged particles produce secondary radiation in their interaction with shielding materials that are predominantly electromagnetic showers. Neutral pions, produced by protons and muons through a knock-on process are responsible of electrons and photons that have an energy spectrum from fraction on *MeV* to hundreds of *MeV* [2].

Muons direct contribution to the background is due to their interaction in matter via electromagnetic interaction resulting in high energy electron, positron, photon showers from knock-on electrons, electron pair production and muon bremsstrahlung. The direct hits of muons and protons and their secondary radiation either result in high energy pulses visible as a broad energy peak in the spectrum. Lead shielding affects more the secondary radiation than muons.

Germanium background spectra always show the annihilation peak at 511 *keV* coming from recombination of positron from electromagnetic showers, negative electrons and decaying μ^+. The intensity of this peak depends on the material used as inner shielding layer.

1.4.1 neutron-induced background

The nucleonic component of cosmic rays produces neutrons in atmosphere, in laboratory building materials and in the lead shielding of the counting system. Building materials are usually sufficient enough to slow down most of the neutrons while the neutrons efficiently produced in lead have a high energy spectrum.

The neutrons induced background consists in two components: a small one due to fast and slow cosmic rays neutrons and a larger from fast neutron produced in lead. The main interactions responsible for background signals are:

- Fast neutrons direct elastic and inelastic scattering with detector atoms
- Photons emitted in inelastic collisions of fast neutrons
- Photons from radiative capture of slow neutrons

Neutrons from external environmental activity dominate the activation and scattering processes at low energy [2].

The most important α-emitters from U and Th chain interact through the (α,n) reaction producing neutrons, they are ^{216}Po (α of 6.8 *MeV*) and ^{212}Po (α of 8.8 *MeV*) for the ^{232}Th chain and ^{218}Po (α of 6.0 *MeV*), ^{214}Po (α of 7.7 *MeV*) and ^{210}Po (α of 5.3 *MeV*) for the ^{238}U chain.

Cosmic-ray particles are capable of forming multiple radionuclides within Germanium and Copper layers composing the counting system shielding. Cosmogenic activation is

Energy *keV*	Isotope	Abundance	Process	Isotope source	Half-life
53.4 and 66.7	^{72}Ge ^{74}Ge	27.4% 36.5%	^{72}Ge(n,γ) ^{74}Ge($n,2n$)	^{73m}Ge	0.53 *s*
139.5	^{74}Ge ^{76}Ge	36.5% 7.8%	^{74}Ge(n,γ) ^{76}Ge($n,2n$)	^{75m}Ge ^{77m}Ge	49 *s*
159.5	^{76}Ge	7.8%	^{76}Ge(n,γ)	^{77m}Ge	54 *s*
198.3	^{70}Ge ^{72}Ge	20.5% 27.4%	^{70}Ge(n,γ) ^{72}Ge($n,2n$)	^{71m}Ge	20 *ms*
500.2	^{72}Ge	27.4%	^{72}Ge(n,γ)	^{73}Ge	prompt
562.8	^{76}Ge	7.8%	^{76}Ge($n,n'\gamma$)	^{76}Ge	prompt
595.8	^{74}Ge	36.5%	^{74}Ge($n,n'\gamma$)	^{74}Ge	prompt
691.0	^{72}Ge	27.4%	^{72}Ge($n,n'\gamma$)	^{72}Ge	prompt

Table 1.2: γ energies and reactions of neutrons with Germanium isotopes

typically caused by direct reactions, spallation or capture. In the case of Copper activation the most important source of background is due to ^{60}Co, this isotope is produced in Copper when a neutron reacts with a ^{63}Cu nucleus and emits an alpha particle [2].

The Germanium atom on which the neutron inelastic collision takes place is left in an exited state but falls immediately on the ground state emitting a photon that, if photo-electrically absorbed in the detector active volume, results in a pulse proportional to the sum of the photon energy and the ionized recoiling atom [2].

The background spectrum for thermal neutrons comes from the capture by a germanium atom through the (n,γ), ($n,2n$) and ($n,n'\gamma$) reactions that result in main sharp thermal peaks.

In table 1.2 are listed some energy lines of Germanium isotopes produced by cosmic rays due to interaction with the crystal.

Some other γ lines often produced by cosmic rays and therefore corresponding to a measurement background of the system are shown in table 1.3.

γ energy (keV)	Isotope source	Half-life	Process
511	Annihilation		
651.1	^{114}Cd	Prompt	^{113}Cd(n,γ)
669.6	^{63}Cu	Prompt	^{63}Cu($n,n'\gamma$)
770.6	^{65}Cu	Prompt	^{65}Cu($n,n'\gamma$)
803.3	^{206}Pb	Prompt	^{206}Pb($n,n'\gamma$)
846.8	^{56}Fe	Prompt	^{56}Fe($n,n'\gamma$)
962.1	^{63}Cu	Prompt	^{63}Cu($n,n'\gamma$)
1412.1	^{63}Cu	Prompt	^{63}Cu($n,n'\gamma$)

Table 1.3: Cosmic rays produced γ lines

Chapter 2

Background Reduction

Material radioimpurities and cosmic ray interactions are the most important constituent of background in low level counting system since they induce some spurious counts in measurements. Background rejection methods are then mandatory to reduce as much as possible the counts due to internal or external background sources. These methods can be classified as passive or active methods. Furthermore for low level counting systems materials cleaning and selection are essential to reduce the detector intrinsic background.

2.1 Passive methods

Passive methods exploit the high atomic number Z materials ability to absorb ionizing radiations. They consist in placing such materials around the detector active volume as shield from radioactive background sources.

Shielding and Overburden

Shielding materials must have some important features: good mechanical properties so that they can be fabricated in brick shape, high Z and density values to absorb ionizing radiations and low neutron cross section to avoid interactions in the shielding. High Z suitable materials are Pb, Fe, Cu and W.

As previously discussed Iron is a good material but twice the thickness respect to Lead would be needed to have the same absorption power. Lead is certainly the most used material since it has all the needed features.To suppress the X and γ rays produced

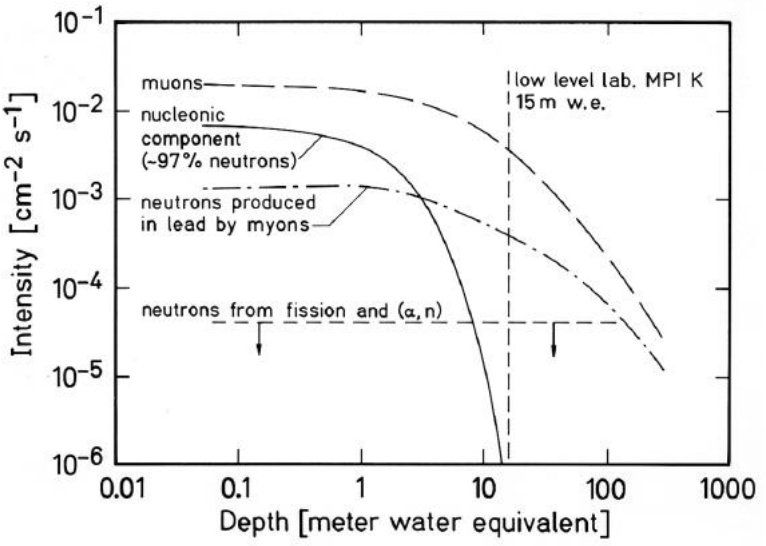

Figure 2.1: Intensity reduction of some background components as a function of the depth (mwe) [2]

in the shielding Lead layers, an inner layer of lower Z material is commonly used. Copper is one of the most suitable materials.

Background in low level system is mainly due to interactions of muons and protons from cosmic rays in the shielding and this effect could only be reduced placing the facility underground. The overburden attenuates the cosmic ray flux depending on the quantity of matter it is composed of.

In figure 2.1 are shown the intensities of muons, nucleonic component and neutrons generated in the shielding at different depths. Until about 5 m.w.e. coverage there is no significant decrease, but above this value the nucleonic components intensity drops. Muons and neutron components need more m.w.e. of coverage to be attenuated. The nucleonic component, 97% of which are neutron, can be reduced also using layers of low Z moderator material, paraffin or polyethylene, outside the shielding to slow down neutrons to thermal energy. Then thermal neutrons can be absorbed through the reaction ^{10}B(n,α)^{7}Li adding Boron to the moderator material.

Since moderator atoms can be excited by radiations causing the emission of γ-rays in the de-excitation process, this shielding can not be used as internal layer. The only way to suppress neutrons generated in the interaction of muons with the shielding materials

is to increase the coverage.

Most facilities are placed in buildings basement and have only the overburden of the building walls and floors that generally can reduce the muon flux by 10-20%. Overburden can be estimated with the number and the thickness of floor plates above a laboratory, but for a more accurate value it has to be considered that some cosmic rays come from declining angles through walls not interacting with some floor plates.

Rare physics event experiments need an efficient coverage from external sources of background. These facilities are generally placed in underground laboratories obtained from tunnels excavated under mountains or unused mines that can have overburdens of thousand m.w.e..

External gamma radiation coming from surrounding materials can be reduced with some expedients. The most practical way is to cover the walls with Iron or Lead, but this is especially done in rooms with whole body counters [2]. Sand and cement of which the walls are made of can be selected as pure as possible when the laboratory is under construction while for underground laboratories a low concentration in natural radioactive elements in special geological formations could be an advantage.

2.2 Active methods

Active shielding is a powerful method to reduce background, it consists in discrimination techniques to distinguish signals from background using different detectors or multiple detection mechanisms.

Background signals rejection could be fulfilled with anticoincidence detectors, known as guard counters or vetoes. The used method consists in the selection of coincidences in decay processes, discrimination of pattern signal (rise time) or detection of different parameters: ionization-scintillation, heat-ionization, heat-scintillation etc. All these rejection techniques need acceptance window cuts since their signal distributions could not form sharp lines and could partially overlap [1]. It is important to reach a complete geometrical coverage of the counting system to efficiently reject all the possible background events, the main detector types used for this purpose are proportional counters, plastic or liquid scintillators and NaI(Tl) or BGO crystals.

Anticoincidence

Anticoincidence technique consists in electronically reject detector signals which correspond, within a very brief time window, with signals of veto detectors surrounding the main one. Guard detectors intercept high energy charged cosmic ray particles that could hit the detector and gamma rays that have interacted through Compton scattering.

Large flat veto detectors, gas proportional and liquid or plastic scintillators are commonly used as anticoincidence shielding for low-level gamma counting system not placed in underground laboratories. Since environmental gamma radiation is randomly distributed it is better to have a uniform active shielding thickness outside the spectrometer; for cosmic rays rejection few *cm* of thickness are adequate. In low-level germanium spectrometer systems, veto detectors should be placed outside the shielding materials covering all the system sides, but this is often not possible for economic reasons.

The background suppression is performed registering a signal in the spectrometer detector only if it is not in coincidence with a pulse in the external veto detectors. This method allows to detect all the pulses due to the measured source eliminating the cosmic radiation that generally penetrates through both veto and main detectors. Among all the veto detectors, plastic scintillators have the best sensitivity to both gamma and cosmic rays ray radiation [4].

Active shield spectrometers

If the active veto is placed inside the shielding, the employment of NaI(Tl) crystal detectors is the most appropriate for space saving reasons since they could have limited dimensions thanks to their high intrinsic efficiency. NaI(Tl) can suppress not only the background pulses from cosmic ray muons, a large part coming from secondary radiation showers, but also pulses of Compton interactions in the spectrometer.

Part of the photons interacting in HPGe detector active volume through Compton scattering mechanism can escape the sensitive volume and only the recoiled electrons are detected. The resulting registered spectrum is a continuum background that affects negatively the gamma ray detection limit in the considered energy range. The scattered photons that have escaped the detector active volume can be detected by a NaI(Tl) with a

suitable size [4]; coincidence with this detector signals can avoid the registration of the background continuum component.

Compton Spectrometer exploits the low angular dependence on scattered photon energy for scattering angles grater than 135 ˚using two detectors. Pulses due to Compton scattering are detected by one detector only if in coincidence with a signal due to the scattered photon on the other one.

Sum Compton Spectrometer consists of two detectors close to each other. Pulse amplitudes registered by both the detectors are summed assuming that one is due to the electron interaction and the other to the scattered photon of the scattering Compton process.

Anti-Compton Spectrometer is used to reduce the background induced by Compton scattering using guards detectors. Pulses in the main spectrometer are registered only if they are not in coincidence with the scattered photons interacting in guards detectors.

Gamma Coincidence

Coincidence is a powerful background reduction technique when measurements of radionuclides emitting γ rays in sequence are considered. This technique consists in the detection of signals registered in coincidence considering a very sharp time window. Therefore, for a radionuclide emitting γ in coincidence, only the pulses from its decay are registered avoiding the background counts. The double coincidence spectrometer is composed of two detectors, they could be two NaI(Tl), a NaI(Tl) and a HPGe or two HPGe. Coincidence counting rate, N_C, for two photons with no angular correlation can be expressed by the formula:

$$N_C = A\varepsilon_1(E_1)\varepsilon_2(E_2)I_{\gamma 1}I_{\gamma 2} \tag{2.1}$$

where $\varepsilon(E)$ are the detectors efficiency at the considered γ energies E, I_γ are the B.R. of the photons and A the activity of the measured radionuclide equivalent to

$$A = N_1N_2/N_C \tag{2.2}$$

N_1 and N_2 are the net counting rates of the two measured photons. A more accurate evaluation of the coincidence counting rate can be achieved considering the corrections for random coincidences, background, sum coincidences, internal conversion probability and coincidence efficiency. Spurious coincidences counts, N_A are evaluated using the coincidence time τ:

$$N_A = 2\tau N_1 N_2 \tag{2.3}$$

To simultaneously detect the radiations of annihilation and de-excitation of β^+ emitters radionuclides it is possible to use a triple coincidence technique. The detectors commonly used are three NaI(Tl) or two NaI(Tl) and a HPGe. Although this method allows a good events selection and a reduced background it has a very low efficiency [4].

Pulse Shape Analysis

Particles of different types can give pulses of similar amplitude but different shapes when detected, the difference can arise in the rise or in the decay part of the pulse. Exploiting this feature it is possible to discriminate different particles interaction obtaining a considerable background reduction. For example the interaction of an electron can be distinguished from the one due to a multi-scattered photon considering the temporal development of pulses. This method is often used in rare event physics experiments to eliminate background events.

Venting

To reduce the background due to Radon concentration some Radon-free gases are commonly used: Argon and Nitrogen. Venting one of these gases in the inner detector space can reduce the concentration of ^{222}Rn and its progenies in the inner shielding volume of the counting system [2].

2.3 Materials Treatment and Selection

Materials selection is the most fundamental prerequisite for low level counting systems and low-radioactivity experiments. Contaminations in the components of the system

induce an intrinsic background that could spoiled its sensitivity; the use of high radiopurity materials is therefore mandatory. The most important contaminants in materials are ^{40}K, ^{232}Th and ^{238}U as seen in the previous chapter.

Since materials contaminations should be as low as possible, their selection has to be performed using systems capable to detect very low radioactivities. For this purpose are generally used low level counting techniques, in particular spectroscopy with High Purity Germanium, α spectrometry, neutron activation analysis (NAA) and mass spectrometry.

Another important aspect concerns the materials treatments often needed for surface cleaning and polishing. Acid cleaning with appropriate high radiopurity chemicals under clean room conditions and using ultrapure water on the final cleaning step has been proved to be an effective method. Some precautions have to be considered about the chemicals, for example the use of a Potassium-free lye for metals and semiconductors.

Electropolishing is another effective cleaning method for Cu, Fe and Ni surfaces; although some polishing liquids have not the needed radiopurity it is the final passivation and rinsing step that determines the purity of the chemical process. Electropolishing, in contrast of normal acid cleaning, smooths the surfaces.

Chapter 3

Techniques

3.1 Low level counting techniques

The main purpose of low level counting techniques is to maximize the number of detected signals, due to the event under study, and minimize all the others, the background components. The detected signal rate depends on sample size, detection efficiency and counting time; these parameters should be optimized to reach the needed sensitivity according to the technique used for the measurement.

The sensitivity for radionuclide contamination detection that can be reached, is significant; these techniques are thus employed in many different fields: biological and chemical tracers, archaeological and geological dating, investigation of natural and induced radionuclides and the study of fundamental particles [9].

A comparison between some techniques sensitivities for Uranium and Thorium detection is shown in table 3.1.

method	**suited for**	**sensitivity for U/Th**
Gamma spectroscopy (HPGe)	γ emitting nuclides	10-100 μBq/kg
Neutron Activation on solids	primordial parents	0.1 μBq/kg
on liquids		10^{-3} μBq/kg
Mass spectrometry (ICP-MS, AMS)	primordial parents	0.1 μBq/kg
Alpha spectroscopy	α emitting nuclides	1 mBq/kg

Table 3.1: Comparison between techniques

Non radiometric techniques commonly measure concentrations of primordial nuclides by weight. To compare results from different techniques the concentration is given in Bq/kg; the conversion factors are shown in table 3.2.

1 Bq/kg of ^{238}U = 81×10^{-9} g/g of U (81 ppb)
1 Bq/kg of ^{232}Th = 246×10^{-9} g/g of Th (246 ppb)
1 Bq/kg of ^{40}K = 32.3×10^{-6} g/g of K (32.3 ppm)

Table 3.2: Concentration conversion factors for primordial nuclides

3.1.1 Gamma spectroscopy

Gamma spectroscopy is a radiometric technique used to measure radionuclides concentrations, it allows the identification of an isotope from the detection of the gamma-rays emitted during its decay. HPGe are the most suitable detectors to perform gamma spectroscopy thanks to their excellent energy resolution and their very low intrinsic background. The typical energy resolution of these detectors not only can distinguish different peaks at close energy but allows also the detection of feeble signal emerging from the continuum.

Emission of gamma rays from nuclei is normally a consequence of an α or β decay. Since the emission is quite immediate, about picoseconds, the detection of γ rays can be directly connected to the previous decay.

Gamma rays are characteristic of a particular radionuclide decay and their energy and emission probability are well defined, for these reasons their detection can give a clear information on the presence of the radionuclide that originates them.

The typical HPGe detector spectrum consists in an energy distribution featuring many peaks and a significant continuum component. When the incident radiation is completely absorbed in the active volume a full-energy peak is present in the spectrum at the corresponding energy. Whenever part of the incident photon is not absorbed by the active volume, the spectrum will show an escape peak at the energy corresponding to the difference between the full-energy and the escaped energy.

The Germanium characteristic X-rays escape peaks are generally due to low energy radiation since the photoelectric process is more probable and the interaction occurs close to the detector surface.

For high energy γ-rays the pair production is the most probable interaction process, forming an electron-positron couple in the interaction point. The positron annihilation creates two 511 keV energy photons; if both are absorbed the process will contribute to the full-energy peak. If one annihilation photon escapes the active volume, a single escape peak at the energy corresponding to the incident energy minus 511 keV is formed in the spectrum, while a double escape peak, at the energy equal to the difference between the incident γ and 1022 keV, corresponds to the loss of both annihilation photons.

Background reduction is crucial for this technique since the acquired spectrum is easily affected by environmental radioactivity. The counts in the spectrum, registered without samples or sources, can be addressed to cosmic rays interaction in shielding, detector and shielding material contaminations, presence of Radon and environmental γ emissions external to the system. These background counts should be minimized to enhance the system sensitivity.

The background components, external to the system, can be reduced with appropriate shielding and veto detectors or placing the counting system underground. The internal component, the intrinsic background, is due to radioactive contaminations in the system materials. HPGe detectors have the possibility to be realized using materials with very low contamination, by materials selection. The contribution of each material to the background depends on its mass and the distance from the detector active volume; these parameters contribute to the choice of the most adequate material.

Gamma spectroscopy with HPGe allows measurements of huge amount of materials, mainly solid, up to few tens of kg. Quite long measuring time, especially for large mass samples or radiopure materials, are mandatory to provide a sensitive counting statistics.

Sensitivity depends also on another critical parameter: the product between sample mass and absolute detection efficiency; this value should be maximized to enhance the system performance.

The optimization of a HPGe detector measurements involves the efficiency calibration of the system. Efficiency depends either on the detector characteristics, on sample prop-

erties and radiation energy; its value should be evaluated for different source-detector configuration. The source-detector distance gives information about the solid angle covered by the emitted radiation and the sample density determines the possible self absorption. HPGe intrinsic efficiency is commonly evaluated in relation to that of a 3×3 inches NaI(Tl) at the 1332 keV of a ^{60}Co source placed 30 cm above the detector.

In standard approach, the efficiency is generally calibrated using a source with known activity, but the resulting calibration curve can be ascribed only to the specific configuration and radiation energy under study.

A solution, capable to evaluate efficiencies in different source-detector arrangement and for different energies, can be found using Monte Carlo simulations.

Monte Carlo simulations

Monte Carlo method could be approximated to a statistical procedure to calculate the value of a variable I, that identifies the average of a casual variable X on a number N of samples. The method is based on pseudo-casual numbers generation assuming a probability of density (PDF) coming from theory data, analytical data and data-theory fitting for the physics processes under study.

Simulations involving interaction of radiation with matter generally use the Monte Carlo method to simulate particles trajectories with the support of libraries containing essential information for the process description as photon interaction cross-section with different materials, secondary particles production and physical-chemical materials properties. The hypothesis is that generating a great number of events the method can produce results very close to the expectation value of the variables under study such as the energy deposited by radiation in a detector.

Thanks to its flexibility, Monte Carlo method could be used in many fields.

The algorithm for particles transport through Monte Carlo simulation is contained in software packages: an available one is *Geant4* developed at CERN. This package includes a large variety of instruments that allow:

- Simulation of particle trajectories in matter considering also possible decays and interactions.

- Evaluation of source-detector geometry and material characteristics influence on the interactions.
- Complete registration of event details.
- Acquisition of the simulated events to provide a prediction of the detector response if such interaction should take place.

Furthermore *Geant4* has a great varieties of geometrical descriptions, in order to have the flexibility to simulate the most complicated and realistic geometries.

Monte Carlo simulations are an essential tool to predict detectors efficiencies in various configurations defining detector and source shape and composition: geometry, materials elemental composition and density. Source-detector distance, dead layers thicknesses, densities, source and active volume dimensions are important parameters: they could affect the simulated efficiency if not correctly described. Efficiencies obtained from simulation should be as similar as possible to the experimental data, for this reason Monte Carlo simulation should be optimized for the system under study.

During my work Monte Carlo simulations have been performed with the software *Arby* [18], based on *Geant4* [17] libraries. It needs an input file in which all the parameters are defined while the contaminations are simulated using the libraries database in which radioisotopes decays are described. Each component can be defined as absorber, detector or source, according to its role. This method provides the possibility to use single isotope decay and also chain decays starting from the parent nucleus, such as ^{232}Th, until the last stable nucleus.

Therefore simulations provide a method to predict the sensitivity or the response of the apparatus in a considered configuration with a specific radioactive contamination.

3.1.2 Mass spectrometry

The determination of long-lived radionuclides especially in environmental samples, radioactive wastes and high-purity materials is of increasing importance.

Inorganic mass spectrometry is a universal and extremely sensitive analytical method for an almost simultaneous determination of element concentrations in the trace and ultra-trace range. In the last few years this method has been established for the determi-

nation of long-lived radionuclides and their isotope ratio measurements [15].

Inductively Coupled Plasma–Mass Spectrometry (ICP-MS) is a technique capable to perform trace metal analysis; the instruments commonly used are quadrupole, magnetic sector and multicollector. The ICP-MS instrument can measure most of the elements in the periodic table quantitatively. It is divided in 5-Stage Vacuum System Mass Spectrometer (fig. 3.1):

- Ion production
- 8 kV Ion Acceleration and Focusing
- Mass Separation
- Energy Focusing
- Ion Detection

Although this technique can be advantageous in comparison to radio-analytical techniques, the characterization of radionuclides with long half lifetimes at ultra-trace level for the selection of high-purity materials requires a high time consuming for sample preparation; this is in any case a very critical point [15].

The sample manipulation procedures involve the use of acids, to mineralize the sample, and radiochemical treatments, such as ion exchange resins, if there is the need to separate the radionuclides under study from the other contaminants. The overall technique should introduce the least possible contaminants and should have the best efficiency. It generally requires moderate amount of material, few tens of g, and can last few weeks considering treatments and measuring time.

The ICP-MS accurately determines the amount of a specific element present in the analyzed sample. In a typical quantitative analysis, the concentration of each element is determined by comparing the counts measured for a selected isotope to an external calibration curve that should be generated for that element. Liquid calibration standards are prepared using the same procedure used for the sample and are analyzed to establish the calibration curve.

The sensitivity of ICP-MS depends on the sample: the needed sample mass varies with the atomic number of the element under study. For heavy elements the sensitivity

increases thanks to the fact that in the region of high M/Z values, the isobaric and instrumental interferences are less important.

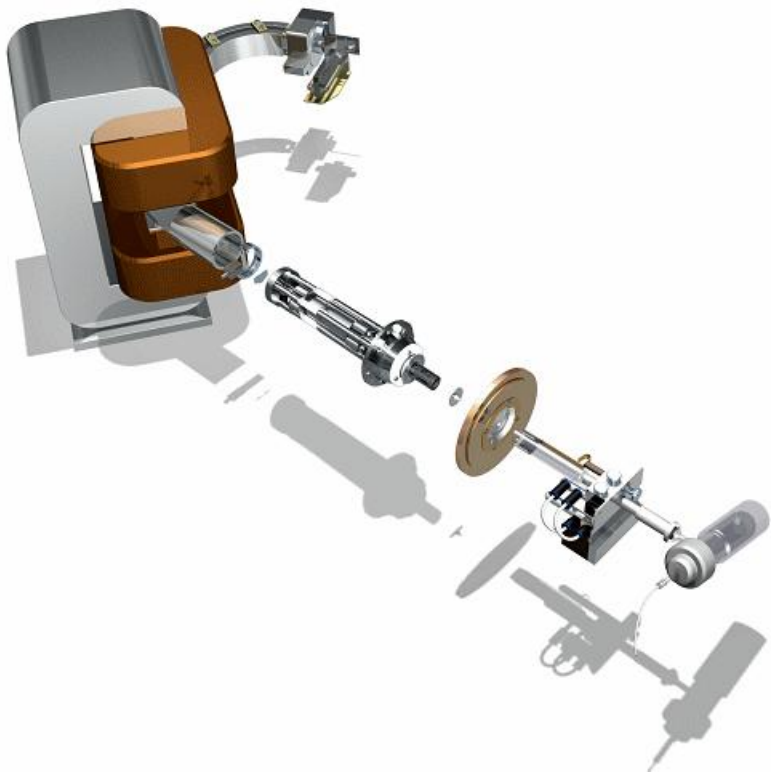

Figure 3.1: HR ICP MS Double Focusing scheme

3.1.3 Neutron Activation Analysis

The nuclear reaction induced bombarding a target material with neutrons can convert a stable nucleus in a radioactive nucleus. Neutron activation analysis principle is the determination of elements concentration in sample, exploiting this process. The analysis can be performed either detecting the instantaneous radiations following the neutron capture (Prompt Neutron Activation Analysis), or if the produced nuclei are radioactive, the radiations emitted during their decays. The nuclear reaction depends on the neutron activation cross section of the target elements and on the neutrons energy.

Activation generally produces a mixtures of radioactive isotopes. To select the ra-

dionuclides of interest and analyze their individual contribution, a feasible approach is the Radiochemical Neutron Activation Analysis (RNAA). In RNAA, the sample is mineralized with acid digestion and the use of Ion Exchange Resin, or other concentration method, provides the separation of the radionuclides of interest.

In order to quantify the separation yield, "carriers" (radioactive or stable isotopes) are added to the sample matrix before the separation. The determination of the carrier recovery provides the separation yield.

The most suitable method to detect the induced radiation is gamma spectroscopy thanks to the possibility to simultaneously detect the produced radionuclides.

Measurements can be performed in short running times, about days, on liquid or dissolved solid samples generally for small amounts of material: less than 1 g.

One on the most sensitive results on ^{232}Th in Copper samples has been achieved with RNAA with a detection limit of 4.88×10^{-13} g/g [16].

3.1.4 Alpha spectrometry

Alpha spectrometry is a technique generally used to determine surface contaminations in sample materials through the detection of the emitted α particles. The high charge and relatively low speed of alpha particles result in significant energy losses even in very thin absorbers. Although the resolution of semiconductors for α-spectrometry is good, the relatively small difference in alpha particles energy between some alpha emitters makes it difficult to separate the peaks [13]. An efficient chemical separation of radionuclide of interest from the interfering radionuclides in sample is therefore required.

Since the detection efficiency depends on the sample thickness it is essential to prepare a thin source. This can be carried out by electro-deposition on metal slabs. Evaporation, co-precipitation, electro-spraying, electrostatic precipitation, spontaneous deposition, molecular plating, and vacuum sublimation are also used to prepare α sources [14].

In environmental samples with very low contaminations a long counting time (1–10 days for the activity of radionuclide lower than 10 mBq) is required to reach a counting uncertainty as low as possible[13]. The main disadvantage of α-spectrometry is the long analysis time due to the chemical separation procedure for the complete separation of the

target radionuclide from the matrix as well as from interfering radionuclides.

Alpha Spectrometry applications which require high resolution, high sensitivity and low background are generally performed with Silicon Barrier Detectors (SBD). The SBD are suitable for heavy charged particle spectrometry since they have a thin entrance window (50 nm) which allows the incoming particle to reach the active detector volume with few energy loss in the dead layer.

The high sensitivity of this method is ensured by the depletion depth of about 100 - 120 μm which will absorb α particles up to 10 MeV, thus covering the complete range of all natural α emitting radionuclides.

Since this technique measures the surface contamination of a sample the detected activity is generally given in Bq/cm^2; to compare this value with the other techniques, converting it in Bg/kg, the sample treatments should be considered.

3.2 Measurements Sensitivity

A system detection sensitivity depends not only on detector features such as intrinsic background, energy resolution and efficiency but also on source and radionuclides that have to be measured. Furthermore it depends also on radioactive background correlated to the presence of other radionuclides not of interest.

Generally, sample measurements are accompanied with background measurements taking into account the system configuration and all the treatments employed to realize the sample; for this purpose blank samples are commonly used. For example since samples that have to be measured with alpha spectrometry are often electro-deposited on a slab, the blank for background measurements is a slab free of contaminants of the same dimension. The background for ICP-MS measurement is performed with a blank produced using the same procedure of the sample preparation.

Blank measurements allow the evaluation of an induced correlated background due to possible contamination in the materials used to realize the sample.

Treatments on environmental samples, measured with gamma spectroscopy, are generally not required. Therefore background measurements should be performed using a matrix, identical to the sample, free from the radionuclides under study. This method

considers also the background correlated with the presence of other contaminants in the sample and the possible absorption of background radiation. Actually, matrix for background measurements are often unavailable, thus a detector background measurement, without a matrix sample, is commonly used. The absorption of radiation due to sample density, however could be evaluated observing the counts under gamma lines present in the background and sample measurements.

A good example is the analysis of the peaks at 583 keV and 2615 keV of ^{208}Tl decay from ^{232}Th chain, if they are not present as contaminations in the sample. If the counts correlated to 583 keV in the sample spectrum are less than those of the background measurement, but those under 2615 keV peak are the same, it is possible to attribute the 583 keV counts lack to the sample absorption; samples density is generally not enough to completely absorb the high energy photon.

Radiometric techniques, such as gamma spectroscopy, measure radionuclides specific activity in samples. When peak counts due to the sample measurement, N, are greater than that of the background, N_B, it is possible to evaluate the contamination of the radionuclide under study. The counting statistics is illustrated in Appendix A.

The specific activity is calculated in disintegration per unit of time and mass (Bq/kg) using the following formula:

$$A_{(Bq/kg)} = \frac{[(full-energy\ peak\ counts)_{sample} - (full-energy\ peak\ counts)_{background}]}{m(kg) \cdot B.R. \cdot T \cdot \varepsilon} \quad (3.1)$$

where the $full-energy\ peak\ counts$ represent counts under the considered energy peak, $B.R.$ is the branching ratio, m the sample mass, ε the absolute efficiency of the detector and T the measuring time (in seconds). To compare the two considered spectra the same measuring time is needed.

If counts in the energy range under study are not present or do not exceed the background level it is possible to estimate the performance of the counting system with different methods.

3.2.1 Detection Limit

The spectrum associated to the sample measurement could have no evidence of counts in the energy range in which the peaks due to the radionuclide under study lye or the counts could be compatible with those of the background measurement. In this case it is possible to set a detection limit. This value is the activity limit that can be measured within a confidence level (c.l.) assuring that the counts fluctuation of the sample measurement exceeds the background counts fluctuation. In table 3.3 the confidence level values are listed as probability that the counts lye within an interval proportional to the standard deviation σ of the registered counts ($\sigma = \sqrt{N}$).

Confidence Level %	Interval
99.7	3σ
95	1.96σ
90	1.64σ
68	1σ
50	0.67σ

Table 3.3: Confidence Levels

If N is comparable to N_B or there is no evidence of a peak, the formula used to evaluate the activity limit is the following:

$$Limit_{(Bq/kg)} < \frac{\sqrt{N}}{m(kg) \cdot B.R. \cdot T \cdot \varepsilon} \tag{3.2}$$

where N represents the continuum counts in the energy range under study. Multiplying the $\sqrt{N}$ by the σ coefficient in table 3.3 it is possible to calculate the desired confidence level.

If the difference between N and N_B is less than a multiple of σ, considered as $\sqrt{N}$, the activity limit can be calculated with the formula 3.3 in which a difference of 2σ is used

as example.

$$Limit_{(Bq/kg)} < \frac{2\sigma}{m(kg) \cdot B.R. \cdot T \cdot \varepsilon} \tag{3.3}$$

3.2.2 Minimum Detectable Activity

The Minimum Detectable Activity (MDA) represents the activity value that can be measured for a radionuclide considering the counts in the background spectrum.

This quantity is evaluable if the sample contamination, at the energy region under study, is compatible with the measured background. To reach a useful MDA, the background correlated to the sample contamination in other radionuclides, should be taken into account.

MDA should be considered as the activity necessary to produce a mean value of net counts high enough to reduce the false-negative rate, that is the missing real activity rate when some is actually present. A 5% false negative probability is commonly chosen. The minimum number of counts, N_D, needed from the source to ensure a false negative rate no larger than 5%, can be calculated from the formula [8]:

$$N_D = 4.653\sigma_{N_B} + 2.706 \tag{3.4}$$

where σ_{N_B} is the square root of the background counts if only statistical fluctuations are considered.
To convert the N_D counts in minimum detectable activity they should be divided by efficiency, B.R. and measuring time [3].

The MDA is a useful quantity when the detection sensitivity for a radionuclide is needed before the measurement takes place.

Chapter 4

Development of Germanium Detectors

The Low Background system under study is composed of two *n-type* HPGe ORTEC coaxial detectors: GMX 100-95-PLUS-LB-S (fig. 4.1). These detectors have a 100% relative efficiency, 95mm of EndCap diameter and have been designed to detect an energy spectrum from 3 keV up to 10 MeV.

Figure 4.1: Detector GMX 100-95 PLUS

The system has been completely developed according to some requirements: electrical cooling system, low intrinsic background, detection of a broad energy spectrum with high energy resolution and coincidence measurements in order to enhance the sensitivity.

The low energy detection has been achieved using *n-type* HPGe detectors that can be realized with thin dead layers allowing low energy radiation to enter the active volume and be detected.

n-type semiconductor

Semiconductor detectors have as their main feature a great energy resolution thanks to the large number of the carriers for an incident radiation event. The fundamental generated carriers in these detectors are electron-hole pairs created along the interaction path of the primary radiation or secondary particle in the detector.

Electrons in the crystalline materials are confined in energy bands (fig. 4.2), set by the periodic lattice of the material, that in semiconductors (and insulators) are separated by forbidden energy ranges. In Germanium crystals the *conduction band* in which the electrons are free to migrate through the crystal, is separated from the valence band, completely filled with electrons, by a *bandgap* of about 1 eV.

At any nonzero temperature some electrons in the valence band could gain enough thermal energy to cross the bandgap and reach the conduction band leaving a vacancy called *hole*. This process will form an *electron-hole pair* that under an applied field will create a motion contributing to the conductivity of the material [3]. The probability of thermal excitation depends mostly on the ratio between the energy bandgap E_g and the absolute temperature T:

$$p(T) = CT^{3/2} exp\left(-\frac{E_g}{2kT}\right) \tag{4.1}$$

where C is a constant depending on the material and k the Boltzmann constant. In absence of an applied field the *electron-hole pair* recombines establishing an equilibrium concentration that will decrease by cooling the material.

To increase the number of free charges that will move under an applied voltage usually

a *doping* process, consisting in adding some impurities, is used. A small concentration of impurities could be already present in the crystals. The resulting semiconductor is *negative* or *n-type* when impurities increase the number of free electrons; for Germanium crystals this can be accomplished by using pentavalent atoms that will take place of a Germanium atom in the covalent bonds with an extra electron lightly bound. These extra electrons populate a level in the forbidden gap near the conduction band, so that a small amount of thermal excitation can ionize a great part of the *donor* impurities creating positively charged ions that allow to maintain the neutrality of the material [3].

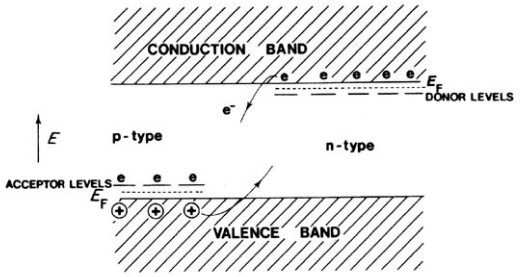

Figure 4.2: Electrons energy bands in semiconductors

Semiconductor radiation detectors exploit the properties of a *p-n junction*, created with *n-type* and *p-type* regions in good thermodynamic contact. The junction is formed in a single crystal modifying the impurities concentrations from one side of the junction to the other, for example diffusing *p-type* impurities on an *n-type* crystal surface that is converted in a *p-type* material.

The density discontinuity of conduction electrons creates a gradient so that the electrons migrate toward the lower concentration region (*p-type*) and the holes toward the *n-type*. The effect of this migration is to create negatively charged space on *p* side and a positively charged space on *n* side resulting in an electric field that, at the equilibrium, prevents a further diffusion. The region in which there is no net charge is called *depletion region* and it works as detector. The contact potential is too low to generate electric fields that will move charge carriers quickly, resulting in a possible incomplete charge collection. Furthermore the thickness of the depletion region is quite small so that only a

small volume of the crystal is sensible to radiation energy release. To increase the active volume a reverse bias is applied to the junction, negative on p side and positive on n side of the material, enhancing the potential difference between contact and consequently the detection volume.

The thickness of the depletion region is given by

$$d = \left(\frac{2\varepsilon V}{eN}\right)^{1/2} \tag{4.2}$$

where V is the reverse bias voltage, N the impurity concentration in the semiconductor, ε the dielectric constant and e the electronic charge.

Gamma-ray spectroscopy requires detectors with great active volume; the only way to further enhance the depletion region fixing the applied voltage is to reduce the impurity concentration N. High Purity Germanium detectors can be produced with impurity levels of 10^9 $atoms/cm^3$ by locally heating the bulk Germanium and passing a melted zone from one side to the other. The process is repeated many times and the crystals are then grown, if the remaining impurities are donor the detector will be an *n-type* [3].

coaxial geometry

The coaxial configuration consists in a long cylindrical crystal where one electrode is fabricated on the outer surface and the other one is provided removing the internal core and placing the contact on the inner surface. In order to ensure a radial field over the whole volume, the inner hole is extended near the front surface and the corners are rounded to eliminate low field regions. For an *n-type* HPGe the outer contact is made as p^+.

The p^+ contact, unlike the n^+ made by diffusion or evaporation, can be produced of only few tenth of a micrometer in thickness implanting boron ions in the crystal surface. Dead layer surface could attenuate the incoming radiation affecting the low energy gamma-ray detection efficiency. The detector in this configuration has a large active volume and a thin surface dead layer that allows the detection of a wide energy range spectrum, from X-rays of few keV up to gamma-rays of several MeV [3].

cooling system

HPGe detectors must be cooled at cryogenic temperature to operate (77 K); this cooling is mandatory to reduce the leakage current that otherwise could spoil the excellent energy resolution typical of such detectors.

Typically the cooling is provided using a dewar in which liquid nitrogen is kept in thermal contact with the detector through the cold finger. Because of the potential condensation of impurity gases on the detector surface it is mandatory to establish high vacuum condition in the cryostat in which the preamplifier and the FET are also generally placed[3]. An alternative to cryogenic liquids, that are quite expensive to maintain, is a mechanical cooling system.

The X-COOLER (fig. 4.3) provides a refrigerator auto-cleaning system during the circulation that traps contaminants through a filter. It is possible to insert the vacuum system in such apparatus.

Figure 4.3: X-COOLER

4.1 Initial configuration: HPGe Pop Top RB

The ORTEC *n-type* HPGe available on the market is a Pop Top Reduced Background configuration (fig. 4.4) that has the following features:

- Electronics and HV Filter placed in the EndCap.
- A Carbon Fiber vacuum structure surrounding the detector.
- Copper Holder, the structure that encloses the crystal.
- Vacuum provided with Molecular Sieve.
- Molecular Sieve, Electronics and HV Filter are placed under the Holder.

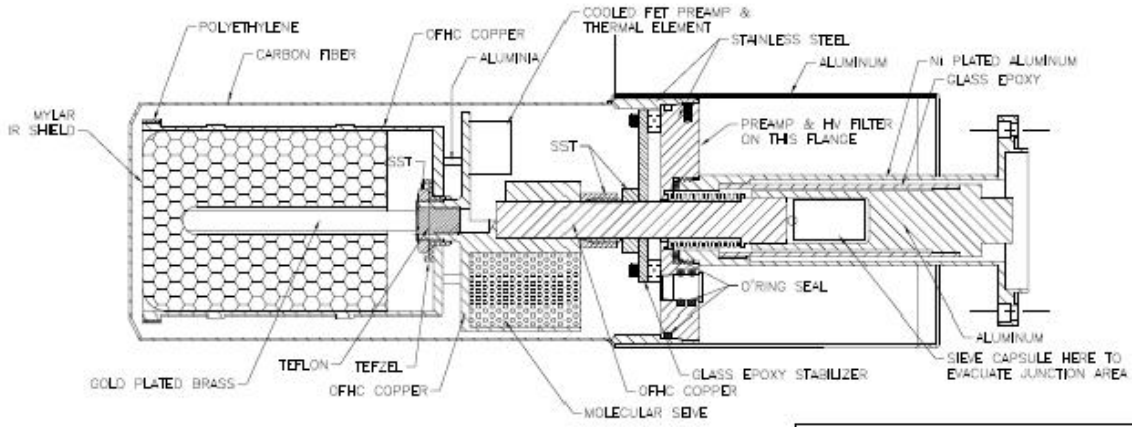

Figure 4.4: HPGe Reduced Background scheme

The manufacturer has provided a technical scheme of the detector in which building materials and their dimensions are completely described.

A scheme of the detector with the material placement is shown in figure 4.5.

1. Carbon Fiber (End Cap)
2. Mylar
3. Polyethylene
4. Gold plate Brass
5. Teflon
6. Tezfel
7. Alumina
8. Molecular Sieve
9. Electronics
10. Stainless Steel
11. Glass epoxy stabilizer
12. Aluminum
13. Copper
14. O-ring
15. Sieve capsule
16. Glass Epoxy

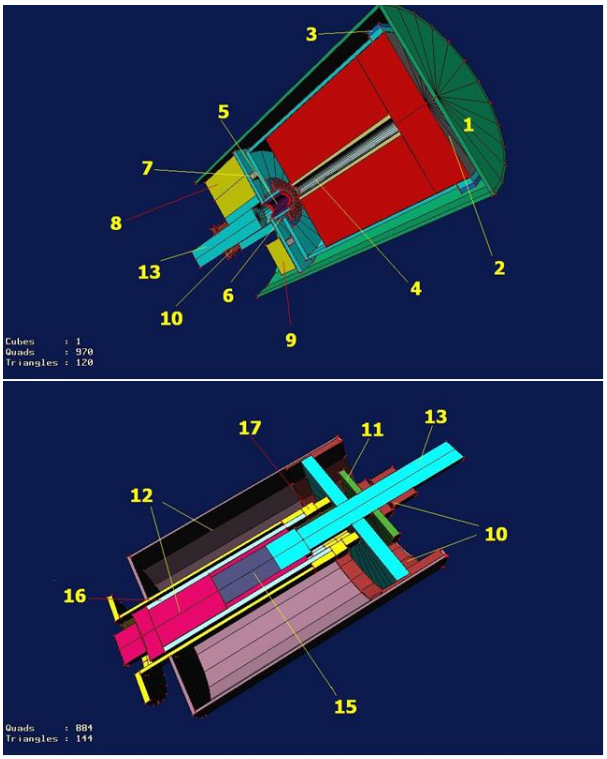

Figure 4.5: default

4.2 Materials selection measurements

Low level counting system are capable to distinguish low rate signals from the measurement background. The high sensitivity of this technique, using HPGe detectors, is achieved by different methods of background reduction, according to the spurious counts sources.

An essential feature of the system under study is a very low intrinsic background, this component is due to contaminations in building materials. Materials used for the detector construction should have a minimal intrinsic radioactive contamination, in particular those closer to the crystal active volume, in order to minimize the effects on the sample measurements.

Starting from the *n-type* Reduced Background HPGe configuration, it has been pos-

Material	^{40}**K** (Bq/kg)	^{232}**Th** (Bq/kg)	^{238}**U** (Bq/kg)
Molecular Sieve	7 ± 2	12.9 ± 0.2	13.9 ± 0.7
Glass Epoxy	56 ± 12	50.6 ± 0.3	23.2 ± 0.8
Electronics	3.4 ± 0.9	4.2 ± 0.1	3.5 ± 0.3
O-ring	< 1	$<$0.7	< 0.2
SST screws	< 0.1	< 0.7	< 0.15
HV-Filter	3.4 ± 0.9	4.2 ± 0.1	3.5 ± 0.3

Table 4.1: Radioactivity of materials composing the Reduced Background configuration measured at Radioactivity Laboratory of Milano-Bicocca.

sible to measure the intrinsic background of the detector through measurements of the materials provided by the manufacturer (ORTEC).

Samples of each building material have been measured at the Radioactivity Laboratory of Milano-Bicocca with Low and Reduced Background HPGe detectors placed in dedicated shieldings. Materials with an intrinsic high purity have been measured at LNGS (Laboratori Nazionali Gran Sasso) with HPGe detectors which can reach a better sensitivity thanks to the underground placement.

The analysis of the materials have been performed through gamma rays spectroscopy, analyzing the characteristic energy peaks associated with the considered radionuclide decay. The specific radioactivity has been evaluated in disintegration per unit of time and mass (Bq/kg) using the formula 3.1.

In order to obtain the configuration efficiency, each component has been simulated as source of radiation, using ^{40}K, ^{232}Th and ^{238}U chains as contaminants. The resulting spectra have then been analyzed to study the counting rate of background due to the measured contamination. Weighting each spectrum respect to the sample mass and contamination, it is possible to reach the overall background spectrum. Particular attention has been paid to contaminations in ^{232}Th, ^{238}U and ^{40}K because they mainly contribute to materials radioactivity. Contaminations of the measured materials are listed in tables 4.1 and 4.2; all the uncertainties are given with a 68% of confidence level.

Since the measured contaminations are particularly significant for some materials, in the following list are described the possible solutions:

Material	^{40}**K** (mBq/kg)	^{232}**Th** (mBq/kg)	^{238}**U** (mBq/kg)
Stainless Steel	< 15	< 2.8	< 100
Aluminum	< 78	$(1.3 \pm 0.1)\times10^3$	$(10 \pm 1)\times10^3$
Mylar	$(1.4 \pm 0.16)\times10^3$	< 26	< 115
Carbon Fiber	$(0.64 \pm 0.12)\times10^3$	25 ± 8	< 30
Gold-plated Brass	< 95	< 67	17 ± 5
Alumina	< 99	$(0.50 \pm 0.05)\times10^3$	$(3.0 \pm 0.4)\times10^3$
Copper	< 19	< 0.06	< 0.05

Table 4.2: Radioactivity of materials composing the Reduced Background configuration measured at LNGS.

- *Preamplifier and HV Filter* (tab. 4.1) have very high contamination values. It was mandatory to realize new ones with other materials. Moreover some components, not replaceable, could have an intrinsic radioactivity. Their presence could led to a new cryostat configuration.

- *Molecular Sieve* (tab. 4.1) is used for the vacuum creation, its high contaminations would led to a change in the cryostat configuration and a new mechanical system to make the vacuum.

- *Glass Epoxy* (tab. 4.1) should be replaced with another material.

- *Alumina* (tab. 4.2) is highly contaminated in all the primordial radionuclides; the solution is to use an alternative material or a more radiopure Alumina.

- *Aluminum* (tab. 4.2) particularly contaminated in ^{232}Th and ^{238}U, an alternative material should be considered.

- *Carbon Fiber* (tab. 4.2): the measured sample is composed of various pieces cut and put together on the HPGe detector with an overall mass of 0.0974 kg. Measuring time of 570425.64 s was needed to reach the required counting statistics although the low mass value. This material is used for the End Cap; since the detectors are *n-type* and therefore can detect low energy radiation, the measured contaminations of this material would affect the background.

- *Stainless Steel* (tab. 4.2): this cylinder shaped sample has a 76 mm diameter and 13 mm height with a mass of 0.4598 kg. The sample has been measured for 570389.9 s with the possibility to evaluate only limits of contamination. Since these limits are quite high the use of this material depends on its position in the cryostat.

Contamination in primordial radionuclides such as ^{232}Th and ^{238}U radioactive chains are the most insidious for materials used in rare events physics experiments. Isotopes of the decay chains can emit gamma rays cascade that can result in coincidence background counts between the two detectors depending on the position of the source material even though some materials show low radioactivity level. This background contribution should be considered since the system composed of two detectors is conceived to work in coincidence.

To evaluate the coincidence background due to building materials, all the simulations have also been performed in coincidence.

Low Background HPGe

Considering the total simulated intrinsic background and each contribution it has been necessary to replace some materials with less contaminated ones. According to position in the detector and compatibility, different alternative materials have been selected and measured. Simulations of the intrinsic background contribution due to their contaminations have been performed with the technique already described.

In particular the two following materials have been selected:

- *High Purity Aluminum* (tab. 4.3) sample shape is a disk with a diameter of 76 mm and 13 mm height. This is a quite radiopure material and the sample mass was only 0.1563 kg, thus a long measurement (1946468 s) was needed to reach a feasible counting statistics.

- *Monocrystalline Alumina* (Al_2O_3) (tab. 4.3) measured sample consists in 11 rings with a overall mass of 0.1119 kg. Its measurement lasted 254438.6 s.

Material	^{40}**K** (mBq/kg)	^{232}**Th** (mBq/kg)	^{238}**U** (mBq/kg)
High Purity Aluminum	< 37	< 5	< 2.4
Monocrystalline Alumina	42 ± 14	< 3	< 50

Table 4.3: Contaminations of alternative materials measured at LNGS.

After this analysis the following changes have been made:

- End Cap: in the Reduced Background configuration it was made of *Carbon Fiber*, but due to the important contamination of ^{40}K the chosen alternative material was *High Purity Aluminum*: *Cryal2. Aluminum* not only could be manufactured with low radioactivity level but has also a low atomic number needed to have a high transmission at low energies.

- *Alumina*: the one used by the constructor was too contaminated. Several samples of this material, produced by different factories were measured, and the one with the lowest contamination was selected (*High Purity Alumina* in table 4.3).

- *Glass Epoxy* was substituted with *Mylar*.

- *Copper*, the material of the Holder, the part of the cryostat closest to the crystal, was replaced with *High Purity Aluminum* due to its lower atomic number that allows a better low energies detection.

Since the components of the preamplifier and the HV Filter contribute critically to the background the only solution has been to place the electronics as far as possible from the crystal. Moreover it has been necessary to modify the cryostat structure because of the high contamination in the *Molecular Sieve* used to make the vacuum in the End Cap. The production company modified the cooling device so that it could also make the vacuum with a mechanical method.

4.3 Final Configuration: GMX 100-95 LB

The materials selection and the changes of the cryostat have brought to a new, improved configuration: both detectors have a Low Background configuration with the electronics outside the End Cap, a mechanical method for cooling, a dedicated system to make vacuum and a cryostat made of *High Purity Aluminum*. The mechanical cooling system is provided by using an X-COOLER for each detector; a configuration scheme is shown in figure 4.6.

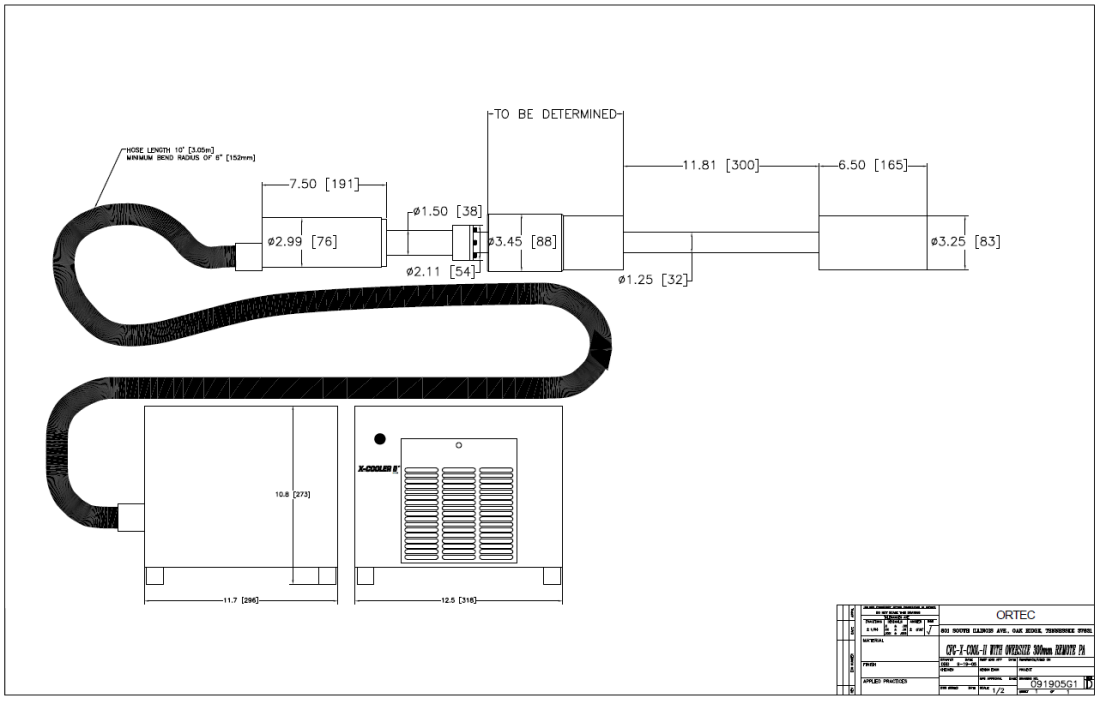

Figure 4.6: X-COOLER and GMX scheme

The system is composed of two *n-type* GMX 100-95 characterized by ~ 100% relative efficiency, 95 mm of End Cap diameter and a detected gamma rays spectrum from 3 keV to 10 MeV.

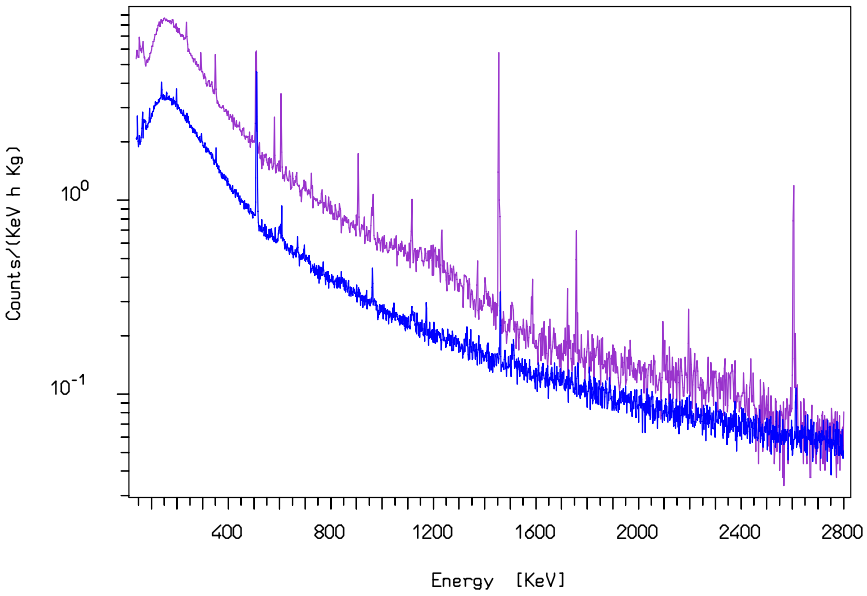

Figure 4.7: Background spectra of GMX, 100% relative efficiency, Low Background configuration (blue) shielded with 15 cm Copper and 20 cm of Lead and GMX, 45% relative efficiency, Reduced Background configuration (violet) with 5 cm of Copper and 20 cm of Lead as shielding

To evaluate the improvement due to materials selection it is possible to compare the intrinsic background spectra resulting from the contributions of the measured materials contaminations of the initial and the final detector configuration, weighted by the detector mass. In figure 4.7 the light blue spectrum corresponds to the final configuration, Low Background GMX, shielded with 15 cm of Copper and an external layer of 20 cm Lead. The violet spectrum is that of a Reduced Background GMX (45% of relative efficiency), shielded with 20 cm of Lead and 5 cm of Copper closer to the detector. This comparison shows a significant reduction over all the peaks counts belonging to the ^{232}Th and ^{238}U chains. The amplitude of ^{40}K 1460 keV peak and of the escape peaks are also lowered. Counts per hour comparison in the final (LB GMX) and initial (RB GMX) configuration are listed in table 4.4. The intrinsic background is therefore considerably suppressed with the materials selection that has been performed.

In this chapter I will name the two detectors with their code number: 2019 and 2200.

Parent isotope	**Energy (keV)**	**LB GMX counts/h**	**RB GMX counts/h**
^{232}Th chain	583	0.3 ± 0.1	3.8 ± 0.2
	2615	0.3 ± 0.1	6.6 ± 0.8
^{238}U chain	609	1.2 ± 0.2	7.0 ± 0.8
	1120	0.6 ± 0.2	1.9 ± 0.5
	1764	0.3 ± 0.1	2.3 ± 0.5
^{40}K	1460	1.2 ± 0.2	24±1

Table 4.4: Background count rates of the most intense γ lines in the detector final configuration spectrum (LB GMX) and in the initial one (RB GMX)

4.4 Optimization of the GMX parameters

The first study of the detectors performances has consisted in a series of characterization measurements concerning shaping time, active volume and efficiency.

The characterization measurements have been realized with a multi-γ source that has a certified activity (4.5) and contains isotopes emitting on the whole energy spectrum. The source is a little gel cylinder with density of 1 g/cm^3 put in a plastic vial and placed on the top of the detector.

4.4.1 Shaping Time

The signal to noise ratio of the detector is influenced by the shaping time parameter that, set at the optimum value, can minimize the electronic noise contribution to the

Isotope	Energy (keV)	Certified γ/s
^{241}Am	59.54	704
^{137}Cs	661.66	394
^{60}Co	1173.24	131
	1332.5	131

Table 4.5: Certified activities at the moment of the measurement.

energy resolution. For the characterization the shaping time has been varied from 4 μs to 24 μs measuring the multi-γ source with a Digital electronic chain DSPEC. Evaluating the Full Width at Half Maximum (FWHM) for each peak while varying the shaping time it has been possible to choose the optimum value of this parameter corresponding to the best energy resolution. The optimum value has been set at 6 μs.

4.4.2 Active Volume

The nominal high voltage certified by the manufacturer is -4900 V; in order to study the dependence of the depletion region on the HV, the latter has been varied from -4900 V to -100 V considering the counts under the peaks emitted by the multi-γ source.

From the figure 4.8 it is possible to perceive that the active volume corresponding to a region completely depleted is reached with a HV of -2000 V: in this condition the generated electric field is not enough to prevent the loss of charges due to recombination processes of the electron-hole pairs during the γ interaction. The -4900 V working voltage is set taking into account the energy resolution of the detector that, at this value, is maximized.

The measurements have been performed using the optimal shaping time.

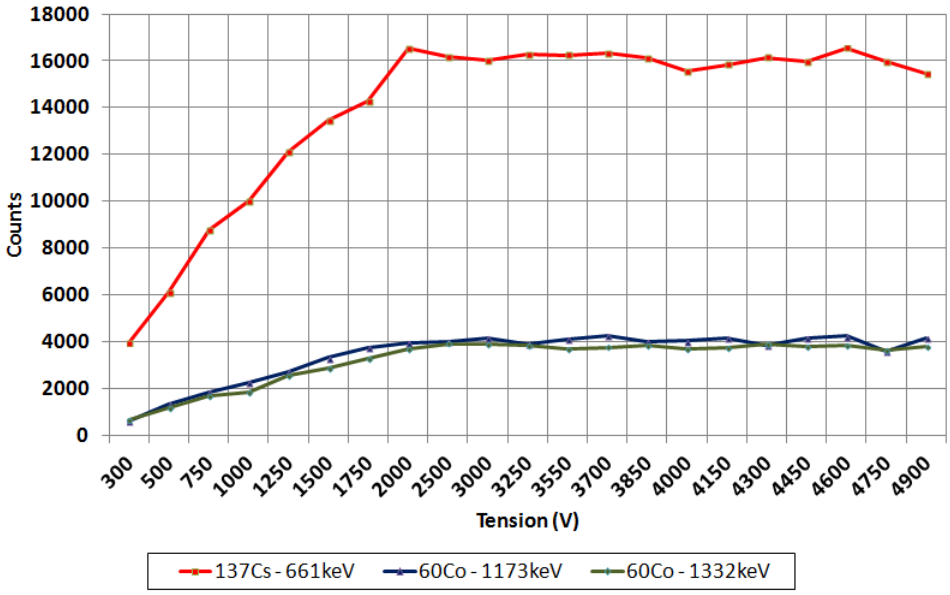

Figure 4.8: High Voltage in function of the measured counts

4.4.3 Efficiency

The efficiency characterization can be performed through the measurement of a source with known activity, considering the emitted γ per second for each peak and analyzing the count rates of the peaks present in the spectrum that correspond to the detected γ rates (fig. 4.9).

Placing the source in contact with the detector End Cap the efficiency for the γ-rays under study are shown in table 4.6.

Energy	Efficiency
59.54 keV	25.2%
661.6 keV	8.3%
1173.2 keV	4.2%
1332.5 keV	3.7%

Table 4.6: Measured efficiencies

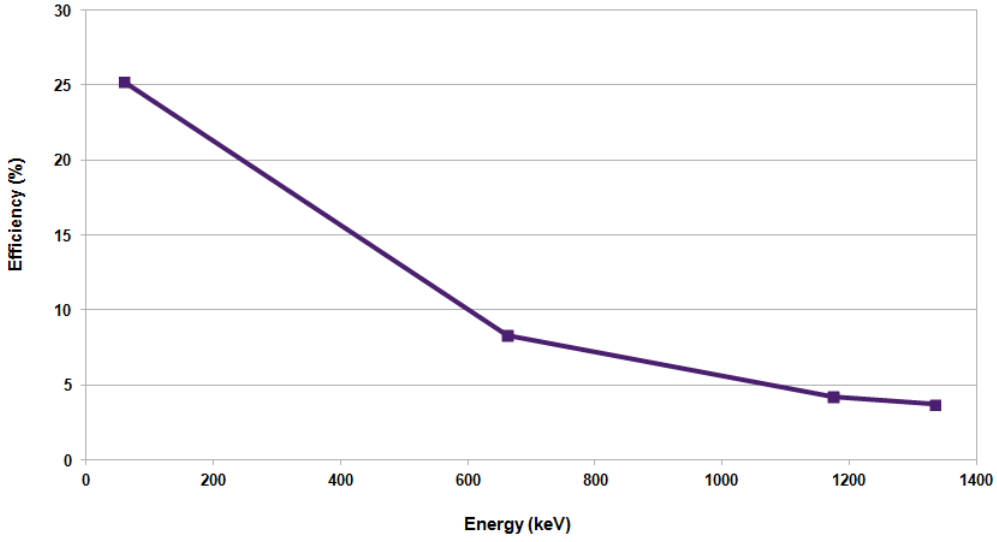

Figure 4.9: Efficiency in function of energy

4.5 Monte Carlo simulation optimization

Monte Carlo simulations are needed for each measurement since they allow the evaluation of the source-detector efficiency for different sample configurations. For this purpose the correct description of the materials and their densities as well as the thicknesses of the dead layers and the active volume is essential.

The used software, Arby, has a graphic interface to visualize the simulated configuration (fig. 4.10) and the particles trajectories.

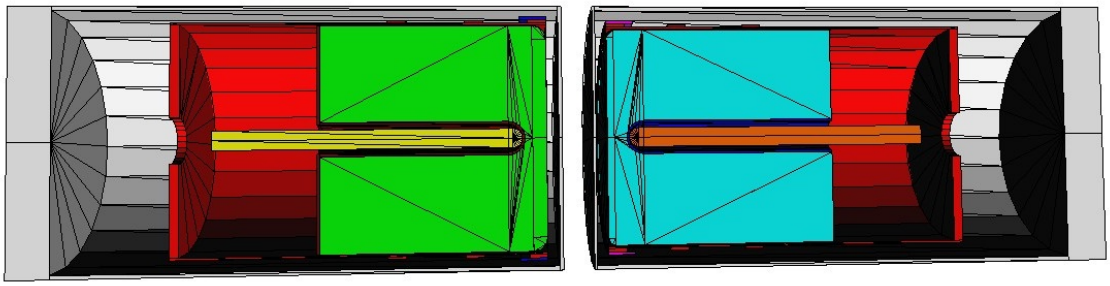

Figure 4.10: Image from MC simulation of the two developed detectors

The source contamination has been simulated using single radionuclide decay considering those contained in the calibrated source used to perform the efficiency calibration: ^{241}Am, ^{137}Cs and ^{60}Co.

The absolute efficiency of a detector is defined as the ratio between the number of detected events and the events emitted by the source; this parameter takes into account

the geometry of the system in particular the source-detector distance, density and thickness of the materials. Starting from the nominal values of the scheme (fig. 4.11), the configuration can be described in the input file containing all the source and detector crucial parameters. Simulated and experimental results are then compared and the discrepancies can be adjusted modifying some of the sensitive parameters in the input file. Efficiency overestimation, for example, can be adjusted by increasing the dead layer thickness, the sample density or the source-detector distance depending on the known information about the experimental configuration.

To verify the simulated results, comparisons using different sources and configurations are suggested. The final discrepancy gives the systematical error of the process.

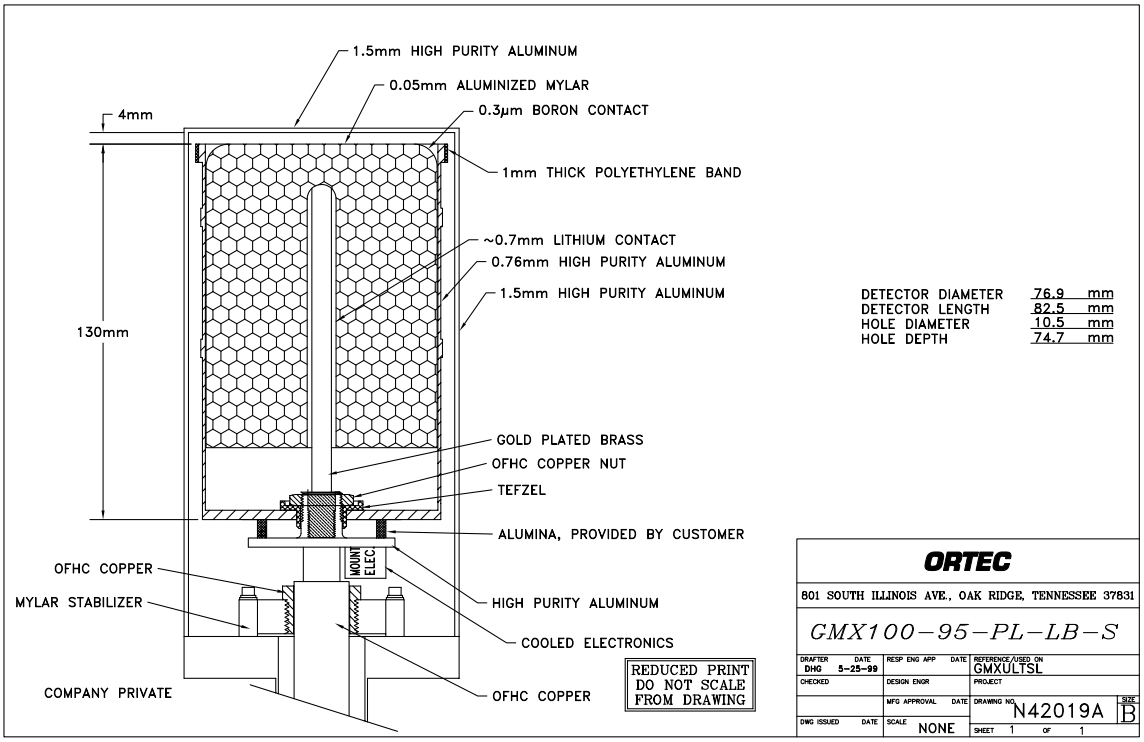

Figure 4.11: GMX HPGe scheme

For the characterization a multi-γ source is commonly used, in order to have a wide spectrum efficiency screening. These measurements have been performed with the same source used for the optimization of the shaping time and the active volume.

Since the GMX detectors are placed on a horizontal axis facing each other, it has been possible to perform measurements at different distances; I have chosen a relative distance among the detectors of 10 cm and 20 cm and for both simulations and measurements have been performed.

The efficiency characterization of the 2019 GMX led to a relative error less than 16%, the optimization results are shown in figure 4.12 and table 4.7.

Isotope	*Energy (keV)*	*B.R. (%)*	*Meas. Eff. (%)*	*Sim. Eff. (%)*	*Err. (%)*
			Distance: 10 cm		
^{241}Am	59.54	35.8	7.111	5.99	-15.76
^{137}Cs	661.66	85.1	2.254	1.947	-13.62
^{60}Co	1173.24	99.99	1.428	1.329	-6.95
	1332.5	100	1.301	1.207	-7.22
			Distance: 20 cm		
^{241}Am	59.54	35.8	2.404	2.210	-8.05
^{137}Cs	661.66	85.1	0.842	0.779	-7.52
^{60}Co	1173.24	99.99	0.568	0.544	-4.22
	1332.5	100	0.525	0.527	0.47

Table 4.7: Simulated and measured efficiencies of the detector 2019.

The same analysis for the 2200 GMX results in a relative error less then 11%. With this value it is possible to evaluate the similarity of the simulated and measured efficiencies; it is used as systematic error associated to simulations. The graphical comparison of efficiency for the 2200 GMX is shown in figure 4.13 and the values in table 4.8.

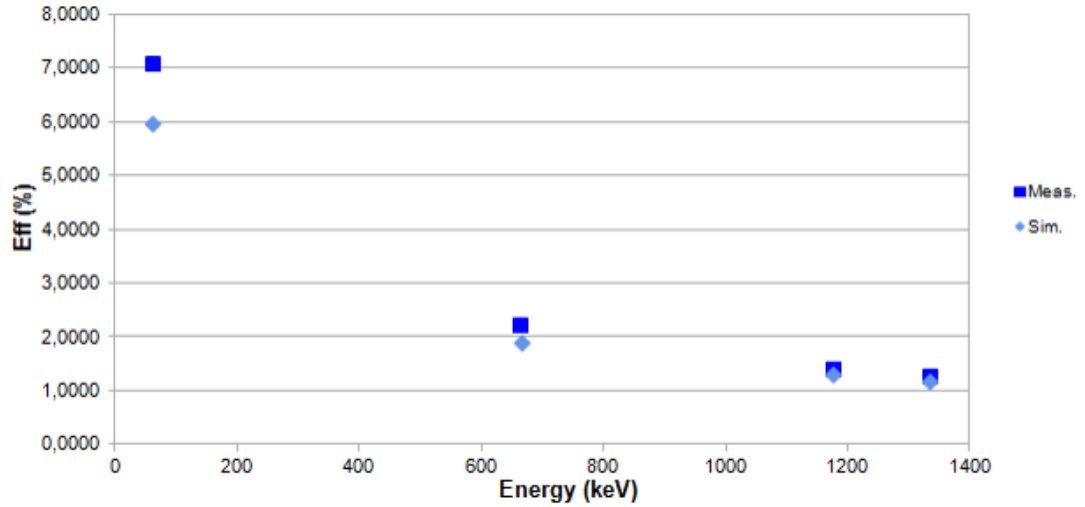

(a) 10 cm distance

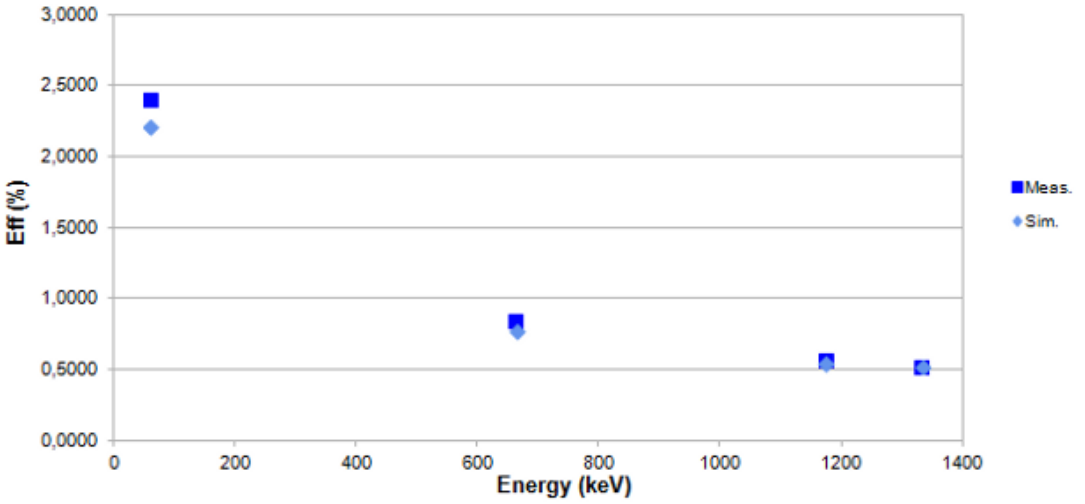

(b) 20 cm distance

Figure 4.12: Comparison between simulated (light blue) and experimental (blue) efficiencies for the detector 2019

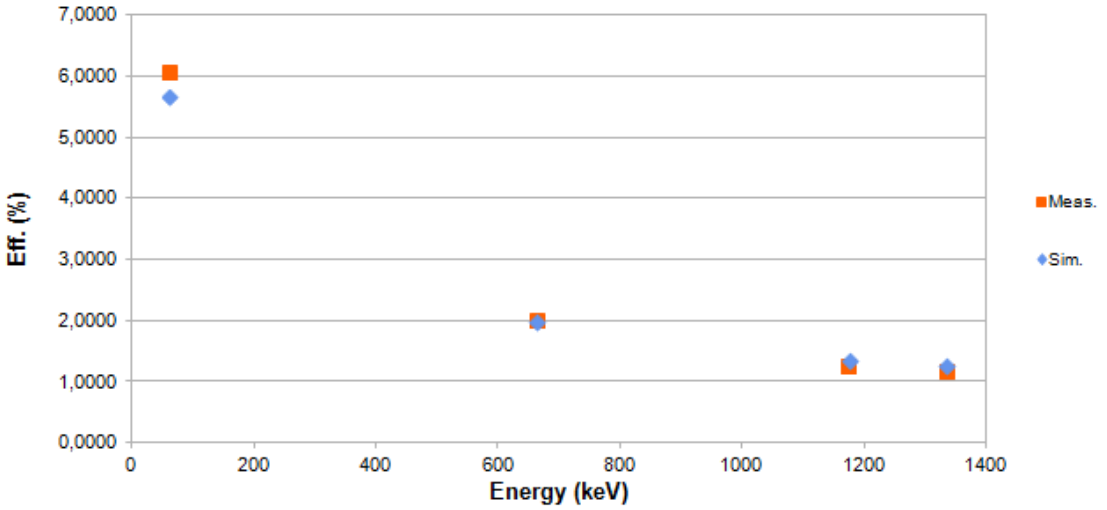

(a) 10 cm distance

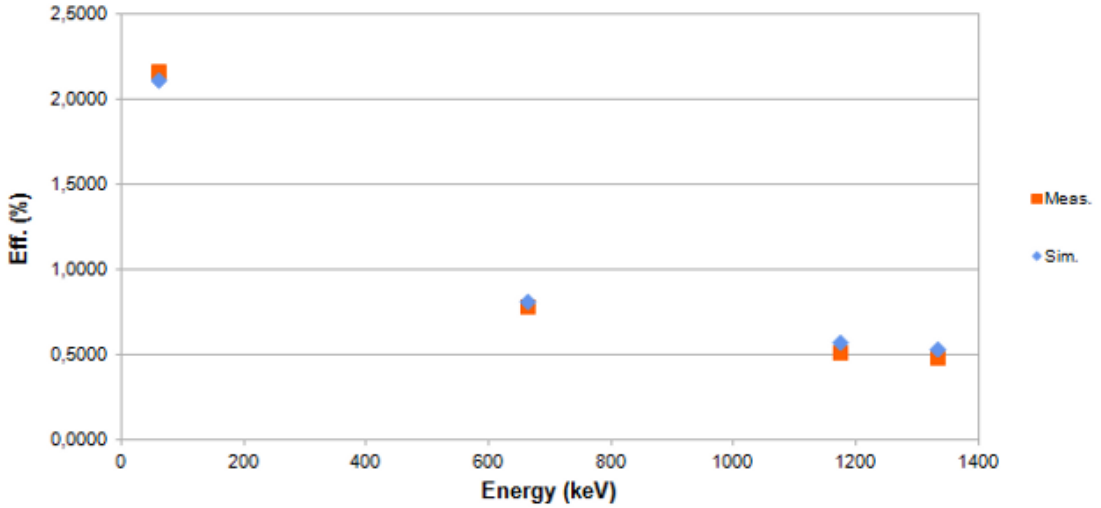

(b) 20 cm distance

Figure 4.13: Comparison between simulated (light blue) and experimental (orange) efficiencies of detector 2200

Isotope	*Energy (keV)*	*B.R. (%)*	*Meas. Eff. (%)*	*Sim. Eff. (%)*	*Err. (%)*
			Distance: 10 cm		
^{241}Am	59.54	35.8	6.074	5.671	6.64
^{137}Cs	661.66	85.1	2.001	2.007	0.16
^{60}Co	1173.24	99.99	1.259	1.366	-8.55
	1332.5	100	1.165	1.273	-9.23
			Distance: 20 cm		
^{241}Am	59.54	35.8	2.173	2.115	-2.68
^{137}Cs	661.66	85.1	0.789	0.821	4.09
^{60}Co	1173.24	99.99	0.528	0.575	8.95
	1332.5	100	0.489	0.541	10.61

Table 4.8: Simulated and measured efficiencies of the detector 2200.

4.6 Shielding

To improve the performances of the measuring system it is essential a dedicated shielding. The GMX detectors are placed in the Radioactivity Laboratory of Milano-Bicocca in the basement of the Physics department building with a shielding composed of an external 20 cm thick layer of (low activity) Lead and a 15 cm thick layer of OFHC Copper closer to the detectors (fig. 4.14). Before the construction all the Lead and Copper bricks have been cleaned in ultrasonic bath using Radiac Wash, a soap with EDTA (Ethylenediaminetetraacetic acid) at 5%, in bi-distilled water.

The electronic part has been distanced from the crystal since some components have a non negligible contaminations, particularly in ^{232}Th. To further shield the active volume from the emitted radiation two cylinders of Roman Lead, one for each HPGe, have been placed covering the whole distance between the End Cap and the electronics. The Roman Lead dates back to about 70 A.C. [21] then the isotope ^{210}Pb that contributes most to the background radiation, with a half life of about 22.3 years, is already decayed.

Both the detectors are inserted in the shielding and can move along a horizontal axis in order to put, between them, samples of different thicknesses.

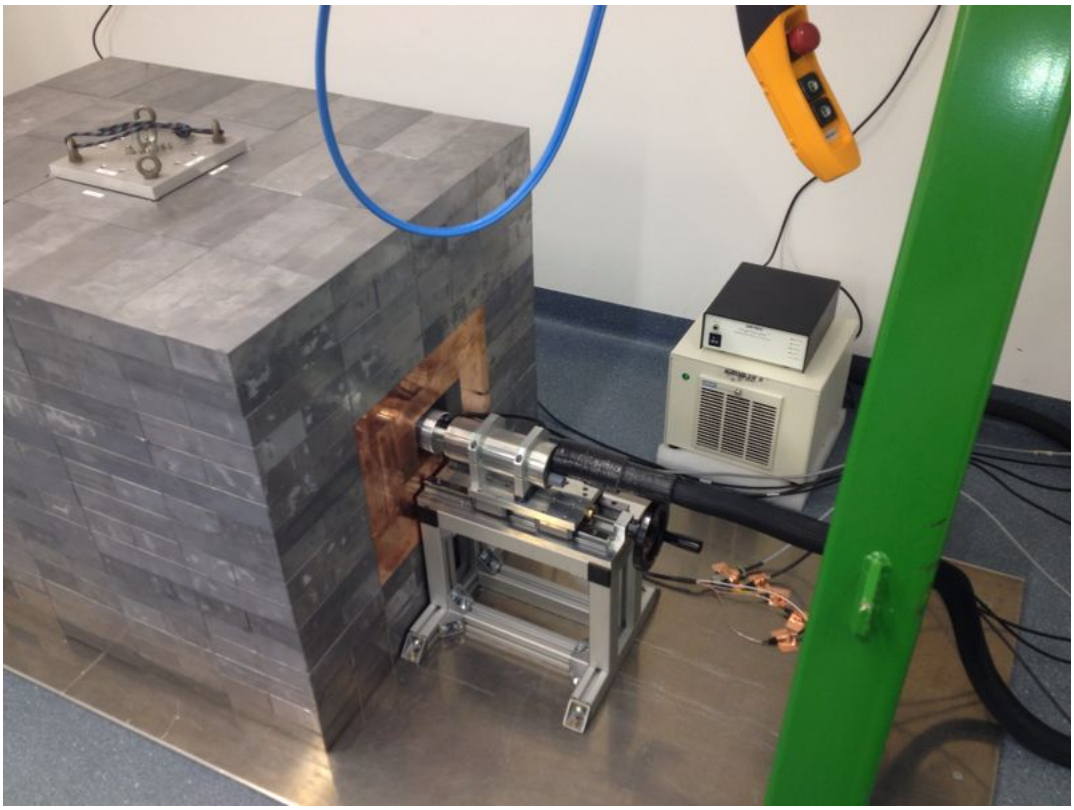

Figure 4.14: Lead and Copper shielding

The shielding is completely closed; a cork has been realized from the center top part corresponding to the space between the detectors. The cork should be lifted to place samples or sources, this is done with a semiautomatic winch moving along a crane whose structure surrounds the whole system as seen in figure 4.15.

The coverage of the Radioactivity Laboratory consists of six floors with walls made of reinforced concrete particularly free of contaminations. The overall coverage has been evaluated detecting the muon flux reduction and estimated to be about 15 m.w.e..

Figure 4.15: Lead shielding and the winch-crane system

4.7 Background analysis

The first important analysis has been the evaluation of the detectors background. These measurements need long time to improve the counting statistic on the various possible peaks.

The background counts per day over the whole spectrum (30-3300 keV) weighted for the detector mass are 75 counts/day/kg.

The two detectors background spectra have been registered simultaneously and compared to verify their similarity. The two GMX have the same features and their signals are processed with the same parameters: gain, shaping time and HV value. They differ in relative efficiency, 103 % the 2200 and 97% the 2019, and it is possible to see from the spectra comparison (fig. 4.16) that they have slightly different energy resolution.

From these spectra analysis it is possible to infer that the background is composed of four main sources: ^{232}Th decay chain, ^{238}U decay series, ^{40}K and induced neutron

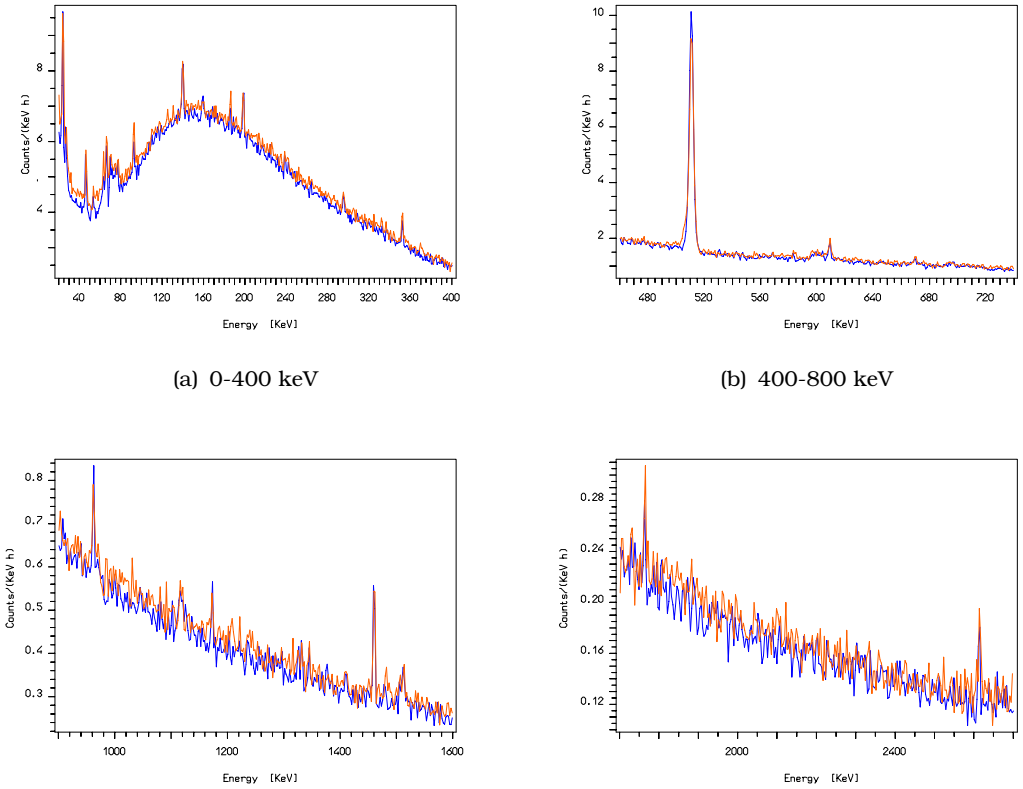

(a) 0-400 keV

(b) 400-800 keV

(c) 920-1800 keV

(d) 2000-2800 keV

Figure 4.16: Background GMX 2019 (blue) and GMX 2200 (orange) spectra comparison

background.

The energy resolution of GMX 2200 is worse than that of GMX 2019 and for this reason some peaks are not visible in its background spectrum.

In table 4.9 the counts per hour under the peaks of the ^{232}Th decay chain present in both background spectra are listed. These peaks are related to the most intense γ-lines of the chain.

The contamination of ^{238}U is more evident for both detectors. Most of the isotopes are from the last part of the decay chain therefore part of their presence could be attributed to contamination in ^{222}Rn. In table 4.10 the counts per hour related to ^{238}U chain isotopes for GMX 2019 and GMX 2200 are listed.

^{232}Th decay chain			2019		2200	
Reaction	γ energy (keV)	B.R. (%)	counts/h	err	counts/h	err
^{212}Pb $\rightarrow$ ^{212}Bi	238.6	43.3	0.87	0.18	0.42	0.26
^{208}Tl $\rightarrow$ ^{208}Pb	583.2	84.5	0.39	0.14	0.32	0.11
	860.6	12.4	0.18	0.10		
	2614.5	99.2	0.39	0.10	0.33	0.10

Table 4.9: Background counts/h of ^{232}Th decay chain isotopes

^{238}U decay chain			2019		2200	
Reaction	γ energy (keV)	B.R. (%)	counts/h	err	counts/h	err
^{234}Th $\rightarrow$ ^{234}Pa	63.3	4.8	1.41	0.24	1.38	0.19
	92.6	5.16	1.39	0.35	1.93	0.34
^{214}Pb $\rightarrow$ ^{214}Bi	241.98	7.4	0.58	0.16	0.58	0.16
	295.2	19.3	0.89	0.19	0.87	0.29
	351.9	37.6	1.13	0.20	1.55	0.29
^{214}Bi $\rightarrow$ ^{214}Po	609.3	46.1	1.16	0.16	1.28	0.19
	1120.4	15.1	0.25	0.10	0.25	0.11
	1238.8	5.79	0.34	0.19	0.15	0.07
	1377.6	4	0.19	0.08		
	1764.5	15.4	0.33	0.13	0.30	0.10
^{210}Pb $\rightarrow$ ^{210}Bi	46.5	3.65	2.1	0.2	2.33	0.32

Table 4.10: Background counts/h of ^{238}U decay chain isotopes

The most significant source of background is probably the neutron induced background. This background is originated by fast and thermalized neutrons from cosmic origin and from those produced in the cosmic rays interaction with Lead in the shielding. The interaction can be divided in two species: the radiative capture, (n,γ), when the neutron is captured by a nucleus producing an isotope in an excited state that consequently emits photons, and the inelastic scattering, (n,n'), where the nucleus on which the neutron interacts is left in an excited state and it will de-excite emitting γ-rays.

The energy peaks rates caused by neutron interactions with the Germanium isotopes in the crystal are shown in table 4.11 for both GMX.

Germanium		**2019**		**2200**	
Reaction	γ energy (keV)	counts/h	err	counts/h	err
^{70}Ge(n,γ)^{71m2}Ge	198.4	2.17	0.34	1.9	0.3
^{72}Ge(n,γ)^{73m}Ge	53.4	0.51	0.13	0.64	0.16
	66.7	3.74	0.38	2.32	0.25
^{74}Ge(n,γ)^{75m}Ge	139.7	2.84	0.34	3.04	0.41
^{76}Ge(n,γ)^{77m}Ge	159.7	1.1	0.2		

Table 4.11: Counts due to neutron induced background: interactions with Germanium

In addiction to the interaction with the Germanium crystal, neutrons can interact with the inner Copper shielding layer. The Copper nuclei emit γ radiation through the same processes of the Germanium nuclei. The energies that constitute the background due to these interactions and their count rates in the corresponding spectra are listed in table 4.12.

The background induced by the ^{40}K contamination is always present since it is a widespread natural radioactive isotope. It decays on ^{40}Ar, emitting an intense γ with an energy of 1460 keV; since it is a primordial radionuclide its half-life is very long.

Counts per hour under the peak corresponding to the γ transition energy are shown in table 4.13.

Copper		**2019**		**2200**	
Reaction	γ energy (keV)	counts/h	err	counts/h	err
^{65}Cu(n,γ)^{66}Cu	185.91	0.80	0.20	1.27	0.25
^{65}Cu(n,n')^{65}Cu	1115.5	0.36	0.11	0.34	0.13
^{63}Cu(n,n')^{63}Cu	669.6	0.49	0.13	0.52	0.17
	962.1	0.80	0.17	0.73	0.16
	1327.0	0.20	0.07		
^{63}Cu(n,α)^{60}Co	1173.2	0.49	0.13	0.34	0.14
	1332.5	0.28	0.08	0.11	0.05

Table 4.12: Counts due to neutron induced background: interactions with Copper

^{40}K			**2019**		**2200**	
Reaction	γ energy (keV)	B.R. (%)	counts/h	err	counts/h	err
^{40}K $\rightarrow$ ^{40}Ar	1460.8	99.16	1.14	0.14	1.20	0.15

Table 4.13: ^{40}K counts per hour in Background spectrum

4.7.1 Background Comparison

To reach a low intrinsic background the two GMX detectors have been realized with selected radiopure materials, the electronics component, placed far away from the crystal, has been shielded with Roman Lead. The spectrometer is inserted in a dedicated shielding composed of 15 cm of Copper closer to the detectors and a 20 cm external layer of Lead. The development of this system can be understood comparing the background spectra of one GMX with a standard coaxial HPGe. In figure 4.17 the spectrum of the GMX 2019 (blue) can be compared with that of a coaxial HPGe, with 30% of relative efficiency, shielded with 10 cm of Copper and the same thickness of Lead; each spectrum is weighted by the detector mass.

Some γ lines rates analyzed in these background spectra are listed in table 4.14.

Parent isotope	**Energy (keV)**	**GMX counts/h**	**HPGe (std) counts/h**
^{232}Th chain	2615	0.3 ± 0.1	3.5 ± 0.3
^{238}U chain	1764	0.3 ± 0.1	1.2 ± 0.4
^{40}K	1460	1.2 ± 0.2	8.4 ± 0.4

Table 4.14: Background count rates of the most intense γ lines in GMX detector spectrum and in a standard coaxial HPGe spectrum

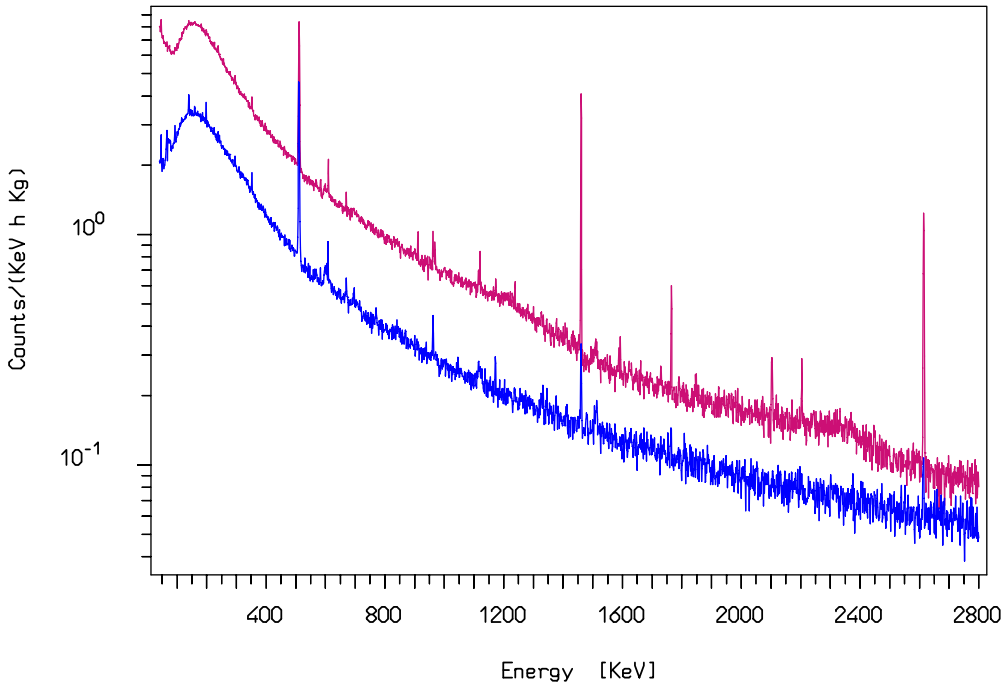

Figure 4.17: Background spectrum of GMX (blue) with 2 kg of active volume shielded by 15 cm of Copper and 20 cm of Lead and of a coaxial HPGe (pink), 30% relative efficiency, with 0.815 kg of active volume shielded with 10 cm of Copper and 10 cm of Lead

Chapter 5

Coincidence Analysis and Data Acquisition Optimization

The system composed of two High Purity Germanium, GMX, detectors has been conceived to work in coincidence. This measurement technique is a background reduction method that allows to select only signals from a particular radionuclide which features a decay with γ-rays cascade.

One possible application of the measurement system is the material selection for rare event physics experiments, whose sensitivity is affected by the background counting rate. The other parameters on which the sensitivity depends, are characteristic of the detector and of the source under study. Although each parameter is optimized, the background is the most crucial. The selection of high radiopurity materials is mandatory to reach an intrinsic radioactive background as low as possible. The main contamination in materials originates from primordial radionuclides as ^{232}Th, ^{238}U and ^{40}K. Some isotopes from the decay series emit multiple γ-rays.

During this work I have focused on the possible coincidences between them, studying the isotopes decay schemes. In particular I have deeply studied the ^{208}Tl of the ^{232}Th chain that features γ-rays emission with high Branching Ratios following a β^- decay.

A dedicated data acquisition and analysis software have been required to perform both single detector and coincidence spectra analyzing the registered signals and selecting the coincidences off-line.

The HPGe detectors have separated, but identical, electronic lines: a high voltage supply and an amplifier.

5.1 DAQ

A high resolution digitizer NI PXI-5122 produced by National Instrument has been chosen for the data acquisition. This high speed digitizer features [12]:

- two channels simultaneously sampled at 14-bit resolution
- 100 *MHz* bandwidth
- up to 512 MB of memory per channel
- 200 mV to 20 V input range
- from 12.2 μV to 1.22 mV sensitivity

The simultaneous sampling and the possibility to use an external trigger make this digitizer suitable for the coincidence analysis.

The NI PXI-5122 has been programmed with LabVIEW framework software. Information about the registered signals and the setting parameters are saved on file to allow the off-line coincidence analysis. The signal waveforms, on both channels, are saved simultaneously with 128 samples per record. For each acquired waveform, the starting time of the event is also recorded. The acquisition time window and the pre-trigger parameters are chosen considering the shaping time and the sampling frequency. Those parameters are important to completely record the waveform.

To register both coincidence and single detector spectra an external trigger has been used. The signals from both detectors preamplifier are summed and amplified to perform a logical OR: if the output signal exceeds a selected threshold, the corresponding logic signal is used as trigger in the digitizer. The trigger is therefore fired whenever a pulse is registered on one or both detectors avoiding coincidences between noise signals. This method not only allows the registration of coincidences but also that of single detector spectrum without most of the noise signals.

The DAQ has a graphic interface showing the acquired spectra and signals, an example of coincidence signals is illustrated in figure 5.1

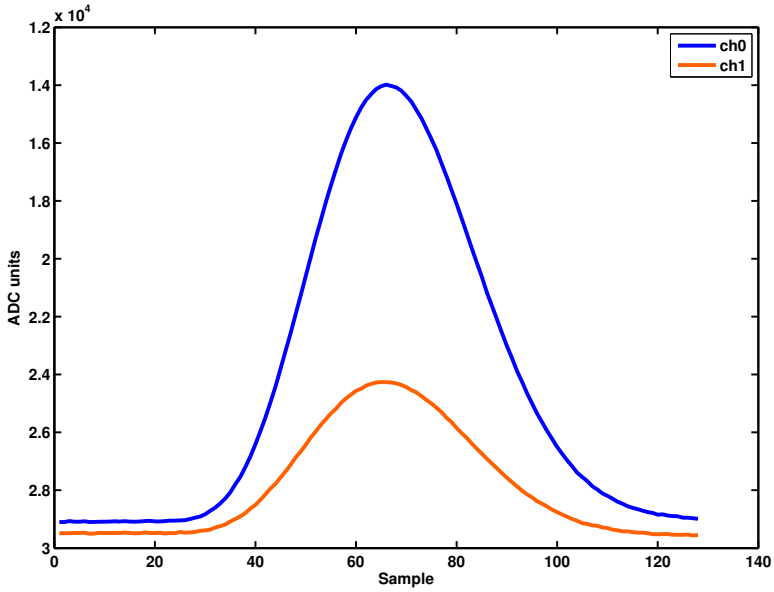

Figure 5.1: Two signals simultaneously acquired

The software produces a binary output file in which the events are inserted in temporal sequence. Each event is described by a collection of informations subdivided in 8 groups, 4 for each channel:

1. a control string of 8 character that indicates a triggered signal on channel 0
2. a short integer (16 bit) containing the number 0 that refers to the first channel
3. a 32 bit unsigned int corresponding to the event registered time in tenth of ms
4. a vector of 128 short integer for the sampled waveform values in ADC units.
5. 8 char for the signal on channel 1
6. a short int containing the number 1 that refers to the second channel
7. a 32 bit unsigned int corresponding to the event registered time in tenth of ms
8. a 16 bit short int vector for the 128 sampled amplitudes.

Signals are always acquired and thus written on file in couple: the first part corresponds to the event on the channel 0 and the second part of that detected on channel 1. The registered time is the same for both because it depends on the common trigger. The measurement output file thus consists in an alternate sequence of channel 0 and channel 1 waveforms, coupled two by two since they are always simultaneously acquired. For every file containing the acquired data, an appropriate header file is created; on this the initial and final date of measurements, the acquisition sampling and time window parameters and the number of channels are saved.

The system electronics and acquisition scheme is shown in figure5.2.

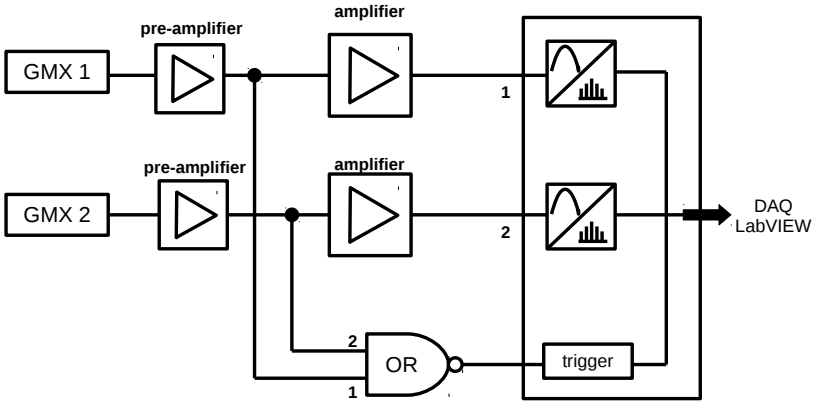

Figure 5.2: Electronics scheme

5.2 Analysis

Because of the peculiarity of the conceived data taking, after some difficulties with an analysis software already used for other detectors, I have developed a dedicated one using MATLAB framework from MathWorks®. Both measured and simulated data should be analyzed, despite the differences in the output files, using the same procedure.

5.2.1 Measurements

The DAQ output file is read considering the 4 binary groups that correspond to a signal registered on one channel. The first step is to simply evaluate each signal amplitude described by the 128 short int. The amplitude of each pulse is calculated as the difference between the maximum and the minimum of the sampled waveform. The pulses are fitted with a spline function, its maximum represents that of the signal, while the mean value of the baseline, calculated on the pre-trigger, identifies the pulse minimum.

The maximum minus minimum amplitudes are saved on file in the same registered sequence so that pulses are coupled in sequence of two to consider the coincidences. Channels pulses can be distinguished according to their position in the file that starts with a channel 0 signal.

I have developed a MATLAB routine to create the detectors spectra from the registered pulses with the possibility of a graphical tool to display and analyze them interactively.

The energy calibration is needed to identify the peaks in the spectrum or the energy region under study; the calibration curve can be evaluated analyzing the spectrum of a known source.

The area under each peak is evaluated by integral counts with the subtraction of a linear background; the software offers the possibility to choose the interval limits of the energy region under the peak and of the background area.

To perform the analysis of a single channel spectrum the pulses can be separated according to their position in the file, which indicates the channel. This analysis is generally used to evaluate the efficiency of the detector for a calibrated source measurement and it is needed to consider the energy resolution. This parameter is particularly important when no full energy peaks are present in the coincidence spectrum and it is used to

perform the integral in the exact energy range of the peaks.

Coincidence analysis can be performed as “peak-peak” or “peak-spectrum” coincidence. “Peak-peak” coincidence consists in selecting a full energy peak on both detectors corresponding to two γ energies emitted in coincidence. The energy range could be set at 2 or 3 σ depending on the desired confidence level. The selection is performed considering consequent signal in the file with amplitudes included in the energy range under study.

“Peak-spectrum” coincidence is performed selecting a full energy peak on one detector and the corresponding spectrum, without energy selection, on the other. In this case the energy selection is performed only on one channel while the coincidence spectrum is composed of all the pulses registered simultaneously to the selected signals. This analysis can give information not only about peaks registered in coincidence but also on the continuum.

5.2.2 Simulations

Efficiencies for each detectors-source configurations are evaluated using Monte Carlo simulations as described in the previous chapter. In order to compare the measured and simulated spectra I have developed a software capable to perform the previous operations also on the simulated spectra. Also for this analysis the software has a graphic display and counts under energy peaks are considered as integral counts with a linear background subtraction.

It is thus possible to analyze a single detector simulated spectrum to evaluate its efficiency for the energy peaks under study. The coincidence spectrum is realized through the energy selection in the simulation output file in which coincidences are represented by the same number of event. This analysis is necessary for the coincidence efficiency evaluation.

The “continuum” study is an important aspect of measurements, to completely understand it, simulations should reproduce perfectly its shape. To compare the measured and simulated shape I have realized a specific graphic software.

All the operations can be performed on both channels, coincidence measurements in fact feature the possibility to combine both detectors results increasing the detection efficiency of the system.

Comparison between simulated and measured efficiencies with the MATLAB software has led to a relative error less than 15%; this result should be considered as the systematic error associated with simulations.

5.3 Assessment

The analysis method has been tested performing a set of measurements with ^{232}Th sources with different known activities. Each source consists in 0.8 mL of water solution with HNO_3 at 5% in volume placed in polyethylene vials. The measured sources, with decreasing ^{232}Th concentrations, have a specific activity of about: 0.4 Bq/g, 40 mBq/g and 4 mBq/g. These values correspond to integral activities of 0.32 Bq, 32 mBq and 3.2 mBq respectively.

These sources has been chosen since in material selection the evaluation of ^{232}Th concentration in sample materials is mandatory. ^{232}Th is one of the primordial radionuclides that contributes most to the radioactive background. Furthermore some of its daughters radionuclides decay emitting many γ in coincidence.

An interesting decay of the series is that of ^{208}Tl on ^{208}Pb, this β^- decay has a chain B.R., respect to the chain progenitor, of about 36% and it is followed by different γ-rays cascades; the decay scheme is shown in fig 5.3.

The evaluation of the possible γ coincidences depends on the emission probability of the whole decay process. This value is a combination of the B.R. of the β^- decay and of the γ-rays emitted from the corresponding level. The energies and the relative intensities, respect to the parent β^- decay, are listed in table 5.1. B.R. are generally given as intensities per 100 disintegrations of the parent nucleus, for the considered γ-rays.

The study of this particular decay led to two leading energy selections and their respective coincidences:

- 583.19 keV selection has 277.37 keV, 510.77 keV and 2614.53 keV as coincidences
- 2614.53 keV is in coincidence with most of the considered γ energies

The “peak-peak” coincidence can be considered selecting the two energies under study from the registered spectra, but the analysis of the energy peaks in the whole coincidence spectrum is also possible.

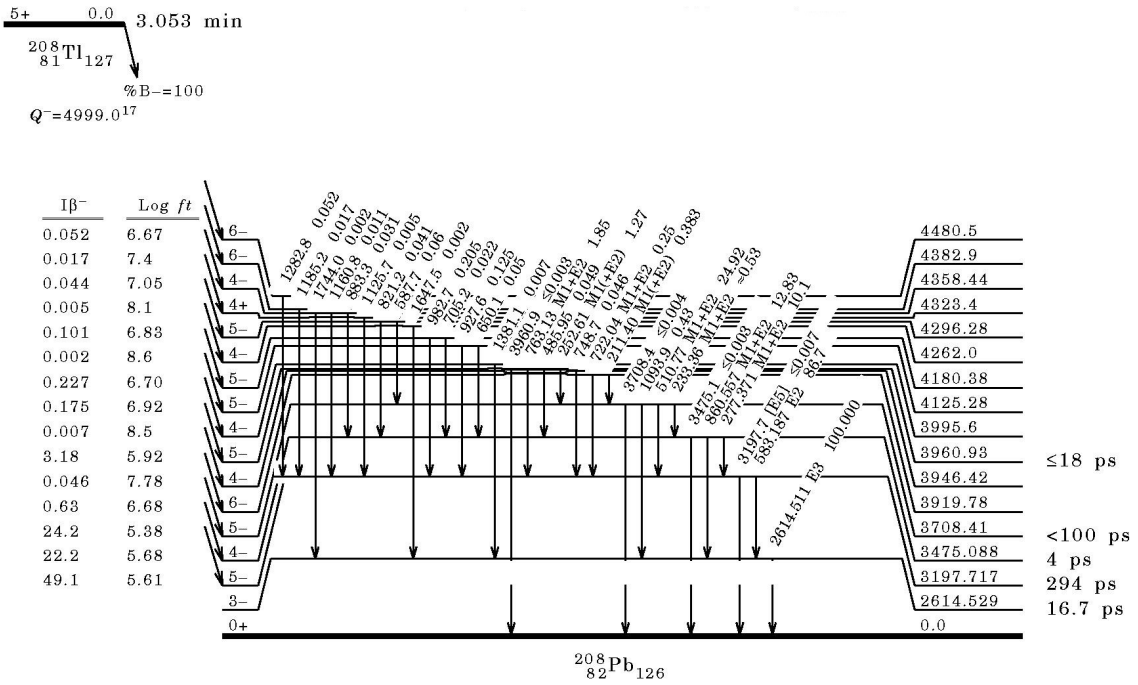

Figure 5.3: ^{208}Tl β^- decay scheme

Level Energy (keV)	**γ Energy (keV)**	**Intensity, B.R. (%)**
3475.09	277.37	6.6
	860.56	12.5
3708.41	510.77	22.6
3197.72	583.19	85.0
2614.53	2614.51	99.8

Table 5.1: Some γ-rays parameters following the ^{208}Tl decay

The complexity of HPGe detector spectrum originates from the peculiar continuum and the secondary peaks. Exploiting the counts under peaks corresponding to energies sum, single and double escape, the coincidence efficiency can be significantly enhanced. Since the processes producing these peaks are more probable for high energies interactions, particular attention should be paid on the 2614.5 keV γ. The sum of different energies is

more probable for this photon since it is in coincidence with all the others.

Considering these aspects I have decided to study coincidences with the selection of the 583 keV photon.

Selections are made on both detectors leading to a final result that is a combination of the two analysis.

The activity of the sources has been evaluated for each calibration measurement through the analysis of single and coincidence spectra. A background measurement, of 286.5 hours, in the same configuration has been acquired; the counts under each analyzed peak in the background spectrum have been subtracted from the source spectrum. For simplicity the detectors are defined as channels: *ch0* and *ch1*.

0.32 Bq

This measurement has lasted about 74.654 hours, the analysis has been performed for coincidence and single detector spectra on both channels.

For the single channel analysis γ-rays with the most considerable B.R. has been contemplated; efficiencies ε have been evaluated by simulations. In order to calculate the source activity, counts under the full-energy peaks in source and background measurements have been considered using the formula 3.1.

In figure 5.4 the comparisons between the source and background spectra for both detectors are shown. Counts due to ^{232}Th source clearly exceed the background; the activity has been evaluated for each ^{208}Tl peak; results are shown in table 5.2. The errors have been calculated through their two main contributions: the counting statistics and the systematic due to simulations.

Since for these spectra different peaks have been analyzed, the activity can be evaluated through the weighted mean of the activities obtained for each single peak with the corresponding error. In table 5.3 the results for both detectors are listed.

It is possible to combine the single detector results considering the entire spectrometer; with this method the detected activity is 0.34 ± 0.02 Bq.

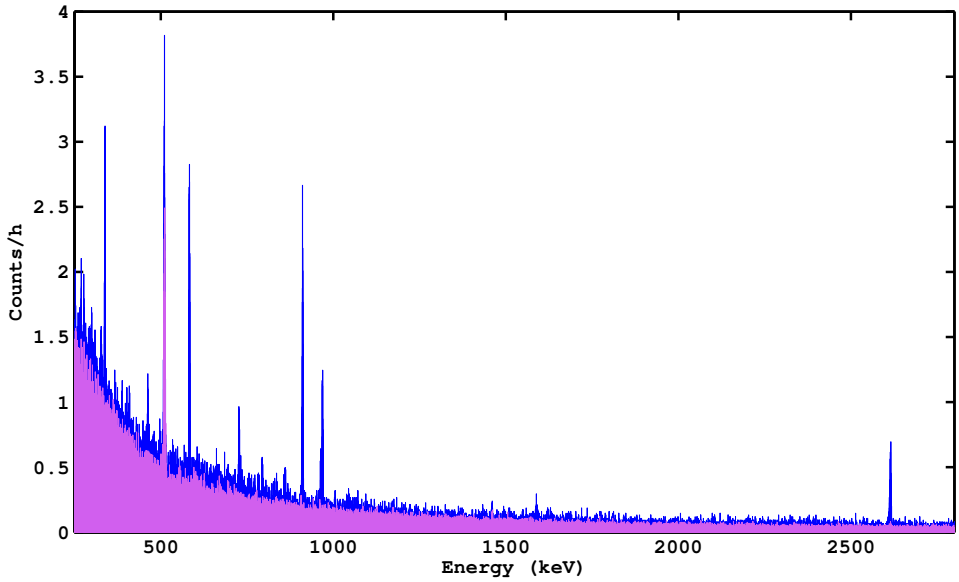

(a) ch0 source spectrum (blue) and background (violet)

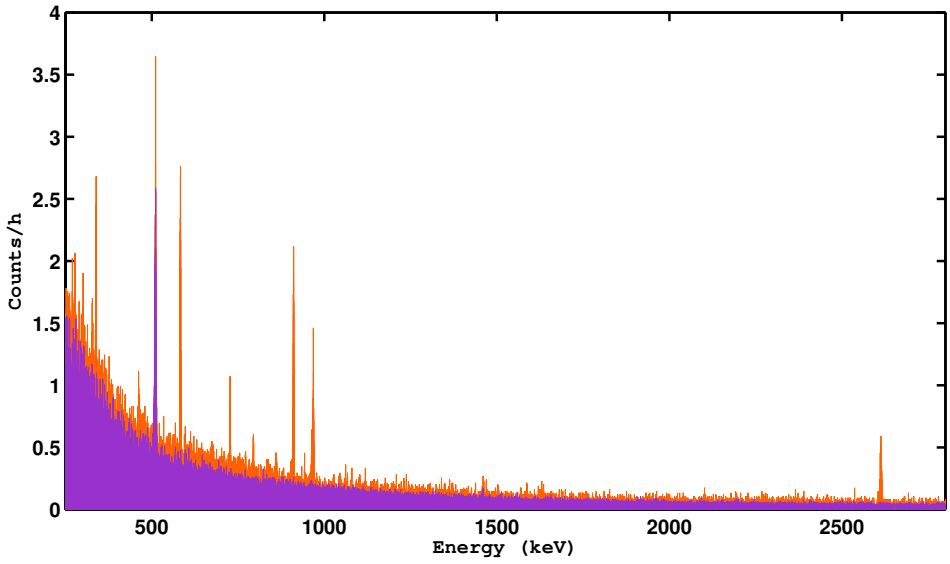

(b) ch1 source spectrum (orange) and background (violet)

Figure 5.4: 0.32 Bq source measurements

	ch0		**ch1**	
Energy (keV)	Activity (Bq)	error	Activity (Bq)	error
277.37	0.32	0.09	0.36	0.10
510.77	0.35	0.08	0.30	0.07
583.29	0.38	0.06	0.38	0.06
860.56	0.31	0.06	0.33	0.06
2614.5	0.31	0.05	0.32	0.05

Table 5.2: Activities calculated for the most intense peaks of ^{208}Tl for both detectors

Detector	**Activity (Bq)**
ch0	0.33 ± 0.03
ch1	0.34 ± 0.03

Table 5.3: Activities calculated as weighted mean of all peaks counts of the 0.32 Bq measurement

The selection of the 583 keV peak, with a suitable energy range, produces a coincidence spectrum on the other detector featuring many coincidence peaks:

- 277.37 keV.
- 510.77 keV, in the single detector spectrum this peak is often superimposed with the 511 keV due to interactions of cosmic rays within the shielding, but the coincidence analysis can select only the events due to the decay.
- 2614.53 keV, the most probable coincidence.
- 2103.5 keV due to the single escape of the 2615 keV gamma.
- 1592.5 keV: the double escape peak of 2615 keV.
- 3125.3 keV peak corresponding to the sum of 2614.53 keV and 510.77 keV.

Coincidence analysis consists in the analysis of the counts under these peaks. The activity can be calculated from the formula 3.1 using efficiencies obtained by coincidence simulations. This analysis has been performed for both detectors.

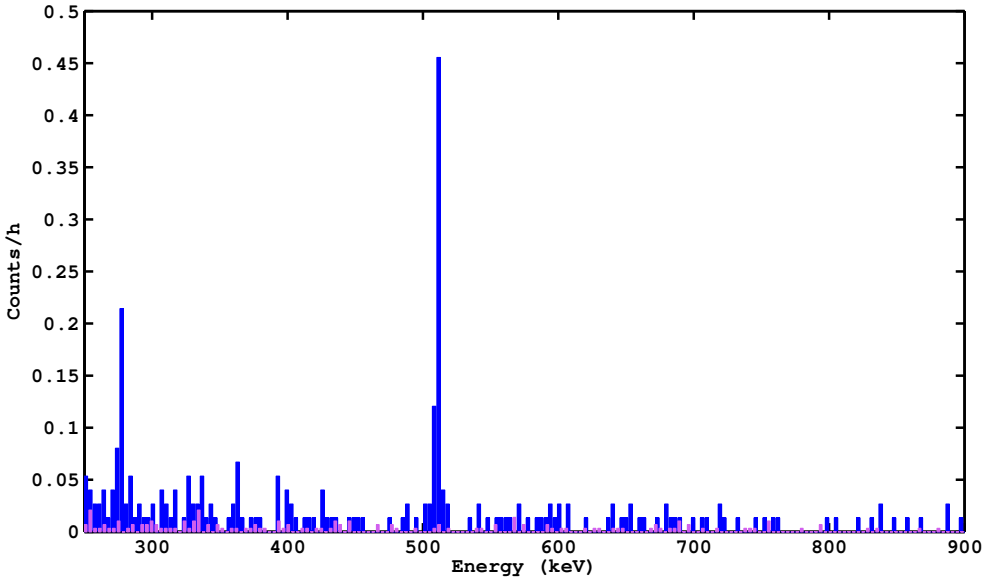

(a) 250-900 keV

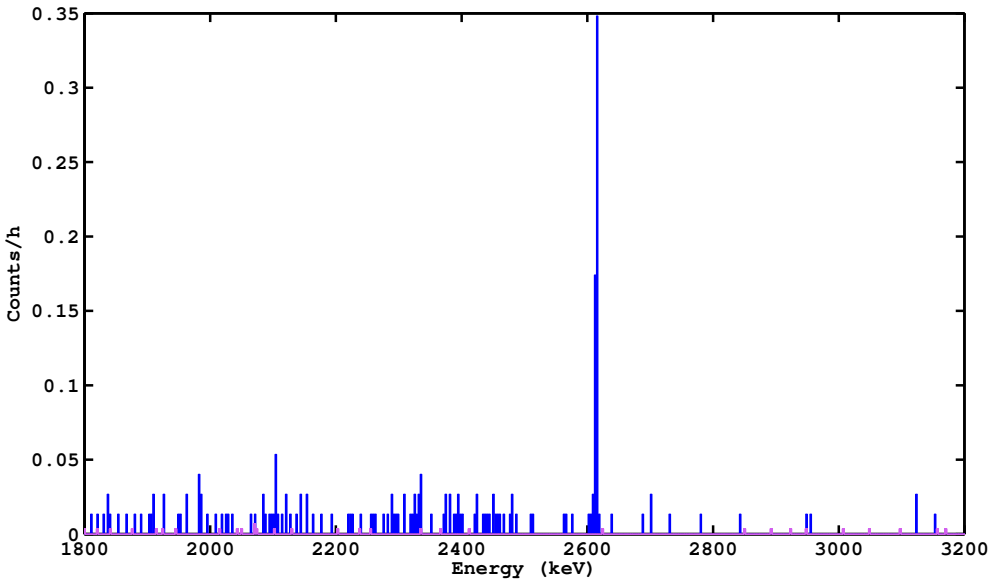

(b) 1800-3200 keV

Figure 5.5: Selection of 583 keV on ch1: 0.32 Bq source (blue) and background (violet) ch0 coincidence spectra

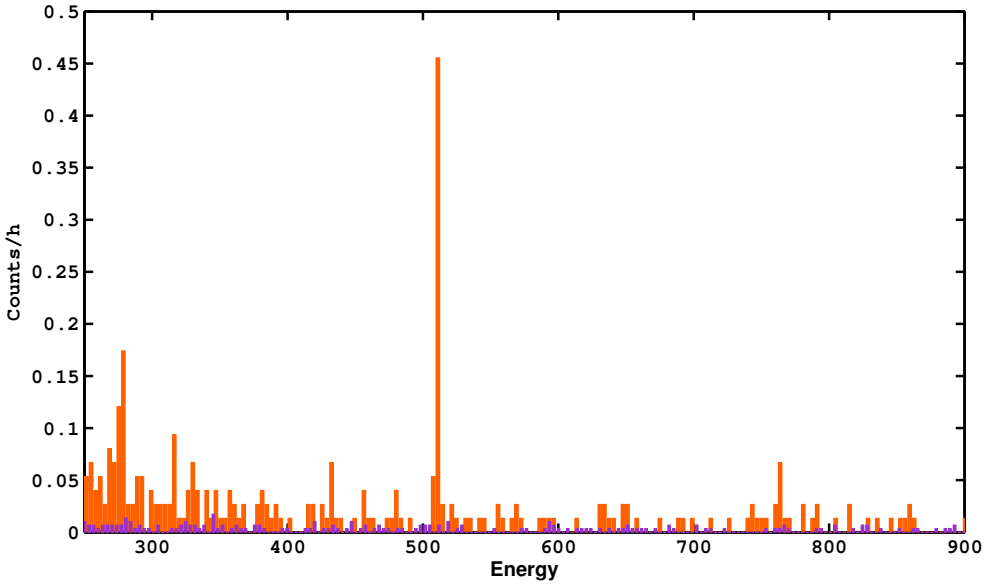

(a) 250-900 keV

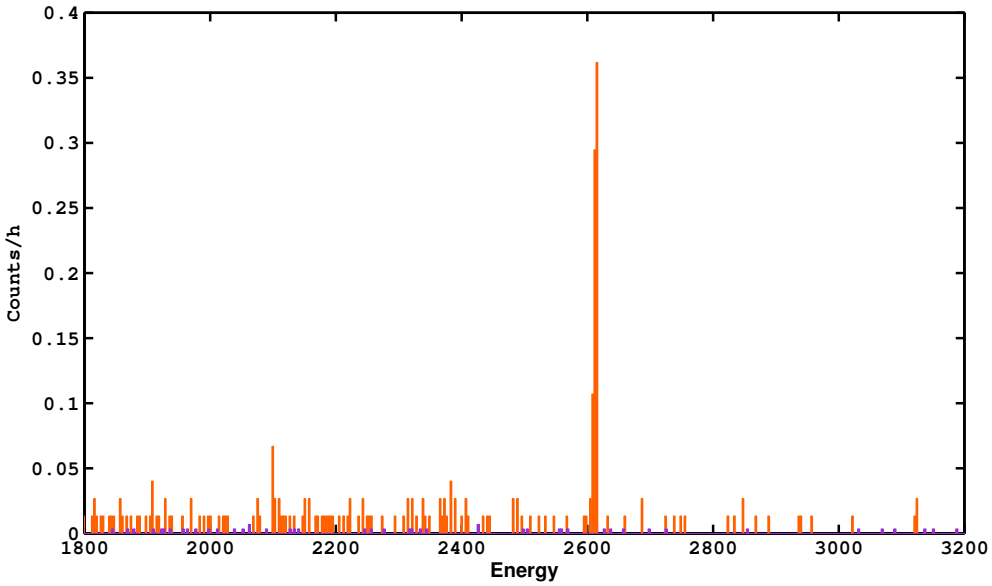

(b) 1500-3500 keV

Figure 5.6: Selection of 583 keV on ch0: 0.32 Bq source (orange) and background (violet) ch1 coincidence spectra

In figure 5.5 and 5.6 the coincidence source and background spectra are compared for *ch0* and *ch1* respectively, the peaks corresponding to 510.7 keV and 2614.5 keV are particularly visible. Background counts contribute only for 277.35 keV and 510.7 keV peaks with less than 0.01 counts/h. There are no spurious counts under the other peaks. The lack of counts in the background measurement, which has a longer counting time, means that counts in those energy range from the source measurement are due exclusively to the source.

The weighted mean of all the peaks contribution for *ch0* and *ch1* are listed in table 5.4. Considering the two detectors as a whole spectrometer the overall activity evaluated by coincidence analysis is 0.30 ± 0.03 Bq.

Coincidence with 583 keV	
Detector	Activity Bq
ch0	0.32 ± 0.04
ch1	0.28 ± 0.04

Table 5.4: Activities evaluated with coincidence analysis for the 0.32 Bq measurement

Each result is compatible with the source activity.

32 mBq

Since this source has a lower activity a longer measuring time is needed in order to reach a statistics suitable for the analysis. The live time has been of 143.308 hours. Both single detector spectra have only two main peaks exceeding the background counts fluctuation: 583.19 keV and 2614.53 keV. Spectra in the energy range of 583 keV and 2614.5 keV peaks for *ch0* and *ch1* are shown in figure 5.7 and 5.8 respectively. In table 5.5 the activities evaluated from each peak analysis and the resulting weighted mean for both detectors are listed. Considering the entire spectrometer the detected activity is 31 ± 4 mBq.

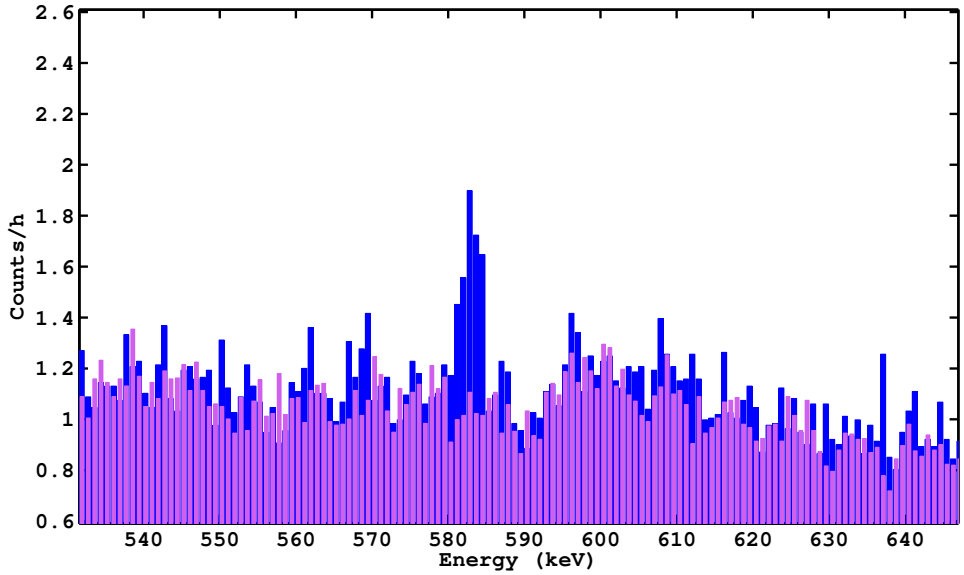

(a) 583 keV

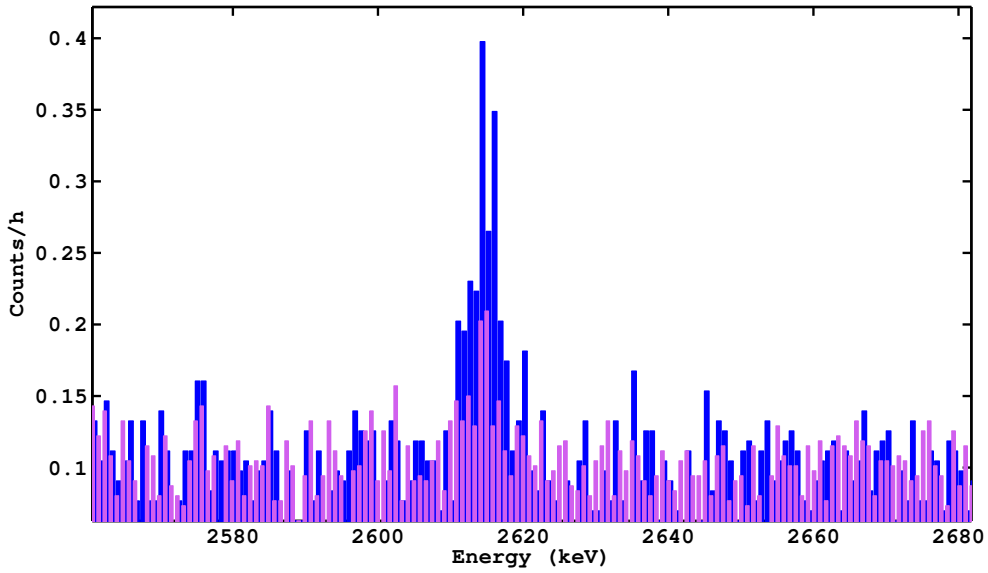

(b) 2614.5 keV

Figure 5.7: ch0: 32 mBq source (blue) and background (violet) single detector spectra

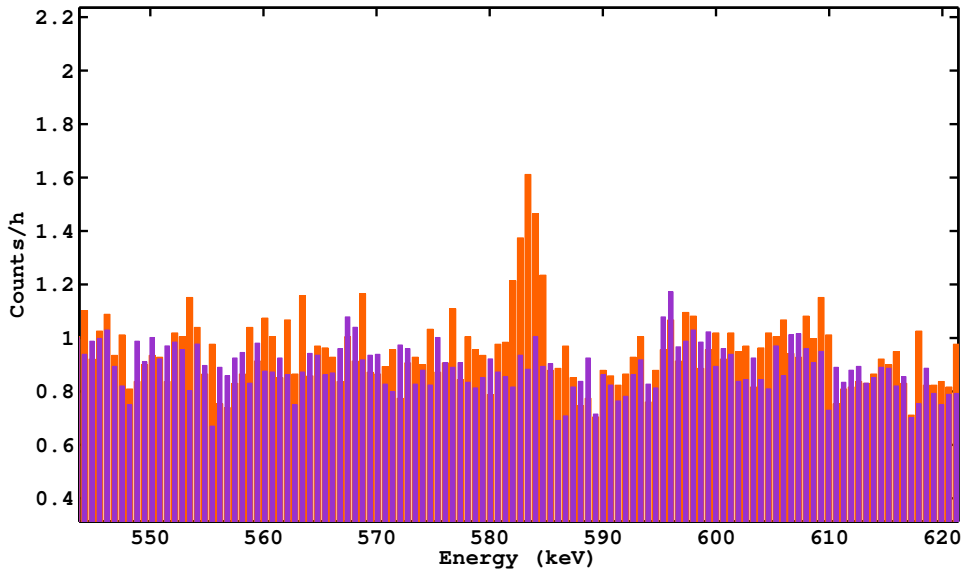

(a) 583 keV

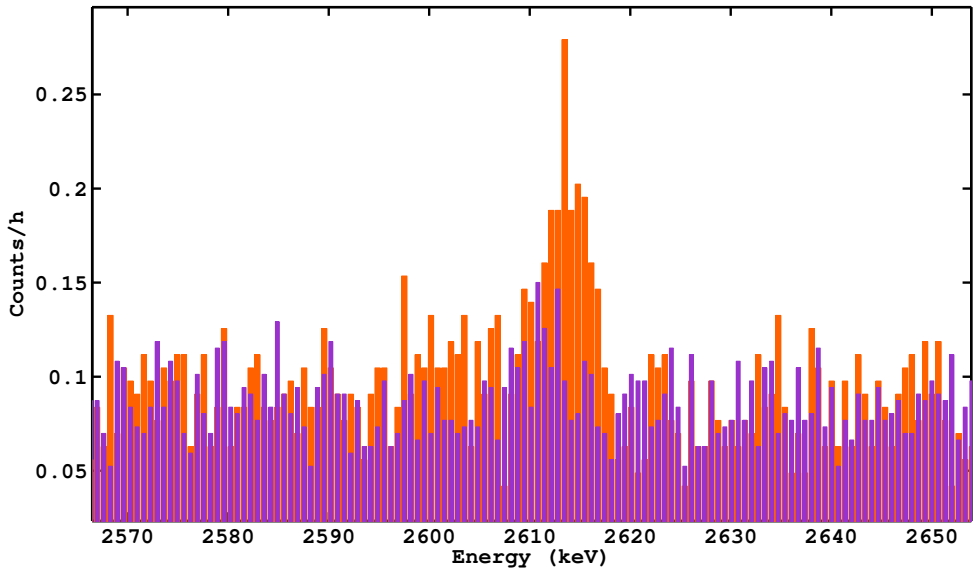

(b) 2614.5 keV

Figure 5.8: ch1: 32 mBq source (orange) and background (violet) single detector spectra

	Energy (keV)	Activity (mBq)	error	**Total Activity (mBq)**
ch0	583.29	57	9	29 ± 6
	2614.5	14	7	
ch1	583.29	57	9	33 ± 6
	2614.5	21	7	

Table 5.5: Activities from single detector analysis of the 32 mBq source

The same previously described coincidence selection has been performed, but in the corresponding spectra only the peaks at 510.7 keV, 2615 keV and 2103 keV are visible. The background subtraction is needed only for the first energy since background has no evidence of coincidence counts in the energy range considered for 2615 keV and 2103 keV peaks (fig. 5.9).

The coincidence spectra analysis can reach a better sensitivity thanks to the selection of events originated from the measured source. This measurement shows a perfect agreement between results and source activity (tab. 5.6). The activity evaluated from coincidence analysis of the entire spectrometer is 32 ± 5 mBq.

Coincidence with 583 keV	
Detector	Activity mBq
ch0	32 ± 8
ch1	32 ± 7

Table 5.6: Activities evaluated by coincidence analysis of the 32 mBq measurement

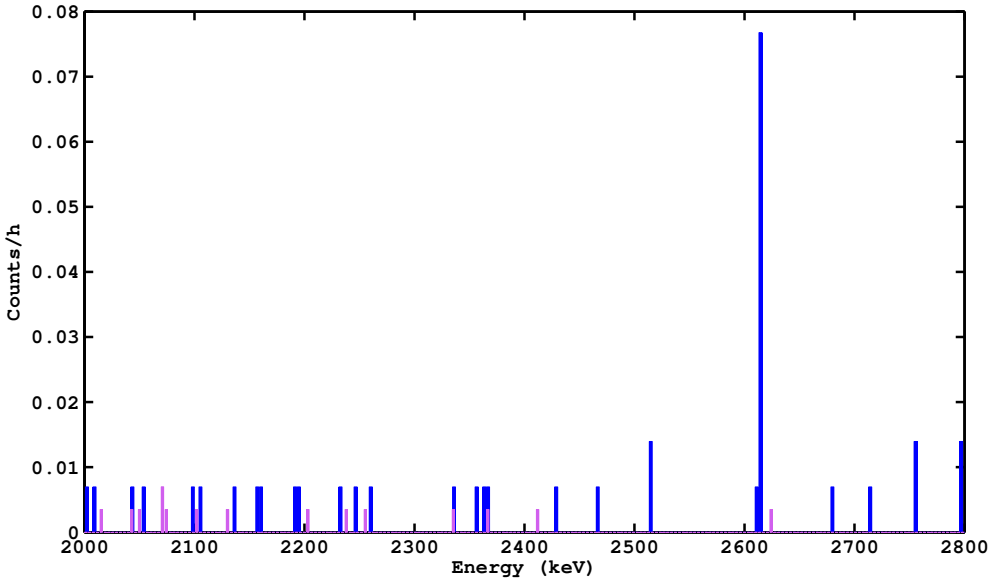

(a) 2614.5 keV on ch0

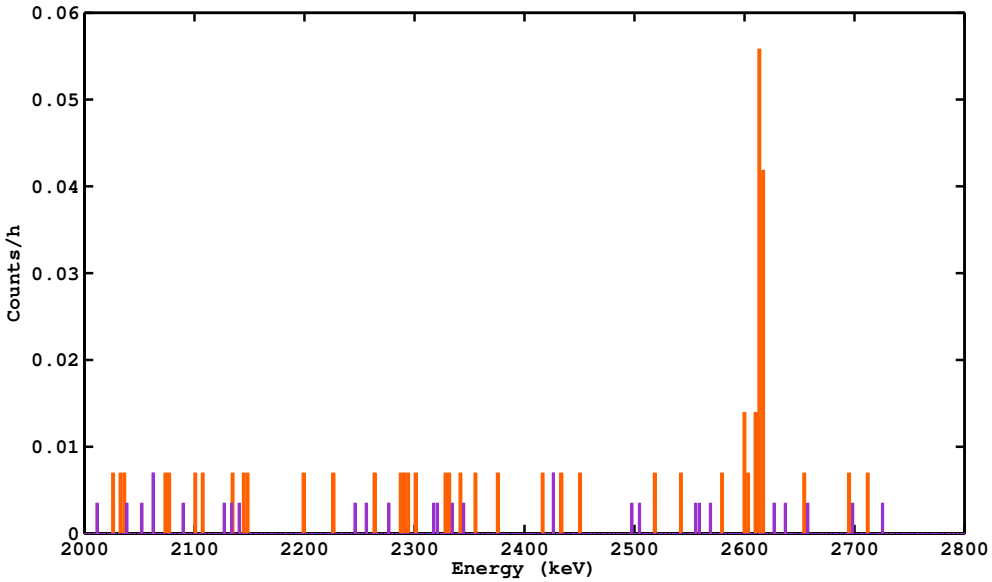

(b) 2614.5 keV on ch1

Figure 5.9: Coincidence spectra of 32 mBq source

3.2 mBq

Although the data taking has lasted 283.3 hours there was not enough statistics to analyze the single detector spectra. Counts due to the source are comparable to that of the background.

The coincidence spectra instead could reach enough sensitivity to have few counts in the energy range of 510.77 keV and 2614.53 keV (fig 5.10). For this measurement it is evident that coincidence selection is a powerful method to reduce the background; it allows the analysis of signals strictly due to the source. The results are listed in table 5.7. Considering the two detectors as one spectrometer the detected activity is 4.3 ± 1.2 mBq that is compatible with the known source activity.

Coincidence with 583 keV	
Detector	Activity mBq
ch0	4.3 ± 1.9
ch1	4.3 ± 1.7

Table 5.7: Activities evaluated by coincidence analysis for 3.2 mBq source measurement

The results obtained from the ^{232}Th sources with different concentrations show that the system works appropriately using the dedicated software and indicate that the measurements of such ^{232}Th concentrations are not affected from the DAQ dead time.

The efficiencies extracted from the Monte Carlo simulations are consistent with the expected values both for single detectors and coincidence measurements. The low intrinsic background and the peculiar data acquisition allow a good sensitivity for each measurement. The assessment measurements have proved that coincidence analysis can enhance the performance of the spectrometer; for these sources it is possible to reach a sensitivity of the order of the mBq in coincidence.

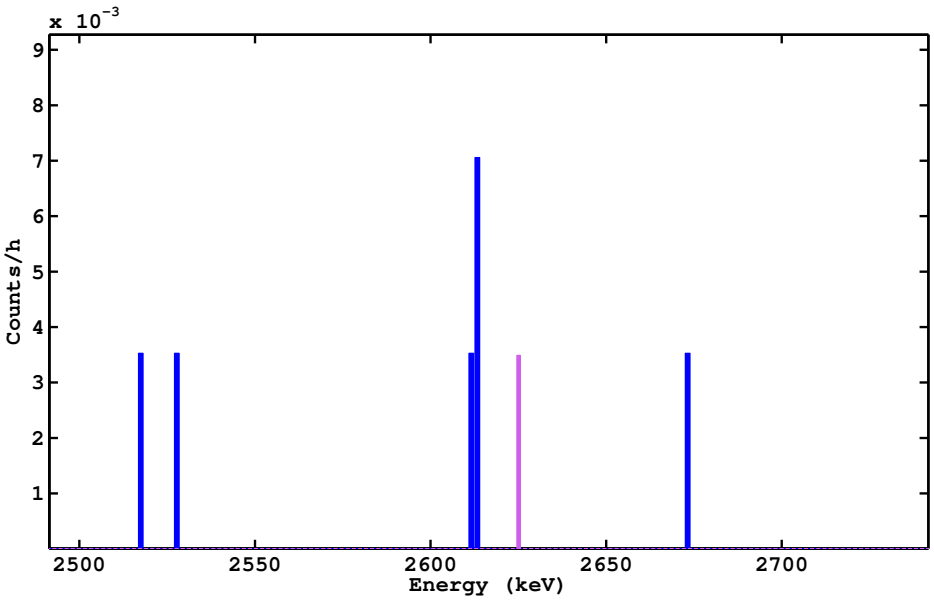

(a) 2614.5 keV on ch0

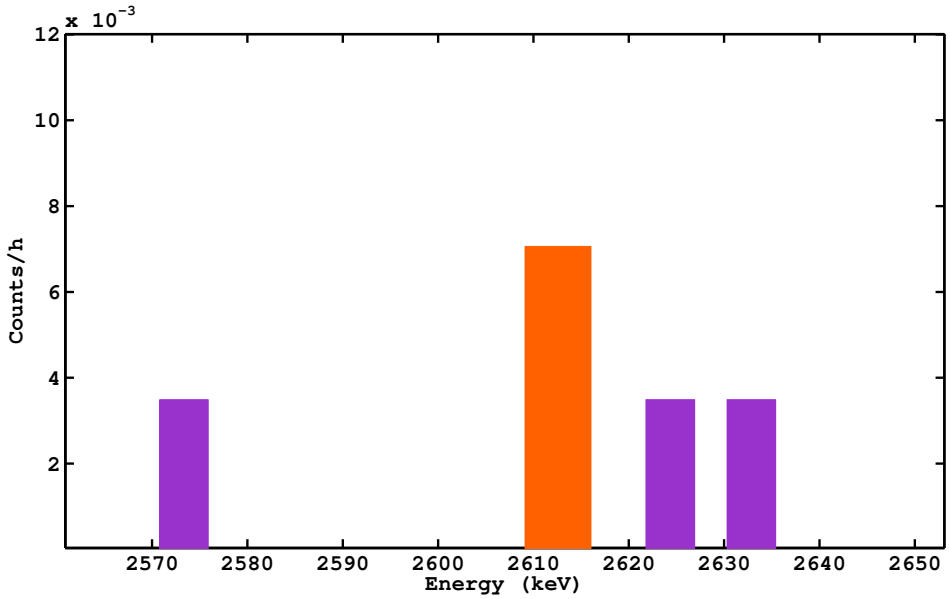

(b) 2614.5 keV on ch1

Figure 5.10: Coincidence spectra for 3.2 mBq source measurement

5.4 Materials selection measurements

The main application of the system composed of the two GMX detectors is the material selection for rare physics event experiments.

Coincidence analysis is possible only if the γ or X radiation following the radionuclide decay is emitted in cascade, therefore the study of the decay schemes is needed for each isotope whose contamination has to be measured.

Various materials used in experiments searching for dark matter and neutrinoless double beta decay signal have been measured considering contamination in ^{232}Th, ^{238}U and ^{40}K. I will present here some of these measurements.

5.4.1 Cesium Iodide

Cesium Iodide (CsI) is commonly used to realize inorganic scintillators that have many applications, for example they can be employed as detectors in the search for dark matter.

The analyzed sample is a Cesium Iodide powder, used for crystal growth, with a mass of 0.197 kg placed in a plastic container (fig. 5.11).

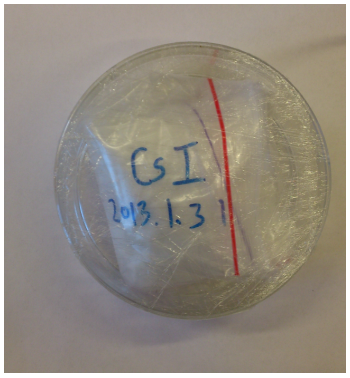

Figure 5.11: CsI sample

The rate due to primordial radionuclides is comparable between source and background spectra within less than 2σ. Concentrations for these isotopes have thus been evaluated as detection limits using the formula 3.2; results are listed in tables 5.8 and 5.9 for *ch0* and *ch1*.

	Energy (keV)	**Detection Limit Bq/kg**
^{232}Th series		
^{228}Ac	911.0	< 0.045
^{212}Pb	238.6	< 0.051
^{208}Tl	583.0	< 0.047
	2614.0	< 0.121
^{238}U series		
^{214}Pb	351.0	< 0.048
^{214}Bi	609.0	< 0.050
^{40}K	1460.8	< 2.9

Table 5.8: ch0: Primordial radionuclides detection limits for CsI measurement.

	Energy (keV)	**Detection Limit Bq/kg**
^{232}Th series		
^{228}Ac	911.0	< 0.038
^{212}Pb	238.6	< 0.056
^{208}Tl	583.0	< 0.040
	2614.0	< 0.151
^{238}U series		
^{214}Pb	351.0	< 0.055
^{214}Bi	609.0	< 0.046
^{40}K	1460.0	< 3.8

Table 5.9: ch1: Primordial radionuclides detection limits for CsI measurement.

The overall contamination of ^{232}Th and ^{238}U can be evaluated as < 0.05 Bq/kg for both decay series.

Moreover the analysis of ^{134}Cs has been requested for this measurement. The β^- decay of ^{134}Cs on ^{134}Ba is followed by the emission of many photons with a significant B.R., the most intense of which are listed in table 5.10.

Level Energy (keV)	**γ Energy (keV)**	**B.R. (%)**
1643.34	604.72	1.48
1167.97	563.25	8.34
1969.92	569.33	15.37
604.72	604.72	97.62
1400.59	795.86	85.46
1969.92	801.95	8.69

Table 5.10: γ-rays emitted from the ^{134}Cs decay

The background spectrum, corresponding to 389.8 hour of measurement, has been subtracted from the measured spectrum in order to analyze only the source counts and to identify peaks due only to the sample; in the single detector analysis the 604.72 keV and the 795.86 keV photons have been considered. In figure 5.12 the comparison between the *ch0* source (blue) and background (violet) spectra in the 600-800 keV energy range in counts per hours is shown,while the 604.72 keV and 795.86 keV peaks of the *ch1* source spectrum (orange) compared with the background are visible in figure 5.13.

The analysis has been performed for both detectors and the results for ^{134}Cs contaminations are shown in table 5.11.

Energy (keV)	**Activity (Bq/kg)**	
	ch0	**ch1**
604.72	0.079±0.007	0.079±0.005
795.86	0.070±0.009	0.070±0.006

Table 5.11: Specific activity of **^{134}Cs** for ch0 and ch1.

The decay scheme (fig. 5.14) shows that the most probable coincidence is between the 604.72 keV and the 795.86 keV photons.

The coincidence analysis has been performed selecting the 604.72 keV peak for the sample and the background measurements. The corresponding spectrum, of the other detector, have been analyzed considering the peak at 795.86 keV; the background rate

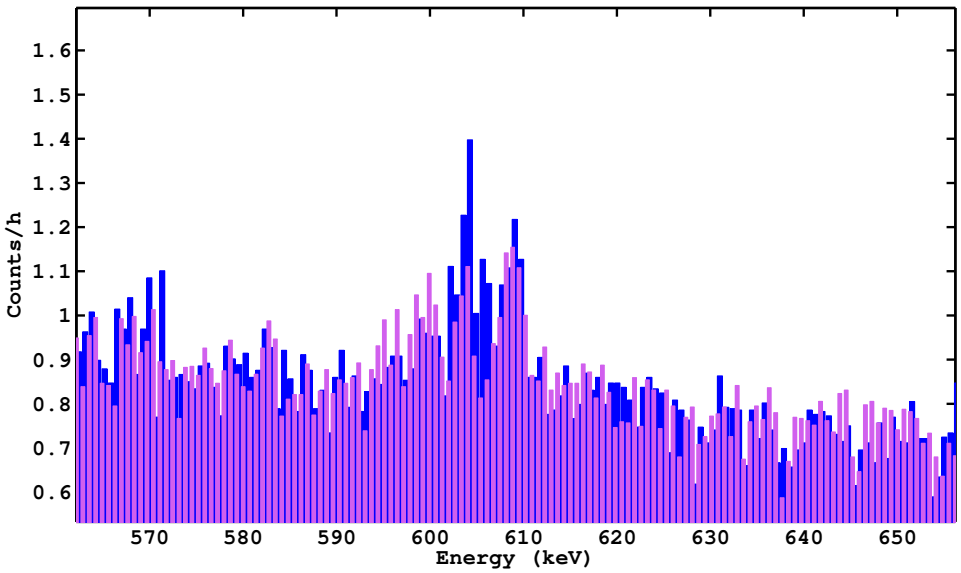

(a) 604.72 keV peak

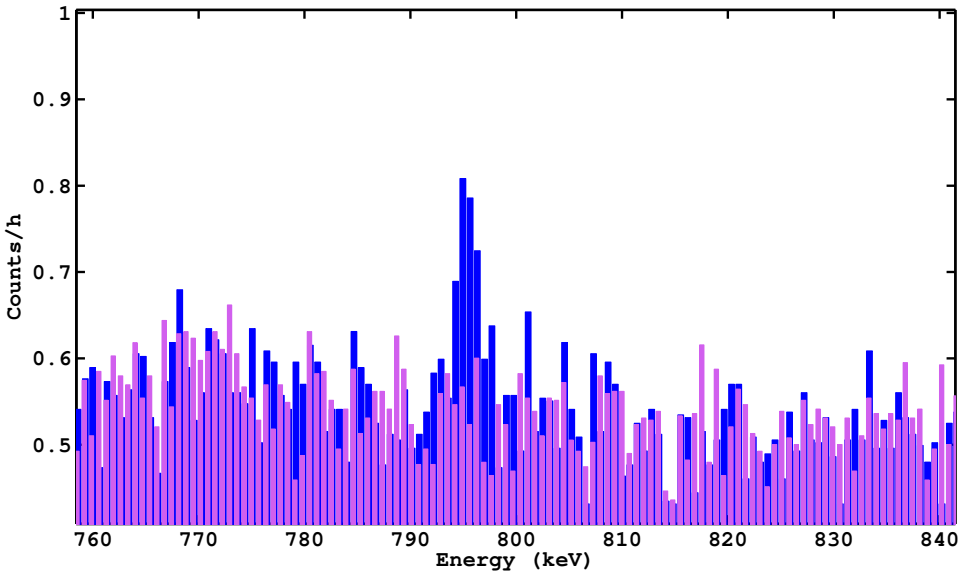

(b) 795.86 keV peak

Figure 5.12: CsI ch0 measurement spectrum (blue) compared with background in the 600-800 keV energy range

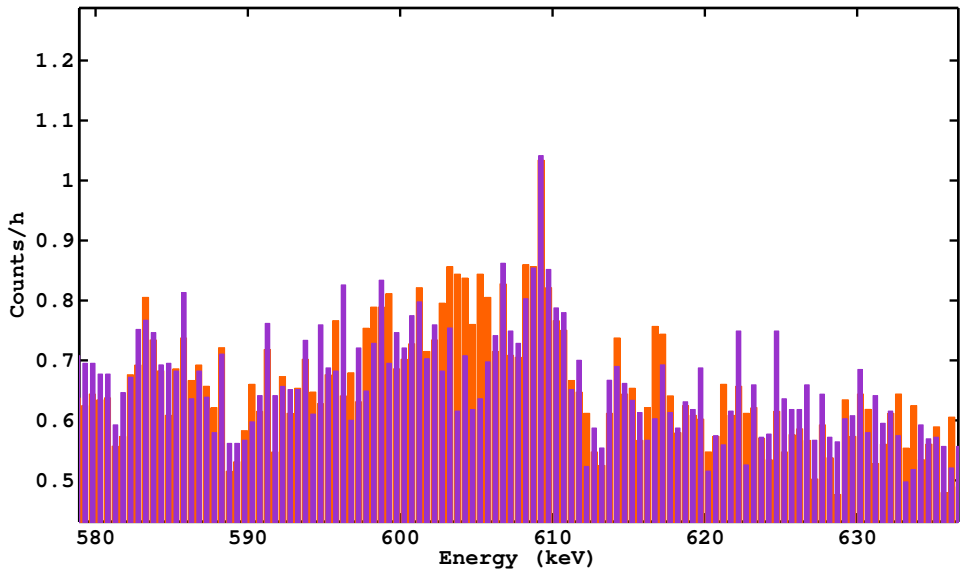

(a) 604.72 keV peak

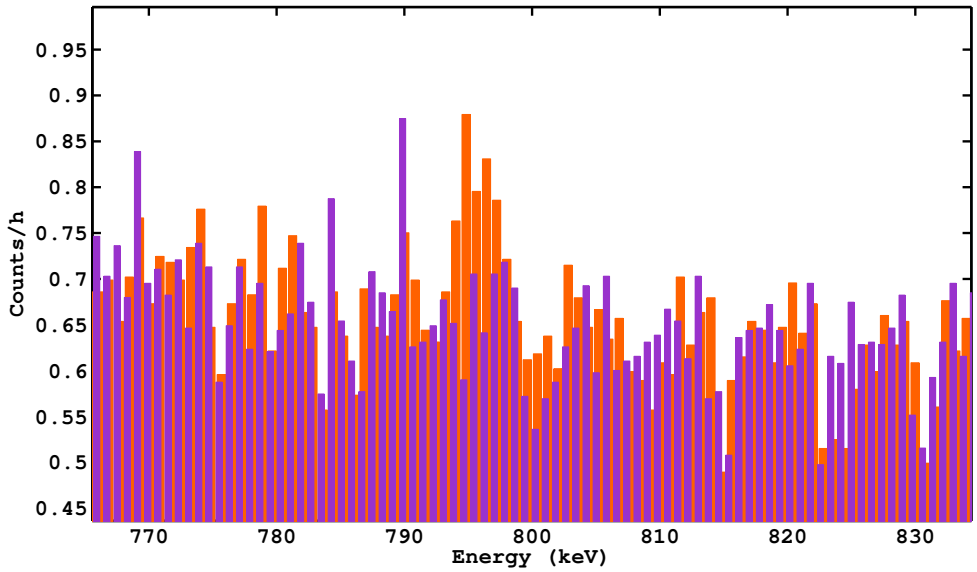

(b) 795.86 keV peak

Figure 5.13: CsI ch1 measurement spectrum (orange) compared with background in the 600-800 keV energy range

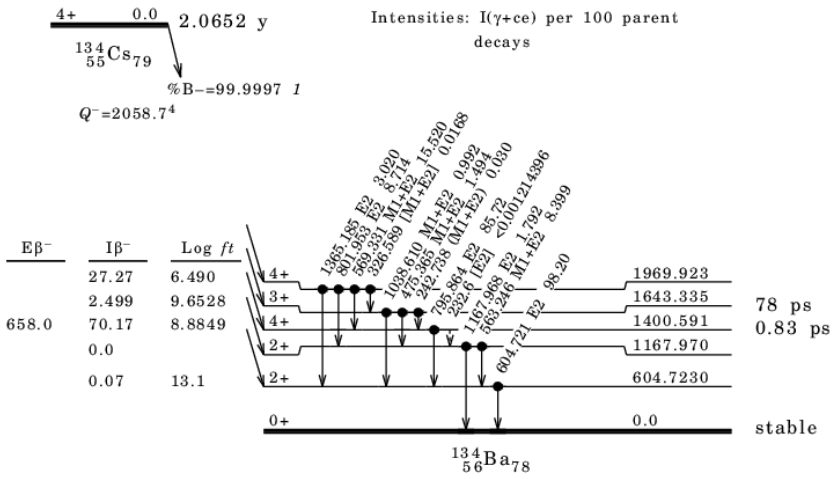

Figure 5.14: ^{134}Cs decay scheme

in the energy range under study has been subtracted from the sample counts. The comparison of the coincidence sample and background spectra for both detectors is shown in figure 5.15.

The coincidence sample spectra show a peak at 795.86 keV, from the analysis of its rate it has been possible to evaluate the ^{134}Cs specific activity in the CsI sample using the simulated coincidence efficiency. Results of this analysis are listed in table 5.12.

Coincidence between 604.72 keV and 795.86 keV	
Detector	**Activity (Bq/kg)**
ch0	0.068±0.021
ch1	0.068±0.022

Table 5.12: ^{134}Cs specific activity evaluated by coincidence analysis

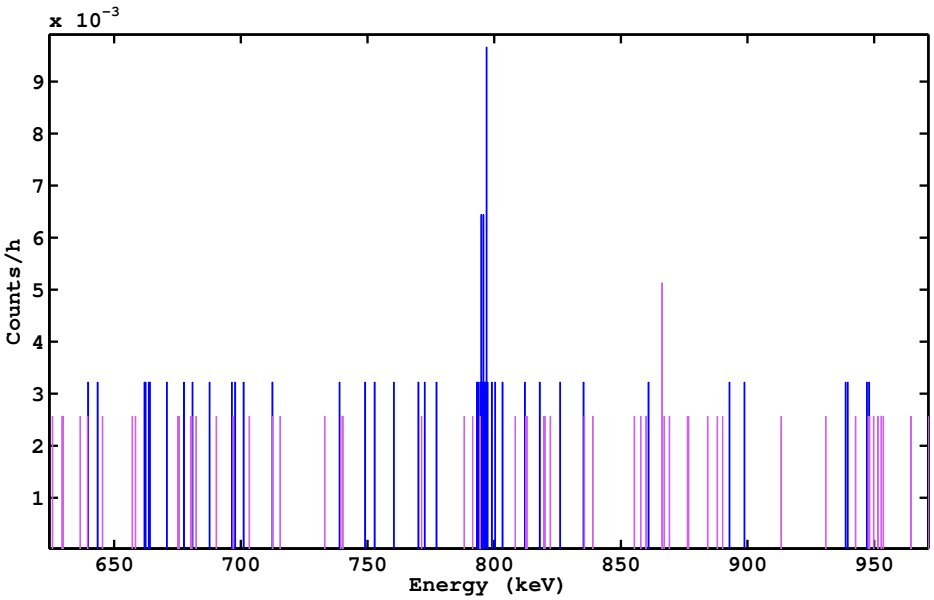

(a) 795.86 keV peak in ch0 sample spectrum (blue) compared to the background

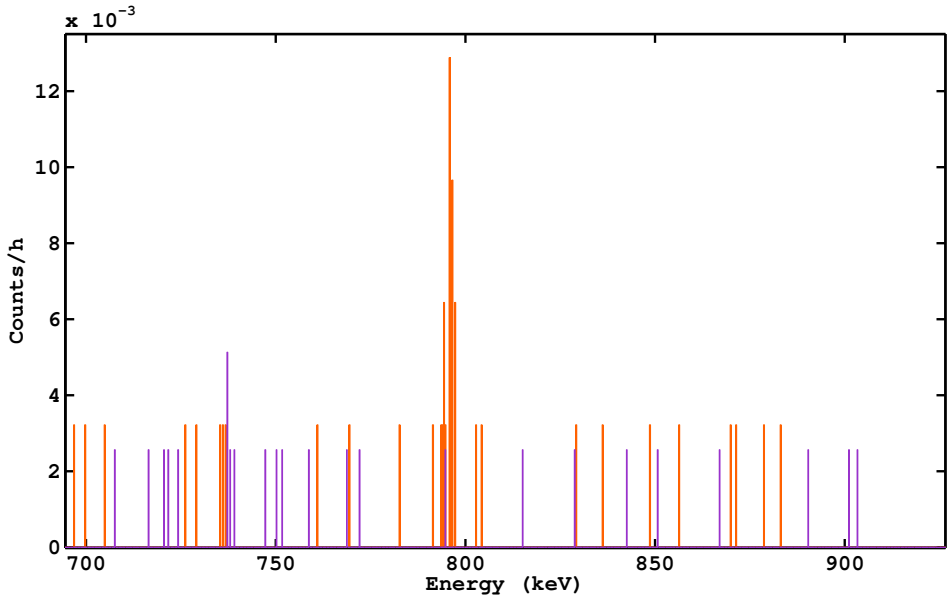

(b) 795.86 keV peak in ch1 sample spectrum (orange) compared to the background

Figure 5.15: CsI coincidence measurement: comparison between sample and background spectra for both detectors

5.4.2 NTD

The NTD39d are neutron transmutation doped thermistors used in the CUORE experiment. They convert the increase of temperature caused by a radiation interaction into a voltage signal recorded by a readout electronic chain.

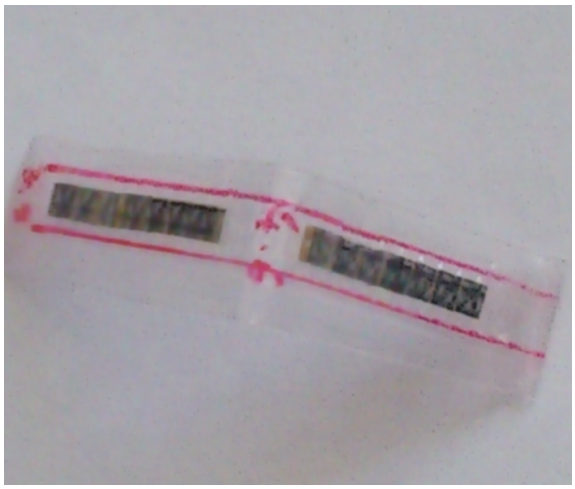

Figure 5.16: NTD sample

The sample consists in two rows (fig. 5.16) of 8 NTDs each for a total mass of 0.0154 kg. It has been placed between the two detectors close to their End Caps. The measurement has lasted 402.716 hours.

The comparison of sample and background spectra exhibits no evidence of primordial contaminations.

Detection limits for ^{232}Th, ^{238}U and ^{40}K are listed in table 5.13 for the *ch0* and 5.14 for *ch1*.

The overall contamination of ^{232}Th and ^{238}U can be evaluated < 0.2 Bq/kg for both decay series.

The background contribution of these thermistors is particularly crucial since they are placed on the experiment crystal detectors. The presence of ^{60}Co should also be considered since it decays emitting two high energy photons in coincidence (fig. 5.17) whose sum is close to the transition Q-value to be measured.

	Energy (keV)	**Detection Limit Bq/kg**
^{232}Th series		
^{228}Ac	911.0	< 0.17
^{208}Tl	583.0	< 0.19
	2614.0	< 0.53
^{238}U series		
^{214}Pb	351.0	< 0.22
^{214}Bi	609.0	< 0.24
^{40}K	1460.0	< 9

Table 5.13: ch0: Primordial radionuclides detection limits for NTD measurement.

	Energy (keV)	**Detection Limit Bq/kg**
^{232}Th series		
^{228}Ac	911.0	< 0.17
^{208}Tl	583.0	< 0.2
	2614.0	< 0.37
^{238}U series		
^{214}Pb	351.0	< 0.20
^{214}Bi	609.0	< 0.29
^{40}K	1460.0	< 8.9

Table 5.14: ch1: Primordial radionuclides detection limits for NTD measurement.

^{60}Co generally contributes to HPGe detectors background due to cosmic rays interactions with the Copper shielding layer. The very probable coincidence between the emitted γ-rays can be exploited to evaluate this isotope contamination using the coincidence analysis. The photons under study have energies of 1173.2 keV and 1332.5 keV both with a B.R. of 99.9%.

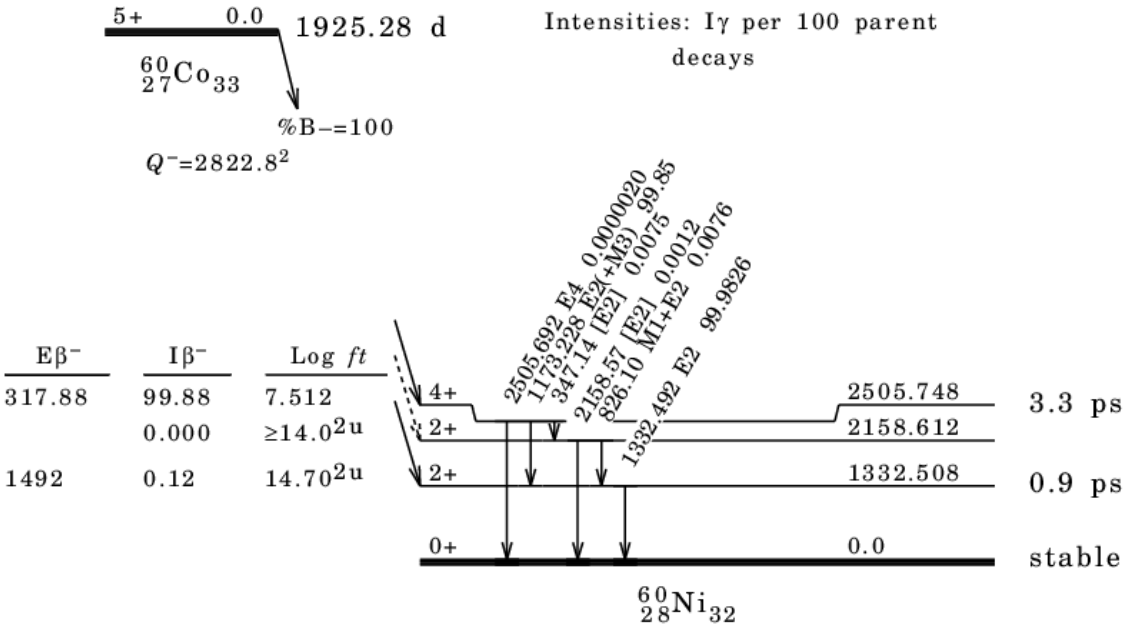

Figure 5.17: ^{60}Co decay scheme

For this decay I have considered a "peak-peak" coincidence selecting the 1173 keV peak on one detector and the 1332 keV on the other. The lack of coincidence events on sample and background spectra can be evaluated using the Poisson statistic in the absence of background. The upper limit for 0 observed events in the absence of background for confidence level of 90% corresponds to a mean value of the Poisson variable equal to 2.30 using the Neyman procedure for Poisson distribution [19].

The detection limit for ^{60}Co, considering the entire spectrometer, can be hence set < 14 mBq/kg.

5.4.3 Superinsulation

The analyzed superinsulation is a thermal insulator used in the CUORE experiment, composed of a thin layer of Mylar (C_{10} H_8O_4), thermoplastic resin characterized by excellent insulating properties on which an Aluminum layer with thickness of the order of ~ 10^{-6} m is deposited.

Several layers of this material are positioned in the space between the external structure of the CUORE apparatus, at room temperature, and the cryostat, cooled at cryogenic

Figure 5.18: superinsulation sample

temperature. Since in this area a high vacuum is maintained, irradiation is the only way the heat can propagate. The material can reflect about the 98% of the incident thermal radiation. Each layer reflects the thermal radiation emitted by the external one, which is at a higher temperature. Because of the high number of layers, the thermal radiation that reaches the cryostat is very low, ensuring in this way the thermal insulation of the cryostat, that in the coldest part has to ensure a working temperature of 10 mK [22].

Because of the position, radioisotopes presence in this material would give a substantial contribution to the background.

The sample mass is 0.0136 kg, it consists in a superinsulation sheet folded several times to reach a suitable size for the system (fig. 5.18).

The lack of a high mass has as consequence a long measuring time to reach a good counting statistics. The sample registered spectra did not show evidence on significant activity compared to the background.

Results from *ch0* analysis are listed in table 5.15, those of *ch1* in table 5.16.

The overall contamination of ^{232}Th and ^{238}U can be considered < 0.2 Bq/kg for both decay series.

	Energy (keV)	**Detection Limit Bq/kg**
^{232}Th series		
^{228}Ac	911.0	< 0.28
^{208}Tl	583.0	< 0.30
	2614.0	< 0.55
^{238}U series		
^{214}Pb	351.0	< 0.35
^{214}Bi	609.0	< 0.38
^{40}K	1460.0	< 15

Table 5.15: ch0: Primordial radionuclides detection limits for superinsulation sample measurement.

	Energy (keV)	**Detection Limit Bq/kg**
^{232}Th series		
^{228}Ac	911.0	< 0.3
^{208}Tl	583.0	< 0.3
	2614.0	< 0.76
^{238}U series		
^{214}Pb	351.0	< 0.30
^{214}Bi	609.0	< 0.42
^{40}K	1460.0	< 46

Table 5.16: ch1: Primordial radionuclides detection limits for superinsulation sample measurement.

5.5 Sensitivity Measurement

Copper is a material characterized by a high radiopurity, it is generally used as material of comparison for different low background techniques. Contamination of ^{232}Th in Copper samples needs a very high sensitive method to be detected. The sensitivity of the system under study has thus been tested through the measurement of a Copper sample placed between the two detectors. The sample is a cylinder with a diameter of 9.5 cm and thickness of 2.5 cm for a total mass of about 1.58 kg. The data taking has lasted 833.831 hours, about a month, although commonly sensitivity measurements can have measuring time from four to six months with a much larger sample mass reaching a sensitivity on the scale of tens of μBq/kg [23].

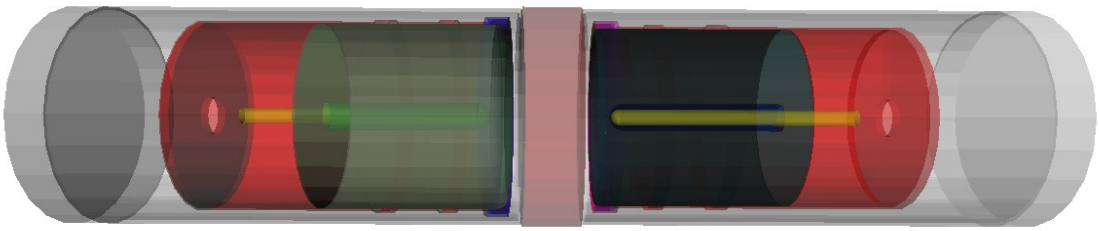

Figure 5.19: System configuration: a Copper cylinder placed between the GMX detectors

The experimental configuration (fig. 5.19) has been simulated to obtain efficiency for ^{232}Th γ lines, in particular those connected with the ^{208}Tl peaks. The simulations have been analyzed for single detector and coincidence spectra.

To evaluate the ^{232}Th contamination through the single detector spectra, the ^{208}Tl peaks lying on 583 keV and 2615 keV have been analyzed. The comparison with the background spectra counts under those energies shows the same counting statistics. In both sample and background spectra a peak at 2615 keV is present, this high energy photon can indeed be originated from an external source since its energy is enough to pass

through the shielding; whereas there is no evidence of a peak in the 583 keV energy range. Detection limits have been evaluated considering the 583 keV peak with a confidence level of 2σ; results for both detectors are listed in table 5.17.

Detector	γ lines (keV)	**Detection limit (mBq/kg)**
ch0	583.2	< 6.8
ch1	583.2	< 6.7

Table 5.17: Detection limits for ^{232}Th in Copper sample for single detector measurements

The selection of the 583 keV peak corresponds to a coincidence spectrum in which counts under the usually considered peaks are zero. The lack of coincidence rate fixes the sensitivity limit for this configuration. The detection limits can be evaluated using the Poisson statistics in absence of background; results in mBq/kg are listed in table 5.18.

Detector	**Sensitivity mBq/kg**
ch0	< 4.5
ch1	< 4.7

Table 5.18: Detection limits for ^{232}Th coincidence measurement of Copper sample

These results can be combined summing the detectors coincidence efficiencies, giving a sensitivity < 2.3 mBq/kg.

Sensitivity depends on the mass-efficiency product and on the counting time; these are the parameters that should be taken into account to improve the detection limit of the system.

A possible method to enhance the sensitivity is the study of the coincidence continuum in addiction to the peaks counts. This technique increases the efficiency since it considers counts over a wider energy range using the same sample mass.

The method has been tested by measuring coincidences of ^{232}Th liquid standards, previously used for assessment measurements, in an energy range between 10 and 3500 keV. Each measurement has been compared with the background subtracting the counts in the region under study for one detector. The simulated efficiency for this analysis is more than twice the efficiency for all the coincidence peaks. Results of the analysis produced for the ^{232}Th vial with activities of 0.32 Bq and 32 mBq are listed in table 5.19.

Source Bq	**Detected Activity** Bq
0.32	0.39 ± 0.06
0.032	0.041 ± 0.009

Table 5.19: Activities for ^{232}Th coincidence continuum measurement

The other ^{232}Th source has a concentration of 3.2 mBq, the continuum rate of this measurement is compatible with those of background, thus it was possible only to evaluate a detection limit < 5 mBq at 90% Confidence Level. This detectable activity has been calculated considering the continuum background counts.

The calibration line evaluated from the continuum counts per hour of the 0.32 Bq and 32 mBq measurements predicts a rate lower than the detected for the 3.2 mBq source. This indicates that the continuum for low activity measurements is dominated by the cosmic rays background and not by the source continuum.

The Copper measurement continuum is therefore dominated by the cosmic rays interactions. The predicted continuum counts can be evaluated performing a simulation. The figure 5.20 shows the measured (orange) and the simulated (dark blue) coincidence spectra. To compare these spectra it has been mandatory to simulate the right contamination so that also in the simulated spectrum there is no evidence of the 2615 keV peak as in the measured spectrum. The efficiency resulting from this simulation can be used to evaluate the expected continuum rate for a assumed activity of 5 mBq/kg: 0.006 counts/h in the energy range from 30 keV up to 2650 keV. This result is more than two order of magnitude lower than the registered rate, 0.68 counts/h, that can therefore be

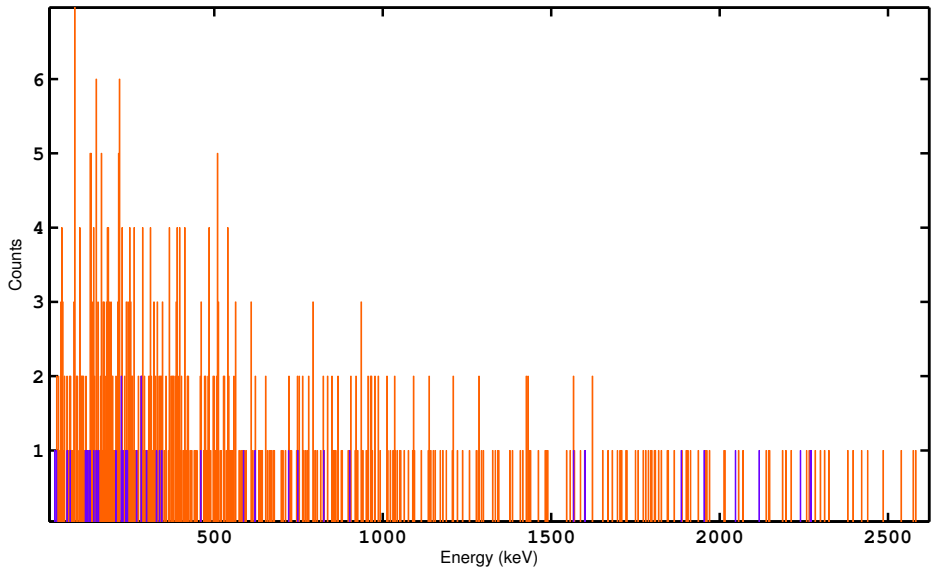

Figure 5.20: Continuum coincidence spectra: expected (dark blue) and detected (orange)

completely attributed to the interactions of cosmic rays that generate a large background also in the coincidence spectra.

The induced cosmic rays background should be reduced using an anti-coincidence method, for instance placing plastic scintillators all over the shielding Lead surface. Background reduction is then performed neglecting signals registered by the spectrometer when in coincidence with signals from the veto detectors within a proper time window.

The other possibility to improve the sensitivity is to increase the sample mass. It is important to optimize the mass-efficiency product without a significant efficiency reduction. Since the detectors are surrounded by a layer of Copper which is made of the same Copper of the sample cylinder, the entire Copper structure can be considered as sample. In the system configuration this corresponds to a total mass of about 176 kg.

This configuration considerably enhances the mass-efficiency product of single detectors, detection limits from the single detector analysis of the 583 keV and 2615 keV γ

lines are listed in table 5.20.

Detector	γ line (keV)	**Detection limit (mBq/kg)**
ch0	583.2	< 1.8
ch1	583.2	< 1.6

Table 5.20: Detection limits for ^{232}Th in Copper structure for single detector measurement

The coincidence analysis for the 175 kg Copper layer has led to a sensitivity < 1.4 mBq/kg for the total spectrometer. Since the Copper layer surrounds almost completely both the detectors (fig. 5.21), the self-absorption and the distance between the Copper edges and the crystals involve a not considerable increase in coincidence efficiencies.

Another parameter that can enhance the system performance is the counting time. If zero counting rate will be observed for longer time, the sensitivity in coincidence measurements can increase linearly with time obtaining a possible final sensitivity in the range below 1 mBq/kg with more months measurement of the same sample. It is possible to reach a sensitivity < 580 μBq/kg considering four months of data taking for the Copper cylinder with no counts evidence for all the analyzed peaks.

It is also possible to consider coincidences of other isotopes of the ^{232}Th decay series, for example those of ^{228}Ac, to further enhance the measurement sensitivity.

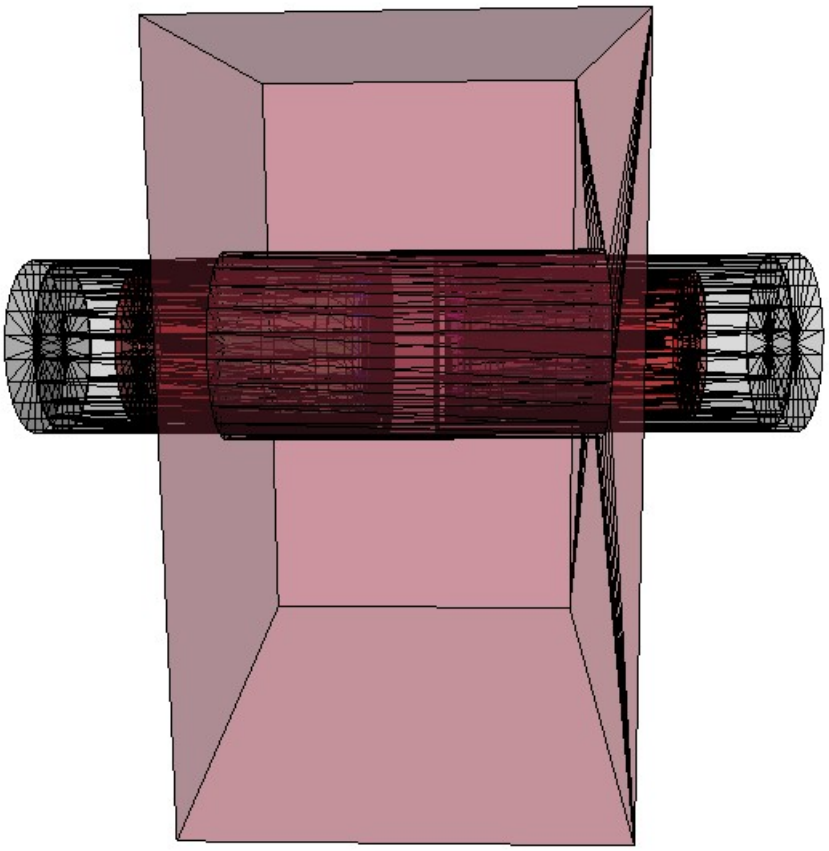

Figure 5.21: System configuration: the GMX detectors surrounded by the Copper layer

Chapter 6

High sensitive measurements with Broad Energy Germanium

6.1 BEGe 5030

The BEGe (Broad Energy Germanium) 5030 is a Low Background detector capable to register a wide energy spectrum from 3 keV up to 3 MeV with a good energy resolution both at low and high energies. The resolution at low energies is equivalent to that of a Low Energy detector whereas the resolution at high energy is comparable to that of coaxial detectors (tab.6.1). The BEGe has indeed a characteristic electric field distribution, due to the small rear contact, that provides a low capacitance and consequently a low noise corresponding to a better energy resolution and a lower energy threshold.

Isotope	Energy (keV)	**BEGe** FWHM	**GeCoax** FWHM	**GMX** FWHM
^{241}**Am**	59.54	0.49 keV	0.9 keV keV	1.0 keV
^{137}**Cs**	661	1.18 keV	1.77 keV	1.7 keV
^{60}**Co**	1173	1.54 keV	1.97 keV	2.2 keV
	1332	1.60 keV	2.00 keV	2.4 keV

Table 6.1: Energy resolution comparison between BEGe, a standard Coaxial HPGe and GMX detector

(a) Bare BEGe crystal

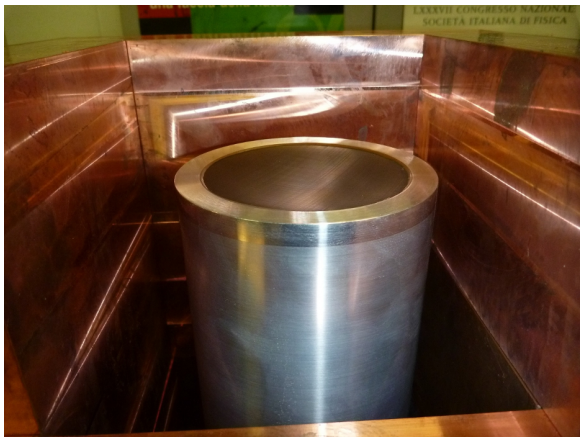

(b) BEGe entrance window and End Cap

The BEGe 5030 detector crystal (fig. 6.1(a)) is a cylinder 30 mm high and has a diameter of 80 mm with a 50 cm^2 area and 50% relative efficiency. The crystal is inserted in a Low Background Aluminum End Cap with a Carbon Epoxy window 0.5 mm thick on the top (fig. 6.1(b)). The window thickness allows the transmission of very low energy radiations.

The configuration of the detector features a Low Background cryostat thanks to the selection of the materials it is composed of. Low energy detection is also permitted by the thin thickness, 0.4 μm, of the dead layer that works as entrance window of the crystal. Thanks to its great active volume the BEGe can detect an energy spectrum with very high efficiency (fig. 6.1) on the whole covered energy range.

In addition to higher efficiency for typical samples, the BEGe exhibits a background lower than typical coaxial detectors because it is more transparent to high energy cosmogenic background radiation that permeates above ground laboratories and to high energy gammas from primordial radioisotopes decays such as ^{40}K and ^{208}Tl of the ^{232}Th chain [5].

6.1.1 Optimization

The BEGe 5030 is placed in the Radioactivity Laboratory of Milano-Bicocca. Each parameter of the electronic chain has been accurately chosen to preserve the excellent

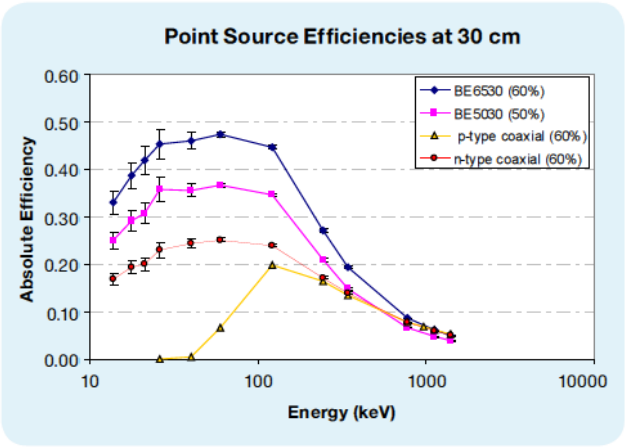

Figure 6.1: Comparison of BEGe efficiency with other standard detectors

features of the detector. The optimization of the shaping time value has been studied using a multi-gamma source containing isotopes that emit γ with energies covering the whole energetic spectrum. Since the BEGe can detect a wide energy spectrum this optimization has been made with different gain values to select different energy ranges.

The optimum value for the shaping time is the one that maximizes the energy resolution. This value has been set at 6 μs evaluating the FWHM of the low energy peaks varying the shaping time from 1 up to 10 μs.

To exploit completely the excellent energy resolution and high efficiency of the BEGe, the signal from the pre-amplifier has been divided to form two signal lines, each of them is amplified with the same type of electronic modules but with different gain. This procedure allows the detection of a low energy spectrum up to 150 keV using a higher gain (fig. 6.3) and the whole spectrum using a lower gain (fig. 6.4). This configuration avoids the losses of some low energy counts, due to the threshold set to remove the noise, on the low energy spectrum (fig. 6.2).

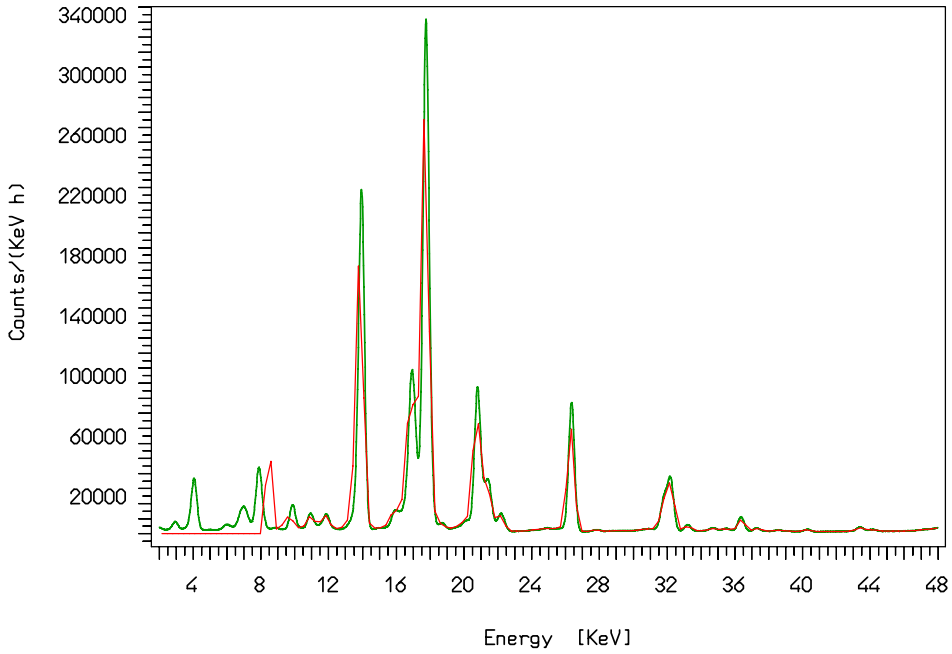

Figure 6.2: Low Energy spectrum with high gain (green) and low gain (red)

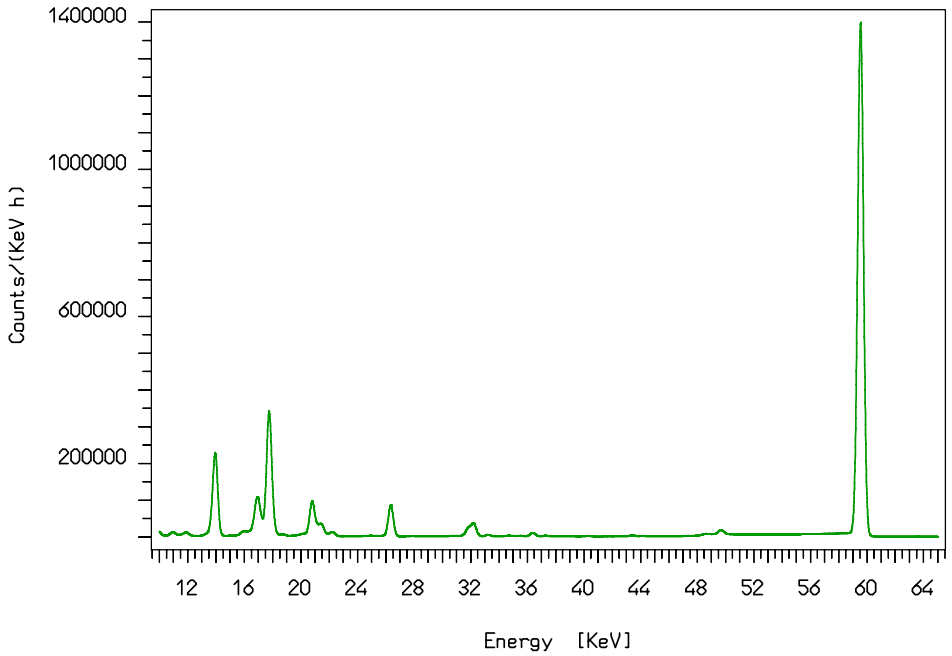

Figure 6.3: Low Energy spectrum

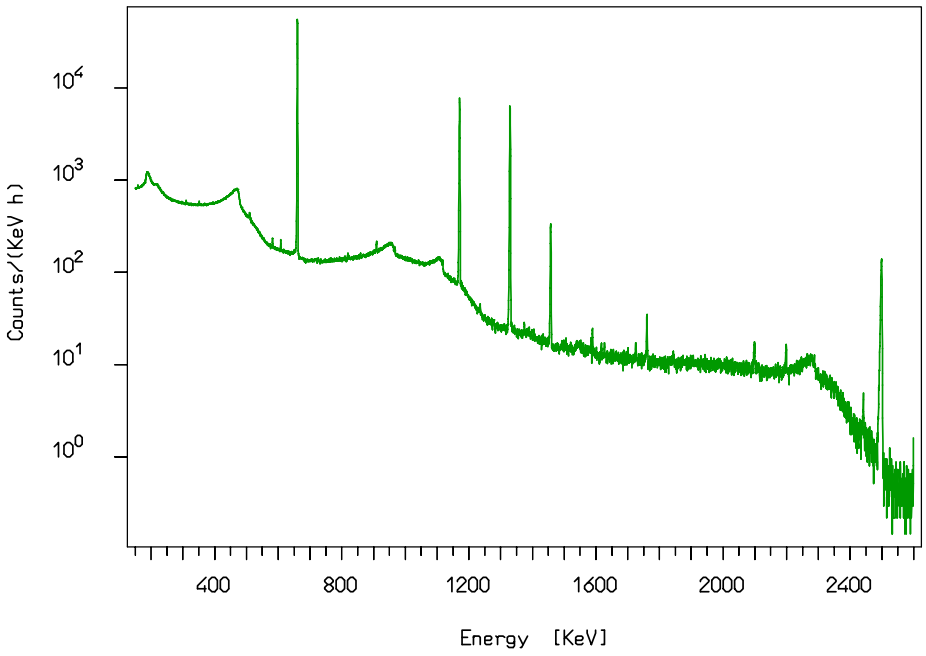

Figure 6.4: High Energy spectrum

6.1.2 Background reduction

The BEGe has then been optimized by studying the measured background in different configurations. Initially the detector was not equipped with a dedicated shielding, but it has been mandatory to reduce the high background due to cosmic rays and environmental radioactivity. A preliminary shielding (fig. 6.5) composed of a 5 cm inner Copper layer surrounded by 20 cm of Lead has been used recording an impressive reduction of background counts on the whole spectrum.

A comparison between low energy background in different configurations is shown in figure 6.6: the higher (dark green) line represents the background without shielding while the lower (light green) is the background spectrum with a preliminary shielding.

The passive shielding reduction method suppresses the background by more than one order of magnitude.

(a) Copper inner layer (b) Lead external layer

Figure 6.5: The BEGe preliminary shielding

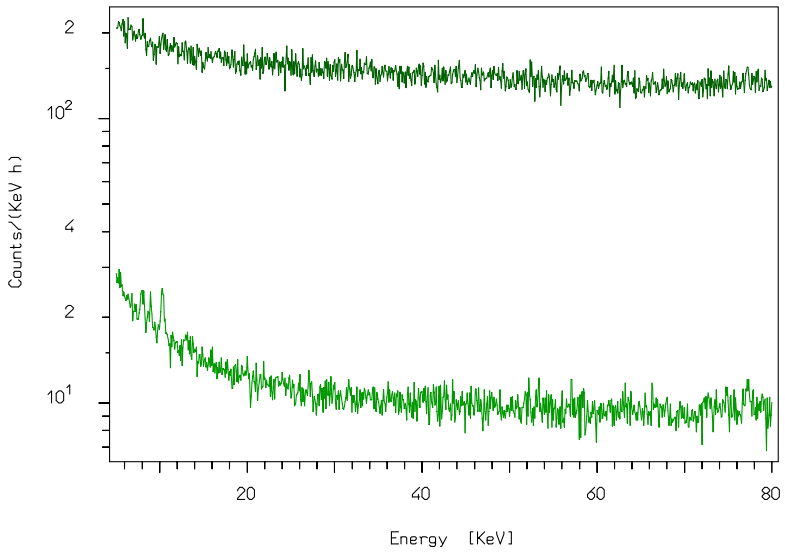

Figure 6.6: Background comparison in different configurations

These results show the necessity of a dedicated shielding (fig. 6.7), now under construction, therefore I have projected a facility composed of an inner 5 cm layer of Copper and an external layer of 15 cm of Lead with a mechanical system to lift the top of the shielding making easier the samples positioning on the detector surface.

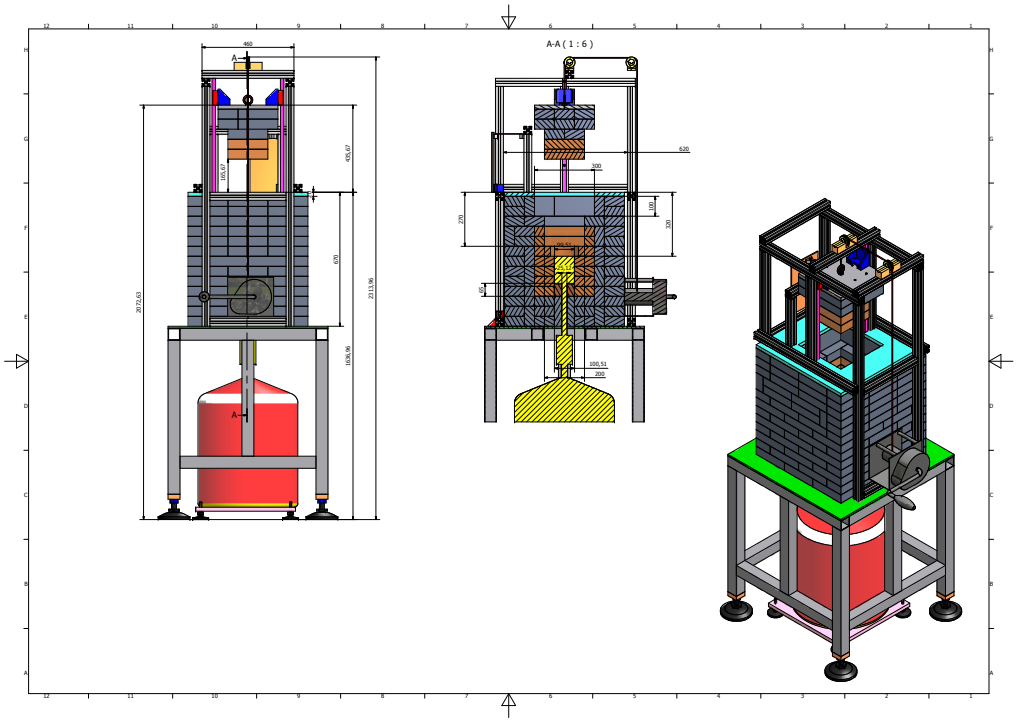

Figure 6.7: The BEGe dedicated shielding

6.1.3 Application

The BEGe performances allow different kind of measurements and has a large application area. For instance thanks to its peculiar features, this detector is also suitable for X-ray measurements and the large upper area allows to measure quite big sample masses providing an enhancement of the sensitivity.

During my PhD work the BEGe 5030 has been used to perform a highly sensitive Plutonium detection for radioactive fallout monitoring.

6.2 Plutonium

Plutonium is a radioactive transuranic element, its presence in nature is for the most part of anthropogenic origin, it is indeed mostly produced in research or commercial nuclear reactors. The main isotopes are the α emitters ^{238}Pu, ^{239}Pu and ^{240}Pu, their decays are followed by many de-excitation γ-rays with very low B.R. and quite low energies. The majority of Plutonium isotopes have short half life compared to geological timescale.

The main sources of Plutonium released in environment are the nuclear tests held since 1945, but also accidents or losses from nuclear plants [24]. As a consequence of a nuclear weapon explosion the released radioactive material is scattered in atmosphere originating the "radioactive fallout" that consists in the fall out of the radioactive particles as ash and fine dust. Once released in environment Plutonium can penetrate in soil and water; its toxicity is not only that of typical actinide metal, but it is due to its affinity with other elements.

In the studies of nuclear monitoring, the measurement of Plutonium concentrations in environmental samples is crucial since it is dangerous by ingestion and hence its presence has to be reduced.

It is of legal and safety interest to constantly monitor areas in which nuclear activity such as nuclear accidents or losses have occurred or places used as nuclear waste storage.

Agencies for ionizing radiations use a reference protocol to set the radiological clearance levels for the dangerous isotopes in environment, these values identify the threshold activity under which contaminations are considered not dangerous.

The Italian Environmental Protection Agency (ISPRA) reports the clearance levels for the considered isotopes as shown in table 6.2.

Isotope	Clearance Level (Bq/kg)
^{238}Pu	140
^{239}Pu	140
^{240}Pu	150

Table 6.2: Clearance levels for some Plutonium isotopes

6.2.1 Measurement techniques

For environmental protection it is mandatory to quickly monitor large areas contaminated by possible radioactive fallout in order to establish the best procedure for site recovering especially for fallout emergency. It is important to use a measurement technique capable to analyze many environmental samples in few hours. Plutonium concentration in environmental samples can be evaluated with different low level counting techniques.

The analytical approach commonly used in radioactive contamination measurements is Gamma spectrometry with High Purity Germanium. This technique can reach low background level and allows a fast and sensitive measurement thanks to the possibility to measure large mass samples and to the absence of samples treatments, that are often time consuming.

Unfortunately the considered Plutonium isotopes are alpha emitters and the gamma rays accompanying the decays have low branching ratios making gamma spectrometry not enough sensitive. Since the γ B.R. are low to reach a suitable sensitivity a quite long measuring time would be needed.

The main techniques to detect Plutonium contaminations are alpha spectrometry and mass spectrometry with ICP-MS. Both these techniques require a preliminary manipulation of the sample that makes the methods quite long.

Alpha spectrometry is generally performed with silicon barrier detectors, for which the measured samples should have peculiar thin layer to avoid α absorption. The environmental samples, generally composed of soil, should undergo chemical treatments: radiochemical separation of the isotopes of interest in liquid solution and then plate electro-deposition. To reach a good sensitivity the whole procedure for this technique is quite long, it takes up to one week for one sample.

Moreover the energy resolution is not enough to separate the characteristic energy peaks related to the ^{239}Pu and ^{240}Pu isotopes.

The other feasible technique, mass spectrometry with ICP-MS, allows the separation of the three isotopes, if no compounds or elements with similar nuclear mass are present in the sample, but the instruments and the needed clean environment are quite expensive. The counting technique is not time consuming, but since the sample should be liquid some chemical pre-treatments are necessary. The sensitivity can depend on the

resins used to separate the isotopes of interest from the sample, on their efficiency and contaminants.

Although the high efficiency of these techniques, the time needed to treat and measure a sample is too long to perform a fast screening.

6.2.2 X-rays spectroscopy

A feasible method to avoid sample treatments is to detect the X-rays associated to the decays of the Plutonium isotopes under study. Each isotope decay is followed by the emission of characteristic X-rays of the daughter nuclei; since ^{238}Pu, ^{239}Pu and ^{240}Pu decay on different isotopes of the same element, Uranium, the emitted X-rays lie at the same energies with different probabilities. This method is more sensitive than γ spectroscopy thanks to the higher B.R. of X-rays; a comparison of the B.R. is shown in table 6.3.

	^{238}Pu		**^{239}Pu**		**^{240}Pu**	
	En	B.R.	En	B.R.	En	B.R.
γ	43.5 keV	0.0395 %	51.6 keV	0.0271 %	45.24 keV	0.04 %
X-L$_{\beta 1}$	13.6 keV	3.69 %	13.6 keV	1.57 %	13.6 keV	3.55 %
X-L$_{\alpha 1}$	17.2 keV	3.9 %	17.2 keV	1.57 %	17.2 keV	3.7 %

Table 6.3: γ and X-rays energies and B.R. of some Plutonium isotopes

Exploiting the higher B.R. of the emitted X-rays it is possible to perform a measurement with a counting time of about few hours using a suitable detector.

This measurement method cannot distinguish between the different isotopes because the emitted radiations lie above the same energies, but can give information about the contaminations of Plutonium in the measured sample.

Since the X-rays under study are in the 12-22 keV energy range it is mandatory to use a detector able to register low energies with high efficiency. The system optimized to perform this measurement is the Broad Energy Germanium 5030 since it can measure large mass samples without the need of pre-treatments and has high efficiency and good energy resolution at low energies.

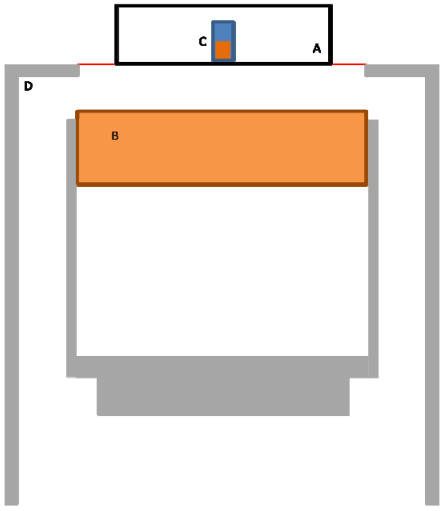

Figure 6.8: source-detector geometry

6.3 Efficiency calibration

6.3.1 Measurements

The efficiency evaluation is a mandatory procedure for the counting system since this parameter is crucial to calculate the activity of a measured sample.

For this purpose simulations are needed and the best method consists in placing a calibrated source, with a certified activity, on the detector and comparing the measured efficiency with the simulated one. To protect the BEGe fragile entrance window a plastic Petri dish has been placed above it with the vial containing the source in it (fig. 6.8).

Using a source containing isotopes with emitted energies covering the whole spectrum it is possible to have a complete calibration. The isotopes commonly studied are ^{241}Am, ^{137}Cs and ^{60}Co (tab. 6.5). The used source is a calibrated multi-γ shaped as a little cylinder of gel with density 1 g/cm^3. The certificate of the source contains all the important parameters regarding the activity of the isotopes to consider (tab. 6.4).

To properly analyze the full energy peaks both low energy and high energy spectra have been registered using different linear gain values set in the amplifiers (fig. 6.9). The efficiency is calculated considering the source activity at the date of the measurement for each photon and dividing the counts per second of each considered peak by this value.

Code	SS-1491
Production date	8/11/1997
Reference date	1/11/1997
Activity of ^{241}Am	1993 Bq
Activity of ^{137}Cs	633.3 Bq
Activity of ^{60}Co	967 Bq

Table 6.4: Certified activities of the multi-γ source isotopes

Isotope	Energy (keV)	B.R: (%)	Type
^{241}Am	13.76	1.07	X
	13.95	9.61	X
	16.82	2.53	X
	17.06	1.53	X
	17.75	5.78	X
	17.99	1.37	X
	20.78	1.39	X
	26.34	2.40	γ
	59.54	35.94	γ
^{137}Cs	31.82	2.04	X
	32.19	3.77	X
	661.66	85.12	γ
^{60}Co	1173.24	99.97	γ
	1332.5	99.98	γ

Table 6.5: Multi-γ emitted energies

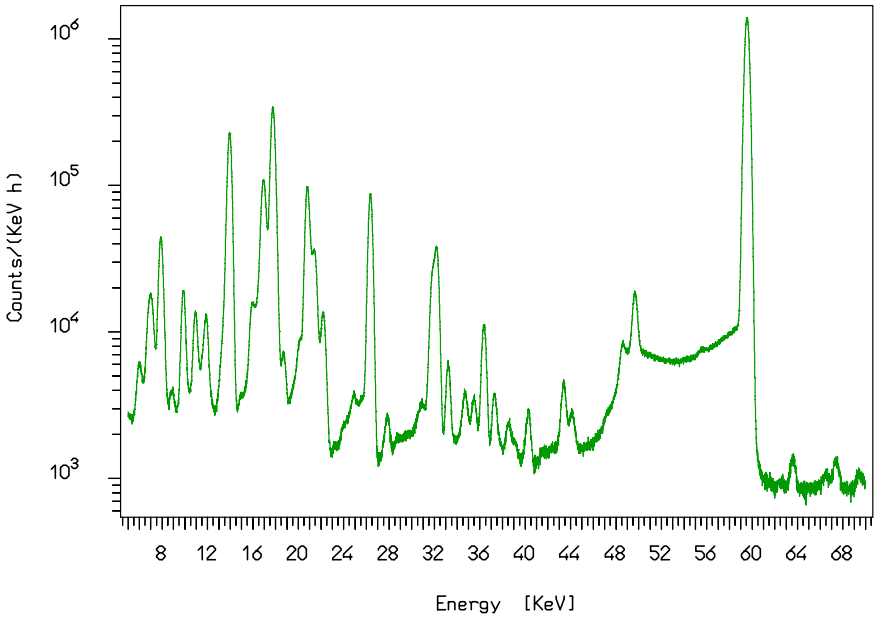

(a) Multi-γ source: Low Energy spectrum

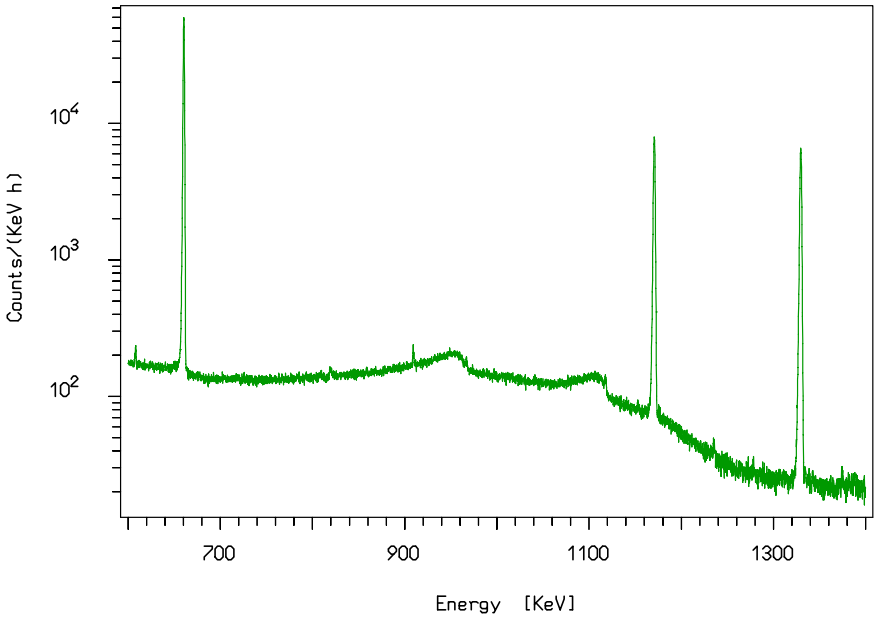

(b) Multi-γ source: High Energy spectrum

Figure 6.9: Multi gamma BEGe energy spectra

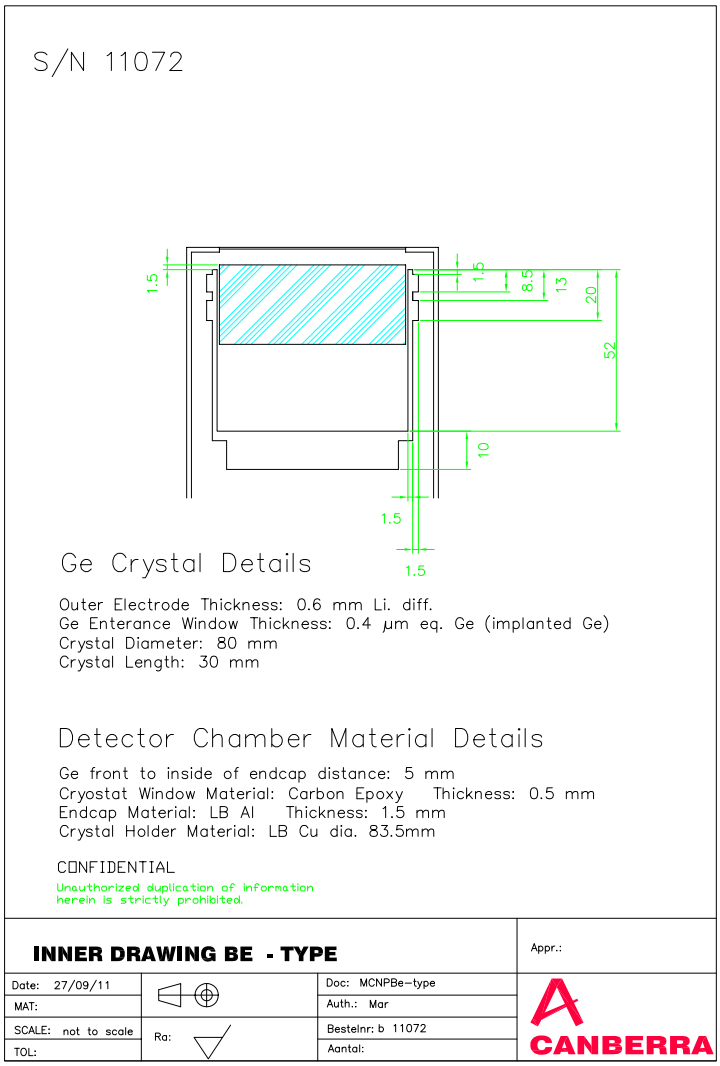

Figure 6.10: BEGe geometry scheme

6.3.2 Simulations

The efficiency calibration with Monte Carlo simulations uses a system scheme (fig. 6.10), provided by the manufacturer, in which some important parameters are defined.

Using the configuration with nominal values the discrepancies between simulated and measured efficiency are quite substantial (fig. 6.11), the relative error is > 24%; this is partially due to the lack of information regarding some parameter values.

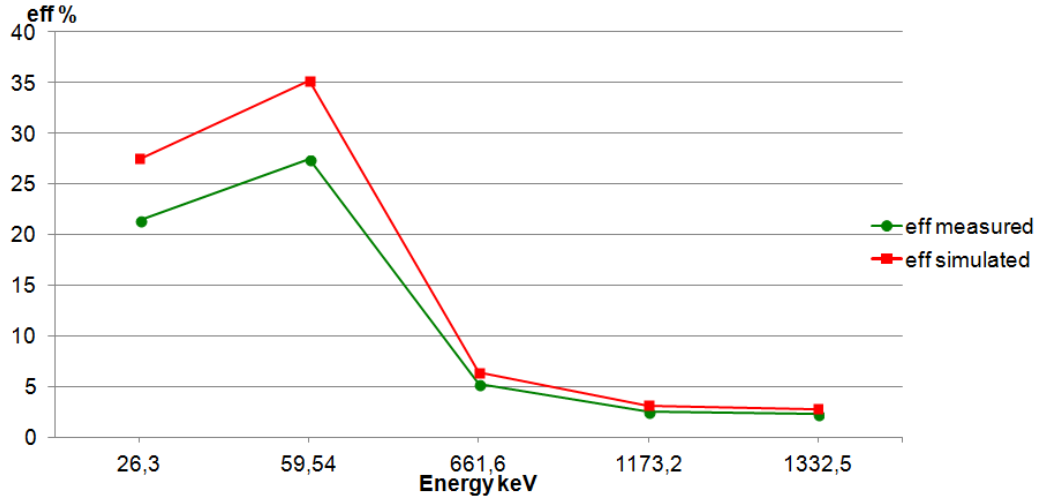

(a) Measured and simulated efficiencies in function of the energy

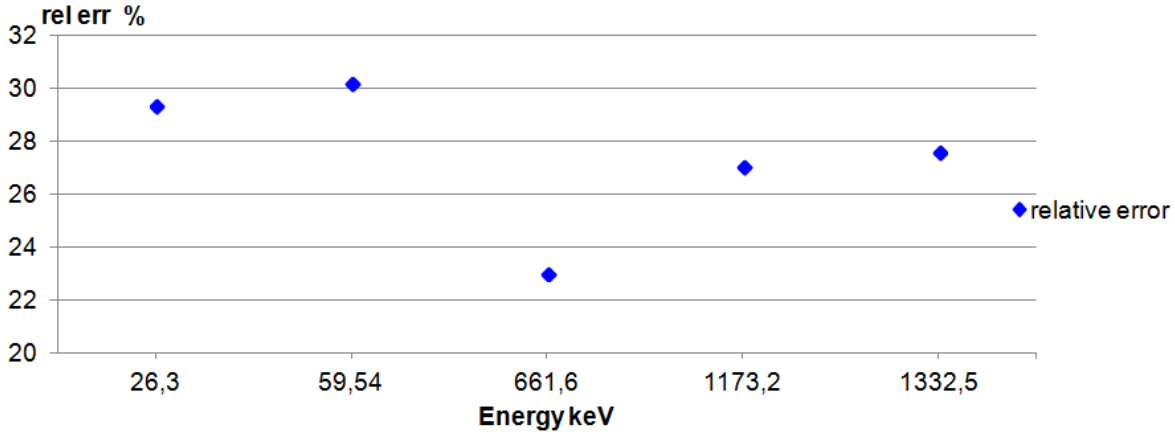

(b) Relative error between measured and simulated efficiencies

Energy keV	BR	eff measured	Δ eff measured	eff simulated	Δ eff simulated	relative error
	%	%	%	%	%	%
26,3	2,402	21,5	0,04	27,5	0,6	29,35
59,54	35,94	27,42	0,01	35,2	0,2	30,19
661,6	85,12	5,34	0,01	6,39	0,0	23,03
1173,2	99,97	2,58	0,01	3,18	0,0	27,05
1332,5	99,98	2,31	0,01	2,83	0,0	27,59

(c) Efficiency values and errors

Figure 6.11: Efficiencies

The input file should be modified to reach results as similar as possible to the measured ones. The most crucial parameters for the efficiency evaluation are:

- crystal-source distance
- entrance window thickness
- dead layers thickness
- crystal active volume dimension

I have modified all these values searching for a compromise between low and high energy efficiencies. Various different simulations have been performed with changes in the input file reaching a final configuration in which the relative error between measured and simulated efficiency is less than 10% (fig. 6.13 and 6.12).

Energy keV	BR	eff measured	Δ eff measured	eff simulated	Δ eff simulated	relative error
	%	%	%	%	%	%
26,3	2,402	21,5	0,04	22,15	1,58	3,01
59,54	35,94	27,42	0,01	27,23	0,42	-0,68
661,6	85,12	5,34	0,01	5,53	0,12	3,49
1173,2	99,97	2,58	0,01	2,81	0,08	9,02
1332,5	99,98	2,31	0,01	2,49	0,07	7,85

Figure 6.12: Efficiency values and errors

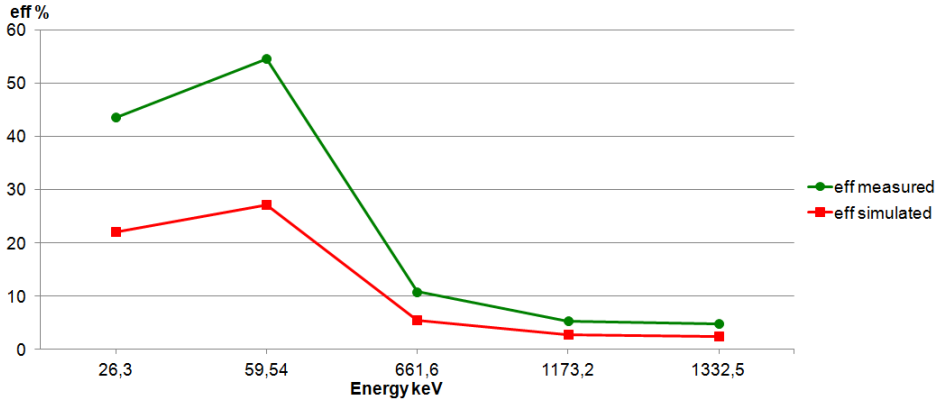

(a) Measured and simulated efficiencies in function of the energy

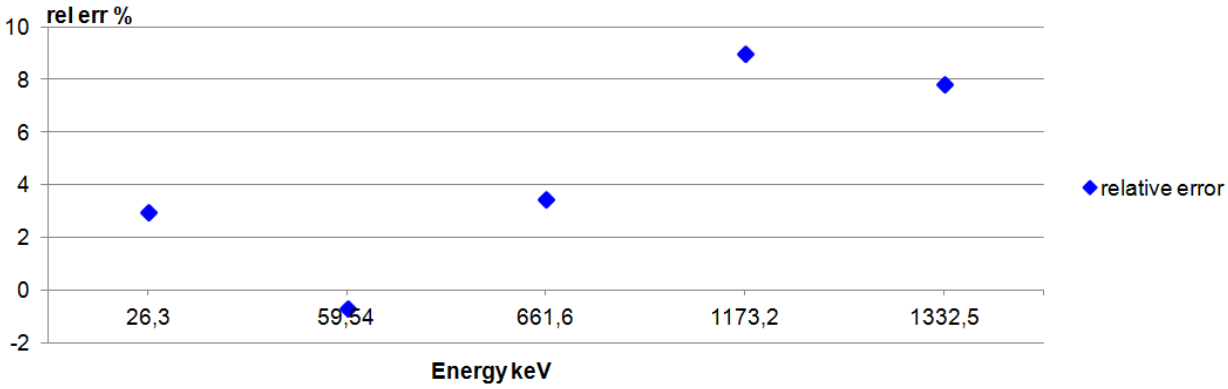

(b) Relative error between measured and simulated efficiencies

Figure 6.13: Efficiencies

6.3.3 Libraries test

Since the BEGe 5030, in this work, was conceived to measure the X-rays, the efficiency calibration is essential in the energy range in which the X-rays from Plutonium isotope decays lie.

The multi-γ low energy spectrum can provide the needed efficiency, in fact the X-rays following the ^{241}Am decay are at same energy range of those from Plutonium isotopes decay. The emitted X-rays are those of the daughter isotope: Neptunium.

I have performed simulations using the optimized BEGe input file and the ^{241}Am as source. In figure 6.14 the great compatibility between measured and simulated result for the 59.54 keV γ line is shown considering both the detector energy resolution and only the γ energy value. The simulated spectrum is displayed with a red line while the experimental spectrum is the green one.

Assignment	X-ray energy
Ge $K_{\alpha 2}$	9.855 keV
Ge $K_{\alpha 1}$	9.886 keV
Ge $K_{\beta 3}$	10.975 keV
Ge $K_{\beta 1}$	10.982 keV

Table 6.6: Germanium characteristic X-rays

The peculiar features of the BEGe permit the registration of a spectrum in which the escape peaks due to the the Germanium characteristic X-rays (tab. 6.6) are particularly notable. During the photoelectric interaction of the incoming radiation with the detector, the Germanium atoms are left excited and consequently emit X-rays in the de-excitation process. If this radiation is not collected in the active volume of the detector, the registered signal has an amplitude identical to the difference between the energy on the incoming radiation and the energy of the escaped X-ray.

In figure 6.15 it is possible to see the quite good agreement between the simulated and experimental energies considering also the escape peaks. The spectra shapes are also comparable.

Although the good agreement reached with the simulation of γ-rays I have noticed,

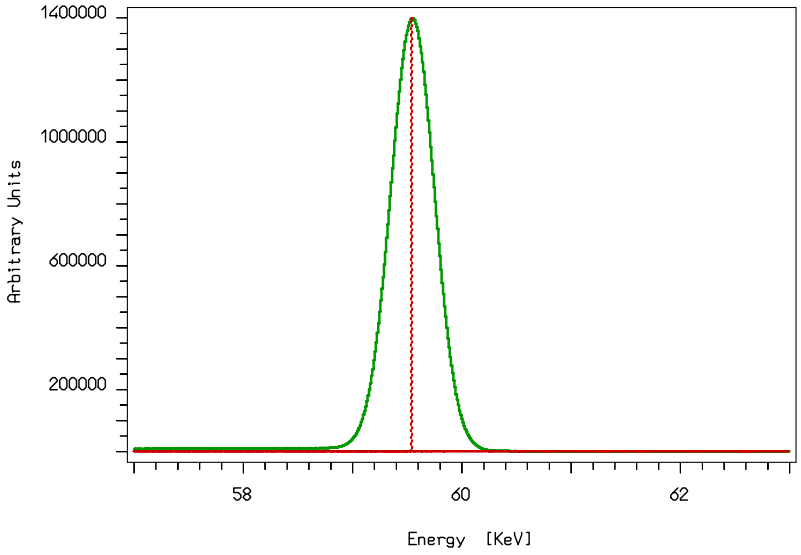

(a) 59.54 keV energy

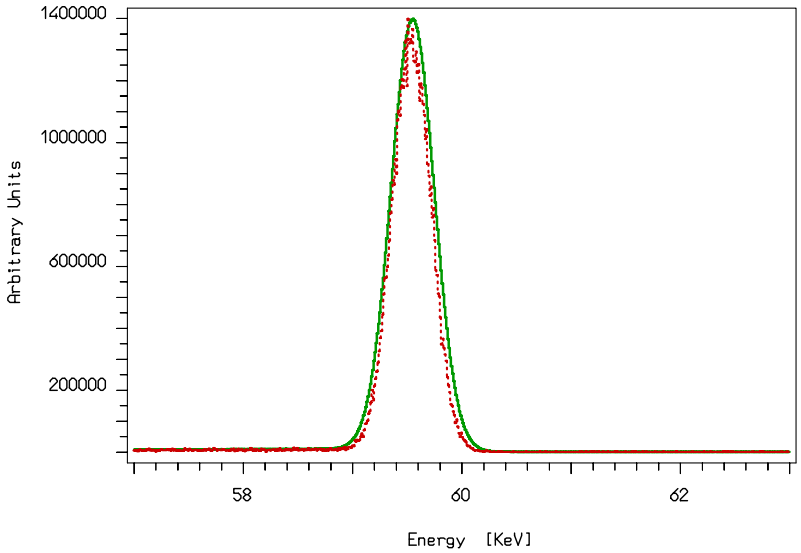

(b) 59.54 keV peak with energy resolution

Figure 6.14: Comparison between simulated spectrum (red) and experimental spectrum (green) of 59.54 keV peak of ^{241}Am

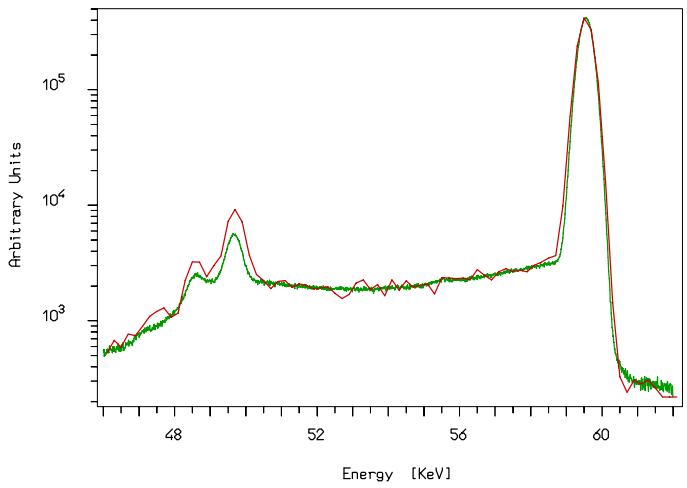

Figure 6.15: Comparison between simulated spectrum (red) and experimental spectrum (green) of 59.54 keV peak with escape peaks

from the discrepancies in the efficiency values, a problem in the simulated low energy spectrum comparing the relative counts between X-ray and γ-ray peaks.

In figures 6.16, where counts has been normalized considering the 17.75 keV peak, it is visible that the X-ray peaks lie at different energies from the measured ones. Also some Branching Ratios are not compatible; this could be seen noticing the discrepancies in the peaks amplitude.

I have searched for a feasible explanation and I have found out that the discrepancies are due to the database used by geant4 libraries: the Evaluated Atomic Data Library (EADL) (tab. 6.7) [20].

Energy		
Measured	Simulated **EADL**	Simulated **X – RayDataBooklet**
13.95 keV	13.96 keV	13.94 keV
16.82 keV	16.86 keV	16.84 keV
17.75 keV	17.84 keV	17.75 keV
20.78 keV	20.89 keV	20.78 keV

Table 6.7: Comparison of Np X-ray energies between X-Rays Data Booklet, EADL library and measured values.

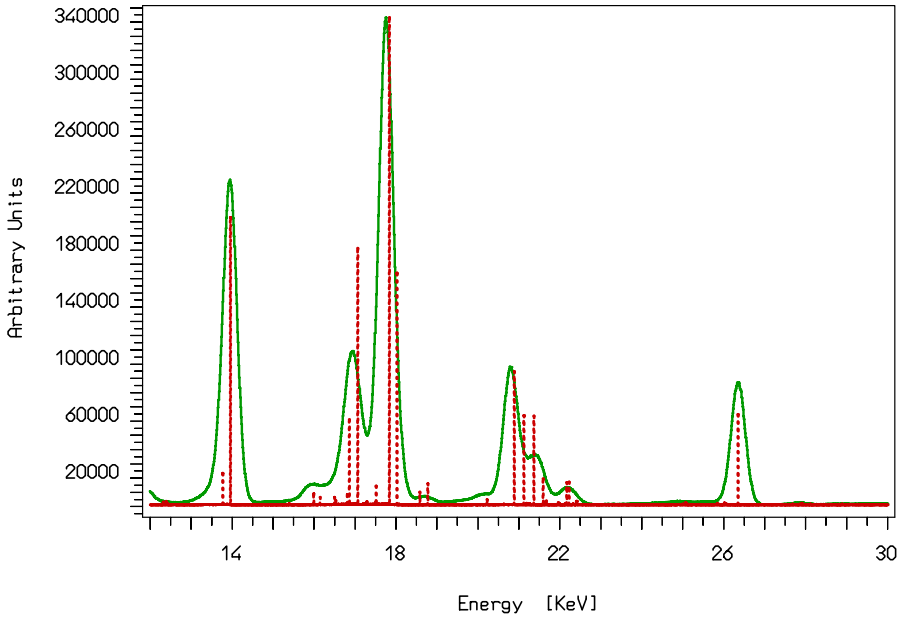

(a)

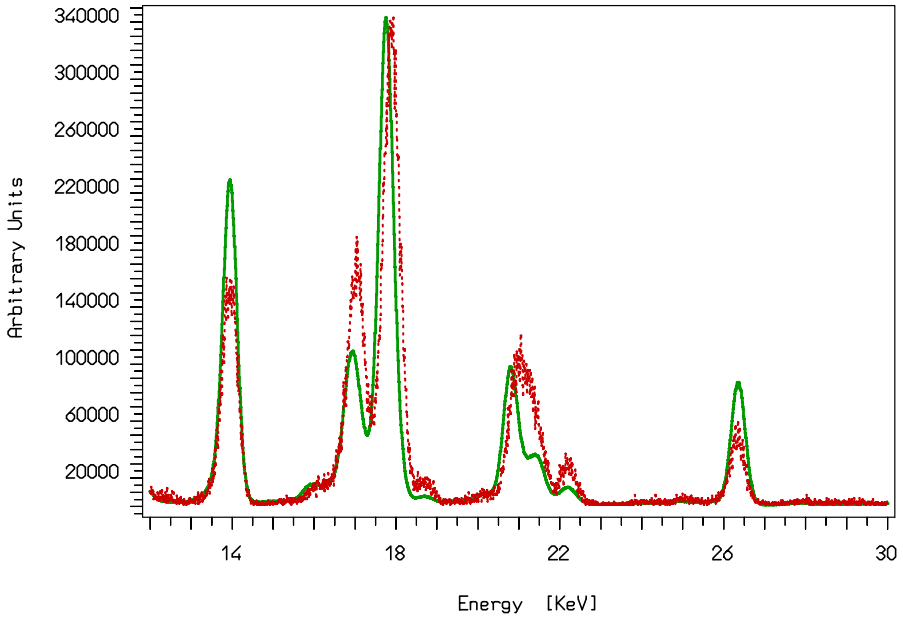

(b)

Figure 6.16: Comparison between simulated, in red, and experimental, in green, ^{241}Am X-ray spectrum

To solve the discrepancies problem I have studied the ^{241}Am in order to realize a chain file to simulate the right energies using the data from the X-rays Data Booklet.

Chain file

The chain file can be used as input source contaminant in simulations, it contains all the data regarding the decay from the parent nucleus to the daughter nucleus and the following de-excitation when the daughter nucleus is left in an exited state. To realize this file it is mandatory to study the decay scheme of the considered isotope in order to select the most probable transitions and the levels involved in the decay. In order to simplify the description regarding the construction of a chain file, the decay of the ^{238}Pu on ^{234}U will be used as example. The decay scheme to which the file, displayed in table 6.8, is referred is shown in figure 6.17.

a.				4								
b.	3											
c.	238	94		2.76760E+09		5.5932						
d.	1											
e.	234	92		0.00000E+00		0.1434						
f.	1											
g.	234	92		2.52000E-10		0.0435						
h.	0											
i.	234	92		0.00000E+00		0.0000						
j.	1	1		0.0011		5.3577						
k.	2	1		0.2898		5.4563						
l.	3	1		0.7091		5.4990						
m.	1	3	0.0001	0.0999	1.34200E+01	0.0000	0.0207	0.4218	0.2861	0.0065	0.1127	0.0810
n.	1	3	0.0004	0.0435	7.13000E+02	0.0000	0.0129	0.3801	0.3366	0.0038	0.1011	0.0940

Table 6.8: ^{238}Pu chain file

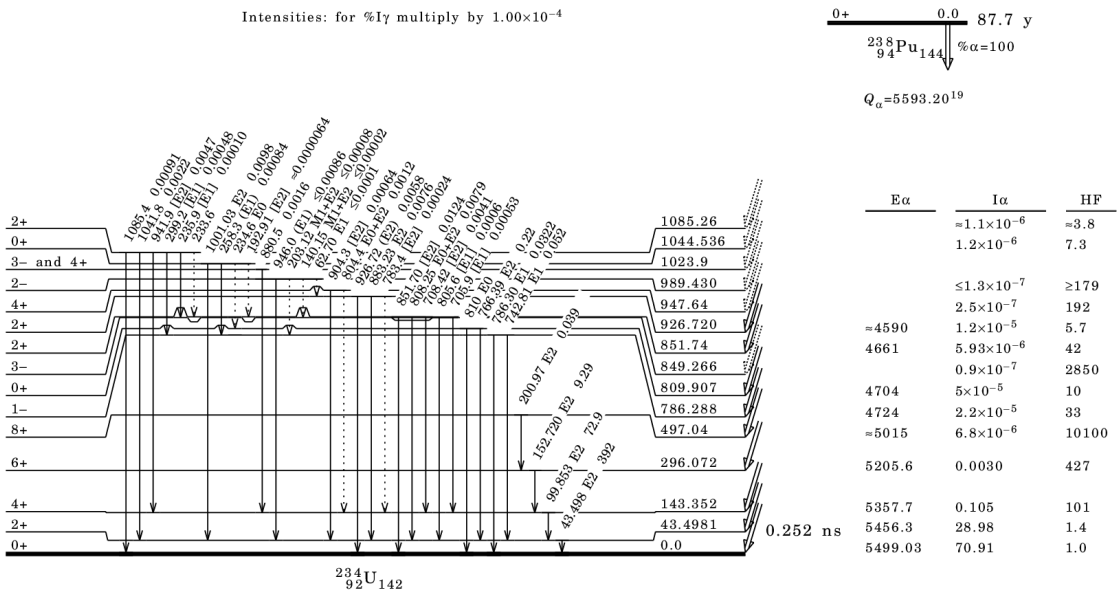

Figure 6.17: ^{238}Pu decay scheme

The file begins with the energy levels on which the parent nucleus decays and for each one are then written all the possible transitions with the corresponding energies and probabilities.

row a. The file starts with the total number of levels considered (4) including the starting level and the fundamental one.

row b. The number in the first row (3) represents the number of decays from the starting level described in the following row.

row c. The description of the starting level is stated by the mass number A (238), the atomic number Z (94), the half-life in seconds and the decay Q-value in MeV.

rows d. & f. The number (1) identifies the number of decays considered from the level described in the next row.

rows e. & g. A, Z, half-life and Q-value are described for an excited state of ^{234}U.

row h. The number 0 means that the underlying level is the stable one.

row i. A (234), Z (92) of the daughter isotope; since this is a fundamental state, half-life and Q-value are 0.

The second part concerns the decay of the parent nucleus. The number of decays has been already stated in row b.

row j. the first number, 1, specifies the number of levels that are skipped by the decay, included the arriving one. In this file this number corresponds to the emission of an α to the first declared level (row e.). If the number is 1 the described level is the first declared after the starting level. The second number, 1, defines the type of radiation:

- α = 1
- β = 2
- γ = 3
- ε = 4, electron capture
- β^+ = 5
- $\beta\beta$ = 6
- for some particular decays, the number 10 is used to describe fictitious levels. For example the complex decay of ^{40}K that features a β^- on ^{40}Ca and an electronic capture on ^{40}Ar.

The third number in the row is the Branching Ratio and the last one is the Q-value. If the described decay is β^+, 1.022 MeV should be subtracted to the Q-value to define the spectrum end point. β decay needs another number to specify if the transition is prohibited or allowed. This number is calculated from the selection rules, the first prohibited transition corresponds to $\Delta J = 0, \pm 1, \pm 2$ with $\Delta\pi$ parity variation.

rows k. & l. these rows are identical to row j., but the first numbers are 2 and 3 indicating that the described decays start from the ^{238}Pu level arriving to the second and the third stated excited levels of ^{234}U respectively.

The last part of the file concerns the γ decays. For γ emission the internal conversion coefficients are crucial to exactly describe the possible emission of X-rays due to the internal conversion.

rows m. & n. the first number indicates the number of skipped levels, the second, 3, is the number corresponding to the radiation type: a γ-ray. The B.R. and the photon energy are the two following numbers. In row n. a 43.5 keV γ with 0.000004% of relative intensity is considered, which follows the 5.4563 MeV α decay. The last eight numbers are the internal conversion coefficients, the first one is the total, the others correspond to the possible electron levels in the following order: K, L_1, L_2, L_3, M_1, M_2, M_3. These values can be evaluated using the database of the *www.nndc.bnl.gov/ensdf* website, inserting the information related to the γ and the isotope emitting it.

For the electronic capture these coefficients are replaced with the electron capture ratios: L_1/K and L_2/L_1.

The chain file describes the decay of an isotope considering the energy levels and emitted radiations, to complete these information a file describing the X-rays and the Auger electrons emission has to be realized. This file is generally named Xray.dat, the inserted parameters are referred to the daughter isotope. The X-rays file contains the following information:

- Energies and Intensities of the K-lines (α_1, α_2, β_1, β_2, β_3, β_5)
- Energies and Intensities of the L_1 lines (β_3, β_4, γ_2, γ_3)
- Energies and Intensities of the L_2 lines (β_1, γ_1, γ_6, η)
- Energies and Intensities of the α_1, α_2, β_{2-15}, β_5 and l L_2 lines
- Fluorescence and Coster-Kronig ratios ω (K, L_1, L_2, L_3), f (12, 13, 23)
- Binding energies (keV) for the K, L_1, L_2, L_3, M_1, M_2, M_3 and M_5 shells
- Auger electrons intensities for the K shell: K-L_1L_2, K-L_1L_3, K-L_1 M_1, K-L_1 M_2, K-L_1 M_3, K-L_2L_2, K-L_2L_3, K-L_2 M_1, K-L_2 M_3, K-L_3L_3, K-L_3 M_1, K-L_3 M_2, K-L_3 M_3.

To describe the ^{241}Am decay and all the other chain files I have used the X-ray Data Booklet database (tab. 6.7) and Evaluated Nuclear Structure Data File (ENSDF).

The comparison between the spectrum simulated with the file I have realized and the experimental spectrum shows a better energy agreement (fig. 6.18) respect to the previous one.

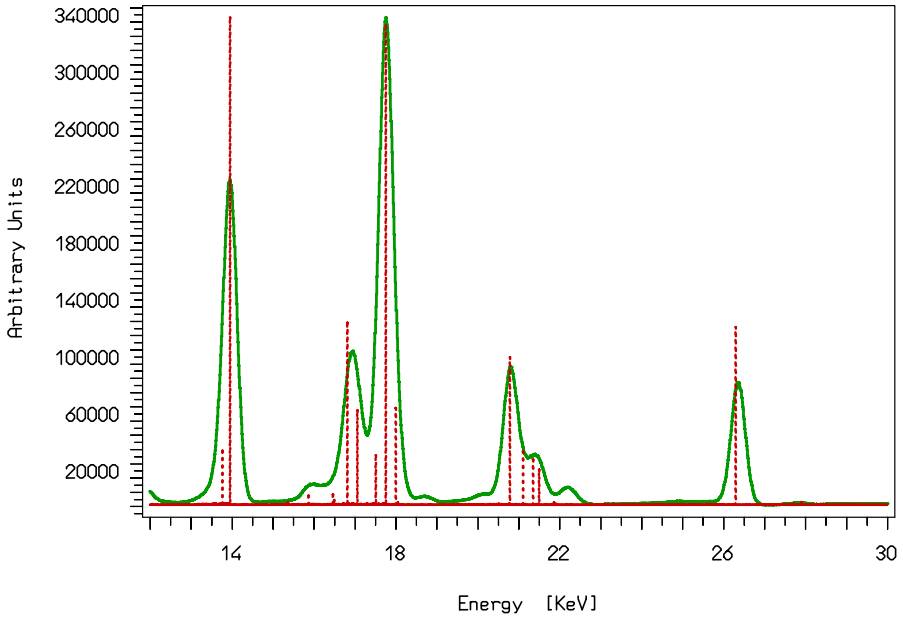

(a)

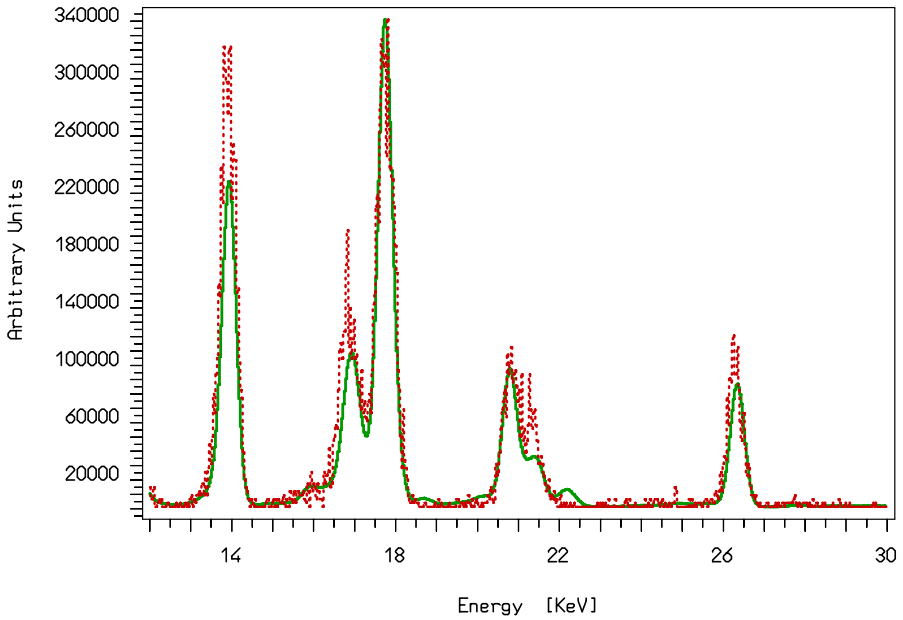

(b)

Figure 6.18: Comparison between simulated spectrum using the chain file, in red, and experimental spectrum, in green, of ^{241}Am X-rays

6.3.4 Low energy efficiency calibration

Because of some difficulties in the B.R. definition for the ^{241}Am decay, the efficiency calibration has been performed using a certified low energy source containing the isotope ^{93m}Nb (tab. 6.9) whose emitted radiations lie in the energy range under study.

Energy	B.R. %	Sum B.R. %	certified γ/s (±3%)	γ/s at 1st March 2013
16.521 keV	3.31	9.60	1632.8	1621.5
16.615 keV	6.29			
18.61 keV	0.49	1.45	316.5	314.32
18.62 keV	0.96			

Table 6.9: Niobium source certified data.

^{93m}Nb decays by internal transition with the consequent emission of X-rays. The source is composed of a powder placed between two very thin plastic layers.

I have performed a simulation with the optimized input configuration file using the geant4 libraries; unfortunately the discrepancies in the X-rays energies are significant also for this decay (fig. 6.19(a)).

Therefore I have realized a chain file describing the ^{93m}Nb decay using the X-ray Data Booklet database. The simulation with this file as input source shows a good agreement with the experimental spectrum (fig. 6.19(b)).

Results of the comparison between simulated and measured efficiencies are listed in table 6.10. It is possible to consider a systematic relative error due to simulations lower than 13%.

Isotope	Energy	B.R. %	Meas. eff.	Sim. eff.	(Sim.-Meas.)/Meas.
Nb-93m	16.61 keV	9.60	25.6%	28.8%	12.5%
Nb-93m	18.6 keV	1.45	27.5%	30.3%	10.2%

Table 6.10: Nb-93m simulated and measured data.

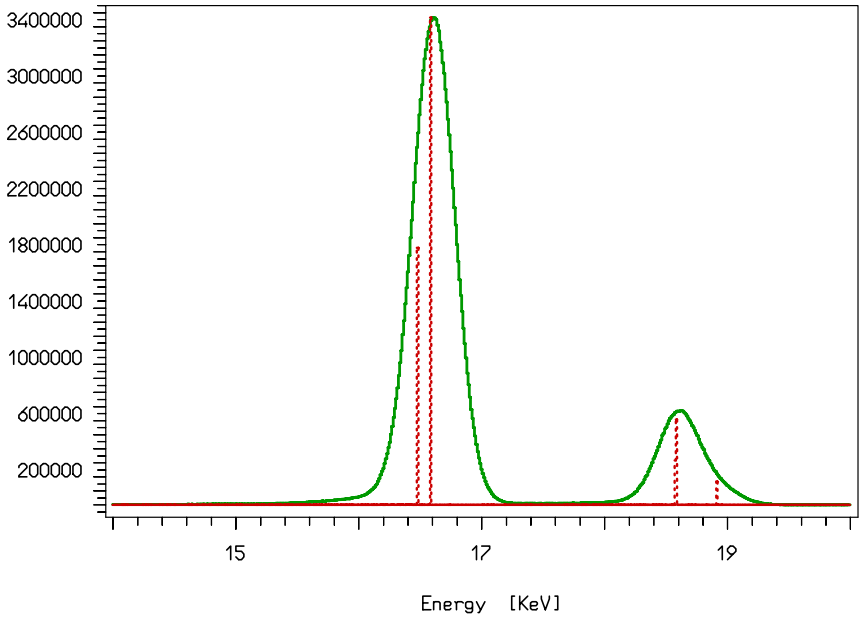

(a) simulation with geant4 libraries

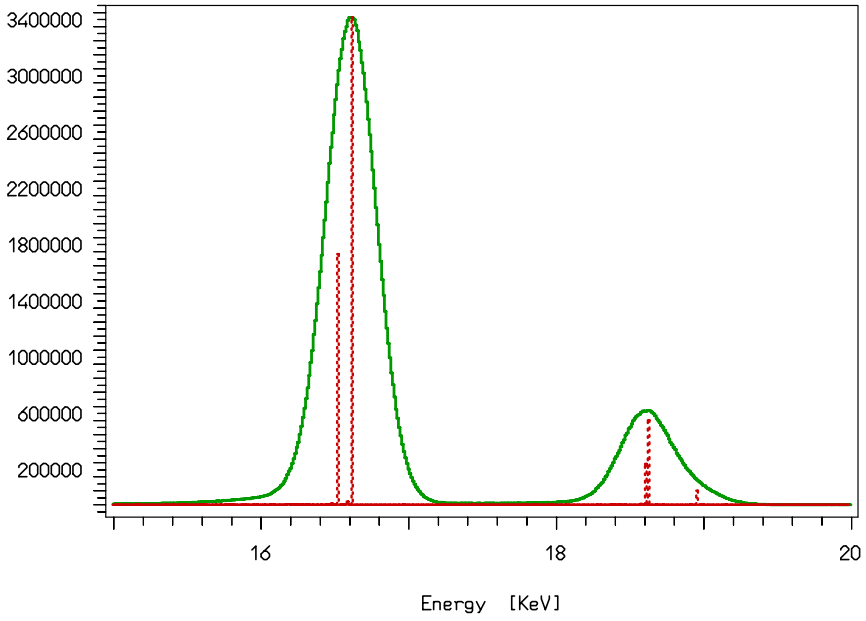

(b) simulation with chain file

Figure 6.19: Comparison between simulated, in red, and experimental, in green, ^{93m}Nb spectrum

6.4 Plutonium calibration measurements

To verify the sensitivity of the X-rays detection method, measurements of ^{238}Pu standards have been carried out. Liquid standards with a specific activity of 2740 Bq/g and 500 Bq and a 3 cm diameter filter with an activity of about 270 Bq, placed at the center of the entrance window have been measured. The count rate guarantees the possibility to detect also the emitted γ-ray of the decay despite the low B.R..

The analysis has been performed considering the counts under the γ full energy peak at 43.5 keV and that of 13.6 keV and 17.2 keV X-rays (fig. 6.20). This analysis provided the calculation of the efficiencies and the activity evaluation from the X-rays counts.

A source of ^{239}Pu liquid standard of 3.5 Bq has also been measured (fig. 6.21) with the same configuration and analysis. It is important to evaluate the product between efficiency and B.R. for the X-rays; this value can be used to consider the contribution of the different isotopes in a sample containing both of them.

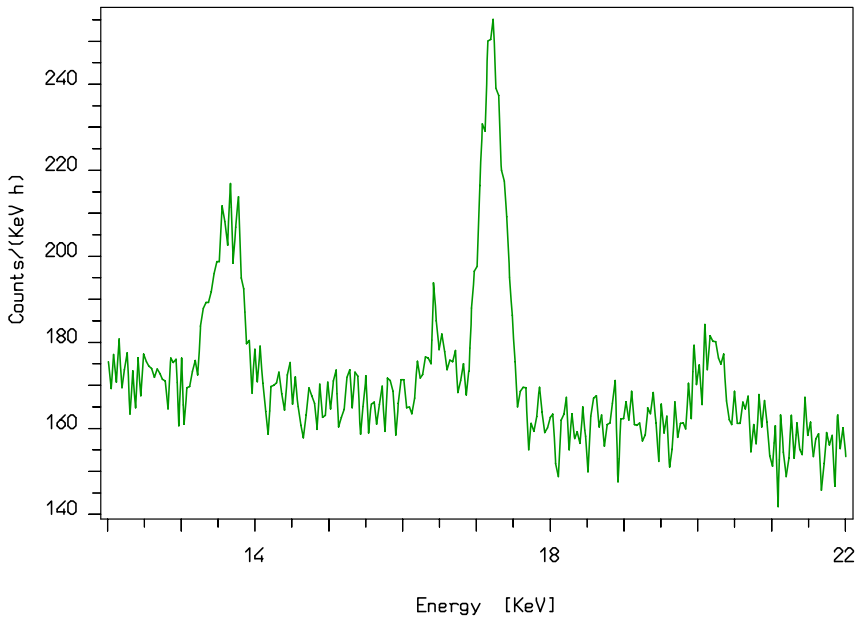

Figure 6.21: ^{239}Pu standard measured spectrum

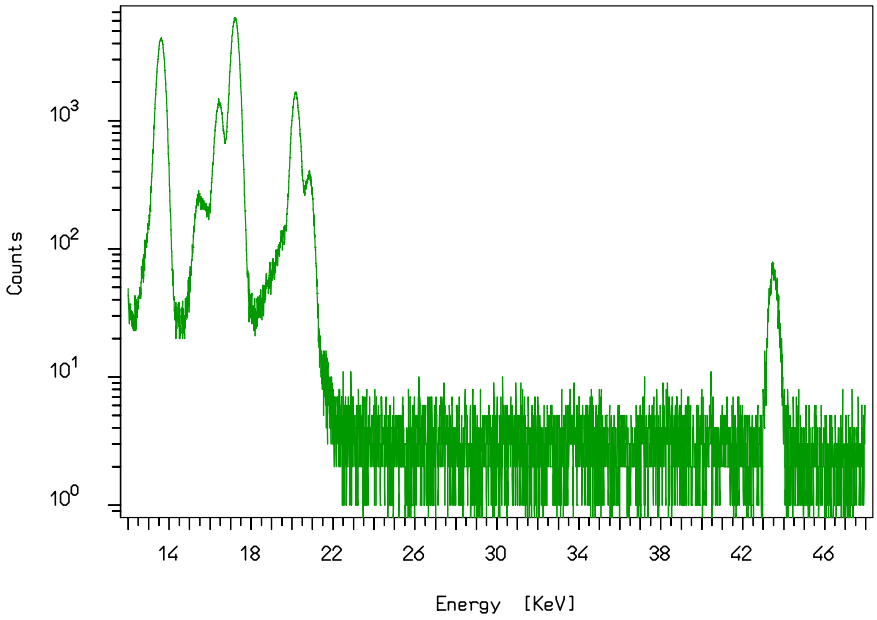

(a) 12-48 keV spectrum

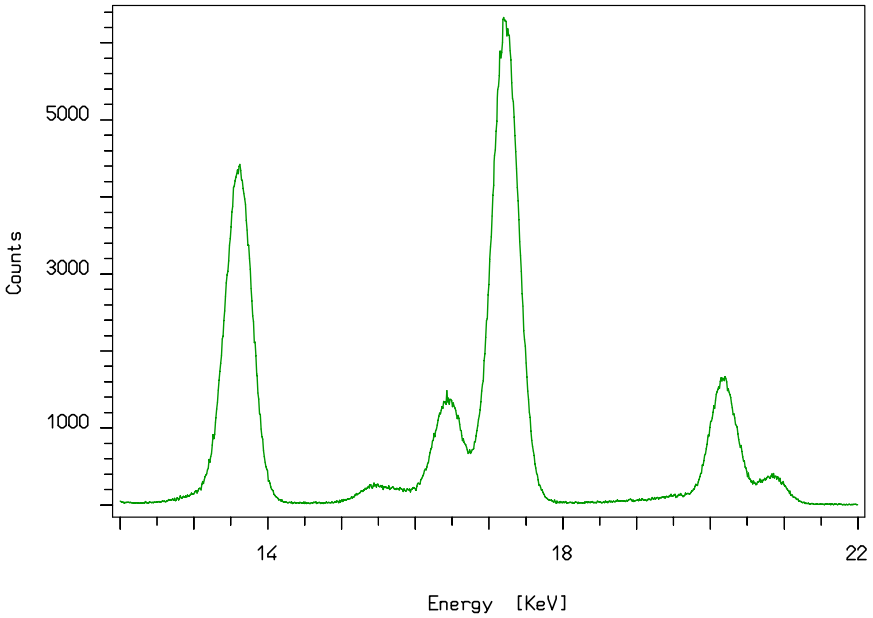

(b) X-rays spectrum

Figure 6.20: ^{238}Pu standard measurement spectra

During the reconstruction of the detector-source geometry for simulations, special attention have been paid on dead layers and source configuration because these are the two most sensitive parameters for low energy detection. For this purpose measurements of different shape and composition sources have been performed. In figure 6.22 the geometry reconstruction of the BEGe 5030 is shown.

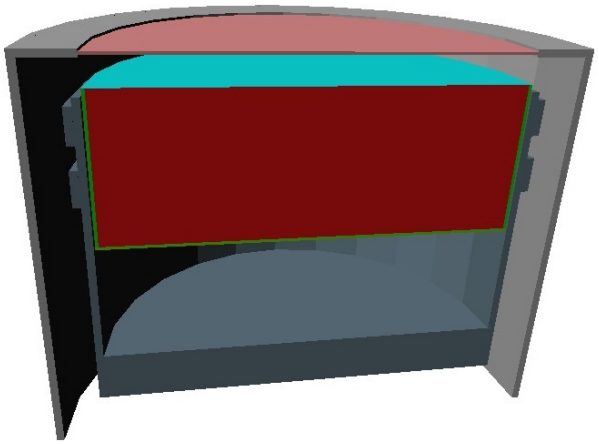

Figure 6.22: BEGe geometry

Considering the measurement of the 500 Bq source and the simulation using geant4 libraries, the activity calculated with the simulated efficiencies has led to a systematic error up to 30% (tab. 6.11) respect to the certified one. In figure 6.23 it is possible to notice that the 17.2 keV peak energy highly differs respect to the measured energy.

Energy	**Activity (meas.)**	Systematic error
13.6 keV	489.5 Bq	30%
17.2 keV	523 Bq	20%

Table 6.11: Activity measured of a standard with known activity (500Bq) of ^{238}Pu for 2 X-ray lines.

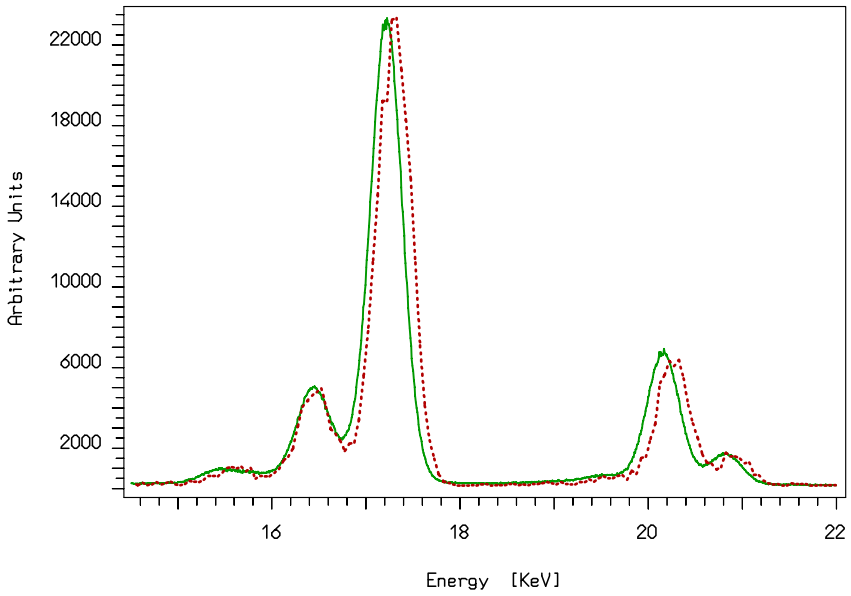

Figure 6.23: Comparison between simulated (red) and measured (green) spectra

Energy (keV)	**Activity Bq**
43.5	298.5 ± 63.8
13.6	285.8 ± 15.5
17.2	328.2 ± 17.3

Table 6.12: ^{238}Pu standard measurement

To improve the system sensitivity I have studied the ^{238}Pu and ^{239}Pu decay scheme in order to create a chain file (fig. 6.8).

The simulations realized with the chain file (fig. 6.24) have been used to evaluate the activity of the 270 Bq source. Comparing the results with the measured efficiencies it is possible to estimate a systematic error of about 15 %. Results for the 270 Bq source are shown in table 6.12.

This method has provided the system optimization using samples of different shape and composition such as point sources or environmental matrix of hundred of grams.

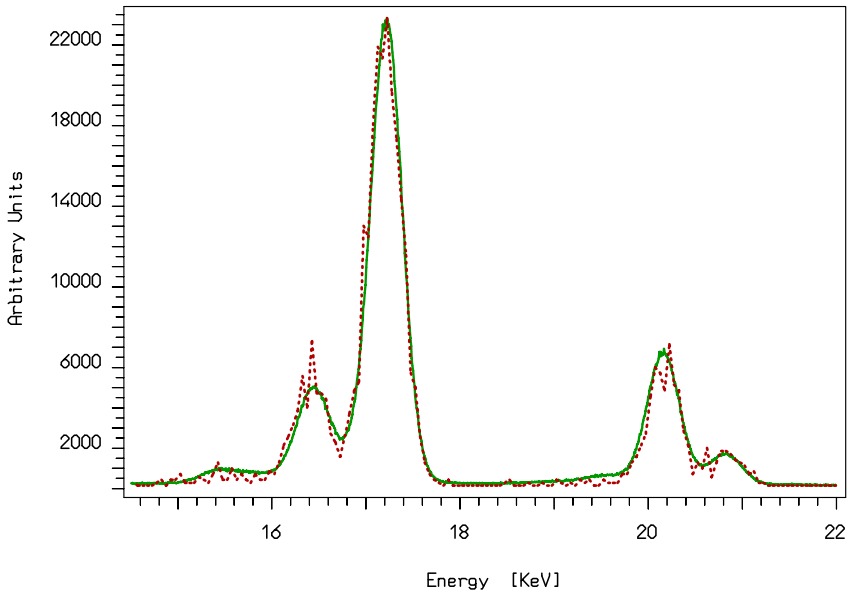

Figure 6.24: Spectrum simulated with chain file (red) compared to the measured spectrum (green)

6.5 Fangataufa sediment measurements

The BEGe 5030 has then been used to measure an environmental sample of sediment collected by IAEA-MEL in Fangataufa Lagoon, where nuclear weapon testing had been carried out. This sample is the IAEA-384 and it was supplied by International Atomic Energy Agency (IAEA). Specific activity values are certified in the IAEA-384 reference sheet [7].

The sum of the three isotopes, ^{238}Pu, ^{239}Pu and ^{240}Pu, concentrations (tab. 6.13) has a certified value of 150 ± 10 Bq/kg. Measurements have been realized using a 50 g of sediment sample in a plastic Petri dish with a 10 cm of diameter placed on the detector.

The analyzed low energy spectrum (fig. 6.25) shows the X-rays energy peaks; in particular the 17.2 keV peak has been considered since it is the one with the highest B.R. for all the isotopes. This peak has a rate of 13.4 ± 0.2 counts/h.

I have described the detector and the sample in every part in the simulation input file. The detector configuration file has already been optimized for the correct simulation of

Isotope	**Activity (Bq/kg)** 95% confidence level
^{238}Pu	38.6-39.6
^{239}Pu	85-105
^{240}Pu	15.1-18.7

Table 6.13: Certified specific activities

the X-rays following the Plutonium isotopes decays, but it is essential to describe appropriately the source. The Fangataufa sediment is a powder and there was no information about its composition.

I have chosen various possible materials with different densities that could be similar to the sample compound.

Of all the simulated spectra the most comparable with the experimental measurement are those with SiO_2 as sample material. The best choice is the compound of SiO_2 and Al_2O_3. Simulations have been performed for all the isotopes under study using this sample description.

The counts under the X-rays peaks of the measured sample have been weighted by the detection efficiencies and Branching Ratios considering the certified activity values ratio, obtaining the expected rate at the 17.22 keV X-ray peak for the three Plutonium isotopes in this sample; results are shown in table 6.14.

Isotope	**Expected counts/h**
^{238}Pu	6.9 ± 1.8
^{239}Pu	6.2 ± 1.5
^{240}Pu	6.2 ± 2.5

Table 6.14: Expected rate for the 17.2 keV X-ray peak

From the expected counts/h at 17.2 keV energy I have estimated a total activity of 159 ± 21 Bq/kg due to the sum of all the isotopes contaminations. This value is perfectly compatible with the certified one.

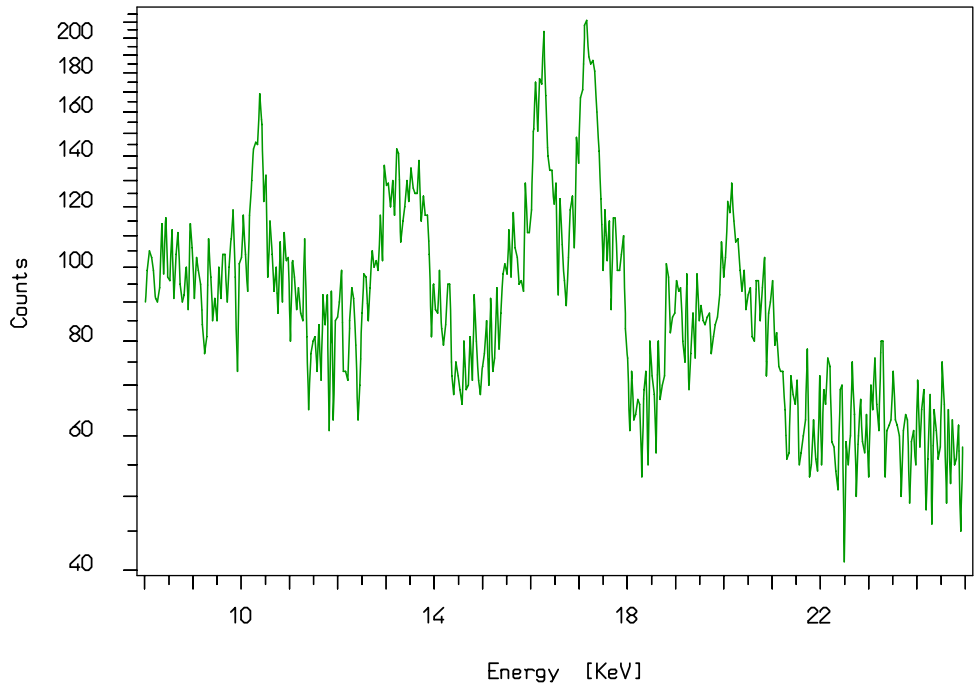

Figure 6.25: IAEA-384 low energy spectrum

The developed method can therefore measure the Plutonium activity due to different isotopes concentrations in few measuring hours. However this analysis is not able to separate concentrations of the three isotopes, but could estimate contaminations comparable to clearance levels for each of them.

A first fast analysis for low Plutonium contamination can give a preliminary result for each isotope. Considering the total counts under the peak of 17.22 keV as a contribution of a single isotope the contamination of this Plutonium isotope is obviously overestimated. Results of this analysis using the product between efficiency and B.R. for each isotope at the considered energy are shown in table 6.15.

Although ^{238}Pu and ^{240}Pu concentrations are overestimated their values lie under the clearance level of 140 and 150 Bq/kg respectively. This means that this kind of analysis is able to give an important and correct information about the sample contaminations establishing if it is whether or not under the clearance level.

Isotope	**Activity Bq/kg**
^{238}Pu	77 ± 12
^{239}Pu	215 ± 32
^{240}Pu	36 ± 5

Table 6.15: Activity estimated considering all the counts under the 17.2 keV peak as due to single isotope

^{239}Pu instead is the isotope with the lowest branching ratios for all the emitted X-rays, so that it is the most difficult to detect, but it is possible to calculate the sensitivity on this radioisotope reachable with the used system.

The evaluation of this sensitivity consists in the calculation of the Minimum Detectable Activity (MDA) from the formula 3.4

The MDA for ^{239}Pu has been calculated considering the counts in the background spectrum of the environmental sample, this allows a more real situation because in the region under study there will be some counts due to other contaminants.
The energy range has been chosen considering the system energy resolution, 400 eV, in this configuration leading to an MDA, for the 17.22 keV from ^{239}Pu decay, of 50 Bq/kg, which is well below the clearance level.
The measuring system is therefore capable to detect this single isotope concentration with a suitable sensitivity.

The X-ray spectroscopy to measure contamination of Plutonium isotopes in environmental samples is thus a fast screening method: considering 150 Bq/kg of ^{239}Pu, the detection of the emitted 17.22 keV X-ray with a BEGe 5030 in 10 hours guarantees a 9σ measurement level.

Chapter 7

Conclusions

GMX Coincidence System

The low level counting system composed of two GMX 100-95 in Low Background configuration has been realized with a low intrinsic background. This feature has been provided with an accurate materials selection. Materials with high radiopurity have been used for the realization of the detectors, considering their contribution to the intrinsic background evaluated through Monte Carlo simulations.

The system is conceived to work in coincidence, for this reason a peculiar data acquisition has been developed; both detectors signals are simultaneously registered thanks to an external trigger that is fired each time a signal is detected in one of the detectors. Waveform parameters are saved on-file in order to allow an off-line coincidence analysis in addiction to that of single detector. The analysis has required some dedicated software that I have developed using MATLAB framework. The goodness of the conceived analysis has been tested using ^{232}Th sources with different concentrations leading to a good sensitivity for coincidence measurements on the ^{208}Tl isotope belonging to the decay chain. ^{208}Tl decay features some high probable coincidences that have been analyzed reaching a detection limit of about 1 mBq for the configuration under study. These measurements have also verified the good reproducibility of the simulated coincidence efficiencies.

A possible application of this system is the material selection for rare event physics experiment.

During my PhD work, after the optimization of the system, some materials for such experiments have been measured in order to evaluate their contaminations in primor-

dial radionuclides. Furthermore coincidence analysis have been performed to study the possible concentration in ^{60}Co and ^{134}Cs whose decay schemes show high probable coincidences between the emitted photons.

The sensitivity of the system has been tested through the measurement of ^{232}Th concentration in a Copper cylinder placed between the two HPGe. The coincidence analysis has allowed a more sensitive result than the single detector measurement. The evaluated detection limit is < 2 mBq/kg. Increasing the sample mass is possible to reach a sensitivity < 1 mBq/kg. It is important to notice that the spectrometer is not placed underground, but it has a coverage of about 15 m.w.e..

This value can be further improved with a longer measuring time of about 6 month; the expected detection limit is < 400 μBq/kg. The sensitivity could also be enhanced using veto detectors to avoid the detection of cosmic rays that are the main source of continuum in the system measurements.

Sensitive Plutonium concentration measurement with BEGe

The Plutonium detection through the analysis of the emitted X-rays has been tested using the BEGe. This detector can indeed detect a broad energy spectrum with high efficiency and energy resolution. It has been optimized using Monte Carlo simulations and calibration measurements of ^{238}Pu liquid standards.

An environmental sample, IAEA 384 Fangataufa Sediments, measurement has been performed; the analysis has been focused on three Plutonium isotopes: ^{238}Pu, ^{239}Pu and ^{240}Pu. Through the detected rates of the X-rays following their α decays it has been possible to evaluate a contamination of ^{238}Pu and ^{240}Pu of about 77 Bq/kg and 36 Bq/kg that are under the clearance level of 140 Bq/kg set by the safety agencies.

^{239}Pu is the most difficult isotope to detect because of its X-rays low B.R.; the detection sensitivity for this isotope has been evaluated as the MDA: 50 Bq/kg. The clearance level for ^{239}Pu concentration is set at 150 Bq/kg, this value can be detected with the BEGe in 10 hours with a confidence level of 9σ with the described method.

Detection of Plutonium concentrations with this method allows a fast screening of samples from potentially contaminated areas, for specific activities relative to clearance

levels. The number of samples needing a further analysis of single isotope contaminations separately therefore can be reduced.

Optimization of the measuring system are in progress. A dedicated shielding optimized for the background reduction is under construction; it will consist in 15 cm Lead and 5 cm Copper closer to the crystal in order to improve the sensitivity of the system.

Appendix A

Counting Statistics

The radioactive decay processes follow statistical laws: the probability that at a certain time t, there will be n decays from N nuclei is evaluated from the Bernoulli binomial distribution:

$$P(n,t,N) = \binom{N}{n}(1-e^{-\lambda t})^n(e^{-\lambda t})^{N-n} \tag{A.1}$$

where λ is the decay constant of the radioisotope under study. This value is related to the nucleus life-time by the relation $1/\lambda = \tau$. Moreover it is possible to define the half life-time as $T_{1/2} = \tau \ln 2$.

Some nuclei do not decay only through single process, but their decays involve different emissions that can be in competition or associated. The decay intensity is defined by the Branching Ratio (B.R.) which is composed of all the partial decay constants:

$$B.R. = \lambda_i/\lambda \qquad where \qquad \lambda = \sum_{i=1} \lambda_i \tag{A.2}$$

Generally a measurement time is shorter than the isotope life-time, thus the probability distribution can be approximated to the Poisson distribution (eq. A.3) with $\bar{n} = N\lambda t$ and $\sigma^2 = \bar{n}$.

$$P(n,t) = \frac{n^{\bar{n}}}{n!}e^{-\bar{n}} \tag{A.3}$$

For low values of $\bar{n}$ the probability curve is asymmetric, increasing the counts the distribution becomes symmetric respect to the mean value. If $\bar{n}$ is greater than ~30 it is possible to consider the normalized Gauss distribution (eq. A.4) with $\sigma^2 = \bar{n}$.

$$G(n) = \frac{1}{\sqrt{2\pi\sigma^2}} e^{-\frac{n-\bar{n}}{2\sigma^2}} \tag{A.4}$$

The probability that a variable x assumes a value between x and $x+dx$ is evaluated as $G(x)dx$: the distribution features a single parameter $\bar{n}$ that corresponds to the x mean value.

The probability that the x value lies between x_1 and x_2 is thus evaluated by:

$$P(x_1 \leq x \leq x_2) = \frac{1}{\sqrt{2\pi\sigma^2}} \int e^{-\frac{x-\bar{n}}{2\sigma^2}} dx \tag{A.5}$$

The equation A.5 can be used to calculate the probability that the difference between x and $\bar{n}$ would be greater than a value ε. Table A.1 shows the probability for some defined values of ε.

ε	0.67σ	1.0σ	1.64σ	1.96σ	3σ
P(| x - $\bar{n}$ | > ε)	0.50	0.68	0.90	0.95	0.997

Table A.1: Confidence Levels

The *Activity* specifies the number of decays per time units; it is defined as :

$$A(t) \equiv \lambda N(t) = A_0 e^{-\lambda t} \tag{A.6}$$

where A_0 is the activity at the initial time.

The activity unit is the *Bequerel* (Bq) or disintegrations per second.

Secular Equilibrium

When a radioactive decay produces an unstable nucleus it is possible to have a series or chain of radioactive decays. The parent nucleus is the first of the series.

If at $t = 0$ there are N_0 parent atoms, is generally assumed that no daughter nuclei are present so that:

$$N_1(t = 0) = N_0$$

$$N_2(t = 0) = N_3(t = 0) = \cdots = 0$$

The decay constants of the involved nuclei are represented by λ_1, λ_2, λ_3, $\cdots$

The decrease of the number of parent nuclei in a time dt is equal to:

$$dN_1 = -\lambda_1 N_1 dt$$

while the number of daughter nuclei increases as the parent decays but decreases due to their decays, this can be written as:

$$dN_2 = \lambda_1 N_1 dt - \lambda_2 N_2 dt$$

The number of parent nuclei at time t can be obtained by:

$$N_1(t) = N_0 e^{-\lambda_1 t}$$

whereas the number of daughter nuclei as:

$$N_2(t) = N_0 \frac{\lambda_1}{\lambda_2 - \lambda_1}(e^{-\lambda_1 t} - e^{-\lambda_2 t})$$

If $\lambda_1 \ll \lambda_2$, the parent isotope has a life-time so long that it is possible to consider a constant decay rate, $e^{-\lambda_1 t} \simeq 1$ and thus $N_2(t) \cong N_0 \frac{\lambda_1}{\lambda_2}(1 - e^{-\lambda_2 t})$.

Therefore the daughter isotope activity, A_2, reaches the limit value $N_0\lambda_1$ establishing the *secular equilibrium* condition in which the daughters activities are equal to the parent activity.

Bibliography

[1] G.Heusser “Low-radioactivity background techniques”, Annu. Rev. Nucl. Part. Sci. 1995. 45:543-90. DOI: 10.1146/annurev.ns.45.120195.002551.

[2] Pall Theodorsson “Measurements of Weak Radioactivity”, World scientific, 1996. ISBN: 9810223153.

[3] Glenn F. Knoll, “Radiation Detection and Measurement, Third Edition”, Wiley, 2000. ISBN: 0471073385.

[4] I. Zvara, P. Povinec and I. Sykora “Determination of very low levels of radioactivities”, Pure Appl. Chem., 1994, Vol. 66, No. 12, pp. 2537-2586. DOI: 10.1351/pac199466122537.

[5] Canberra Germanium Detectors user’s manual

[6] Andrzej Zastawny “The Measurements of low radioactivities”, Lectures for Extramural non-resident, post graduate studies assisted by Internet “Methods of absolute dating and applications”, 2003.

[7] International Atomic Energy Agency Department of Nuclear Sciences and Applications IAEA Environment Laboratories “Reference Sheet - Certified Reference Material IAEA-384 Radionuclides in Fangataufa Lagoon Sediment”.

[8] L. A. Currie, “Analitycal Chemistry” 40(3), 586 (1968).

[9] E. C. Anderson, F. N. Hayes “Recent advances in Low Level Counting Techniques“, Annual Review of Nuclear Science Vol. 6: 303-316. DOI: 10.1146/annurev.ns.06.120156.001511.

[10] The 30-Minute Guide to ICP-MS, technical note.

[11] R. R. Greenberg, P. Bode, E. A. De Nadai Fernandes ”Neutron activation analysis: A primary method of measurements“, Spectrochimica Acta Part B 66 (2011) 193-541.

[12] National Instruments Data Sheet

[13] Xiaolin Hou, Per Roos ”Critical comparison of radiometric and mass spectrometric methods for the determination of radionuclides in environmental, biological and nuclear waste samples“ Analytica Chimica Acta 608 (2008) 105–139

[14] E. Holm, ”Source preparation for alpha and beta measurement“, NKS-40, 2001. http://130.226.56.167/nordisk/publikationer/1994 2004/NKS-40.pdf.

[15] Johanna Sabine Becker ”Mass spectrometry of long-lived radionuclides” Spectrochimica Acta Part B 58 (2003) 1757–1784

[16] Clemenza M., Borio di Tigliole A., Previtali E., Salvini A.,‘Ultra sensitive Neutron Activation measurements of 232Th in copper“‘ American Institute of Physics, Vol. 1338 pp. 37-43 (2011)

[17] Agostinelli, et al., 2003. ”Geant4 a Simulation Toolkit.“ NIM A.

[18] Bucci, C., et al., 2009. ”Background study and Monte Carlo simulations for large-mass bolometers.“ Eur. Phys. J. A 41, 155e168

[19] J. Beringer et al. (Particle Data Group), Phys. Rev. D86, 010001 (2012) and 2013 partial update for the 2014 edition.

[20] ”https://www-nds.iaea.org/epdl97/libsall.htm“

[21] A Alessandrello et al. ”Measurements of internal radioactive contamination in samples of Roman lead to be used in experiments on rare events“, Instruments and Methods in Physics Research Section B, Volume 142, Issues 1–2, June 1998, Pages 163–172.

[22] A. Nucciotti et al. "Design of the Cryogen-Free Cryogenic System for the CUORE Experiment", Journal of Low Temperature Physics, Volume 151, Issue 3-4 , pp 662-668, DOI 10.1007/s10909-008-9723-8

[23] Heusser G., M. Laubenstein, H. Neder ”Low-level germanium gamma-ray spectrometry at the μBq/kg level and future developments towards higher sensitivity“

[24] M. Clemenza, E. Fiorini, E. Previtali, E. Sala ”Measurement of airborne ^{131}I, ^{134}Cs and ^{137}Cs due to the Fukushima reactor incident in Milan (Italy)“, Journal of Environmental Radioactivity 114 (2012) 113e118